2014-09-23

The Evaluation of MS4A4A and MS4A8B Expression in Hematopoietic Cells

Puri, Mandip

UNIVERSITY OF CALGARY

The Evaluation of MS4A4A and MS4A8B Expression in Hematopoietic Cells

by

Mandip Puri

A THESIS

SUBMITTED TO THE FACULTY OF GRADUATE STUDIES

IN PARTIAL FULFILMENT OF THE REQUIREMENTS FOR THE

DEGREE OF MASTER OF SCIENCE

GRADUATE PROGRAM IN BIOCHEMISTRY AND MOLECULAR BIOLOGY

CALGARY, ALBERTA

August, 2014

Abstract

MS4A is a family of proteins with four membrane spanning regions. Currently, among the 15+ human MS4A family members, most remain uncharacterized. A notable exception is MS4A1 (CD20) which displays restricted expression on the surface of B-lymphocytes and forms the immunotherapeutic target of Rituximab. Given the importance of MS4A1 as an immunotherapeutic target our goal was to search for additional members of the MS4A family that may form potential immunotherapeutic targets. Here, I describe the evaluation of I) MS4A8B and MS4A4A expression in select hematopoietic cell subsets, using monoclonal antibodies that were generated against extracellular epitopes, and II) the investigation of whether monoclonal antibodies directed against MS4A4A can induce Fc-receptor independent effects characteristic of immunotherapeutic antibodies such as cellular apoptosis. We found that MS4A8B is not expressed in any of the hematopoietic cell subsets evaluated but is present in the NCI-H69 small cell lung carcinoma cell line. However, we identified that MS4A4A is expressed in select hematopoietic cell subsets. Specifically, herein I report that MS4A4A is expressed in peripheral blood monocytes and monocyte derived M2 macrophages but not resting peripheral blood granulocytes, lymphocytes, or M1 macrophages. I also report that monoclonal antibodies directed against MS4A4A were not capable of inducing cellular apoptosis or influencing select cellular functions in the cells evaluated.

Acknowledgements

Throughout my master's degree I have had the privilege to learn and benefit from the expertise of others. I would like to thank my supervisor, Dr. Julie Deans, for providing me the opportunity to take part in a challenging and meaningful project, her continuous support, and scientific guidance. I would also like to thank Maria Polyak and Ratna Sanyal for providing a stimulating and friendly lab environment, their expertise, and support. I would also like to acknowledge Ratna Sanyal for the generation of data displayed in Figures 3.2, 3.4 and 4.1 and Maria Polyak for the generation of data displayed in Figures 3.1B, 3.8, 4.1B, 4.3 and 4.4. Special thanks to my committee members, Dr. Stephen Robbins and Dr. Frank Jirik for their helpful discussions and to my external examiner Dr. Donald Morris. I would also like to thank Evelyn Lailey for helping me obtain primary blood samples and additional members of Dr. Kamala Patel's lab. A thank you also goes to members of Dr. Dan Muruve, Dr. Christopher Mody's, as well as Dr. May Ho's lab, who provided reagents and everyone else who helped make this thesis possible. Finally, I would like to thank my family for their support and motivation.

Table of Contents

List of Tables

List of Figures

Abbreviations and Symbols

Symbols

α	Alpha
β	Beta
γ	Gamma
ε	Epsilon
μ	Mu

Abbreviations

CD	Cluster of differentiation
C_H	Constant heavy chain
C_L	Constant light chain
D1	Domain proximal
D2	Domain distal
DC	Dendritic cells
Fc	Fragment crystallisable
FcR	Fc receptor
FcαR	Fc receptor alpha
FcεR	Fc receptor epsilon
FcγR	Fc receptor gamma
FcRn	Fc receptor neonatal
GM-CSF	Granulocyte macrophage colony stimulating factor
HAT	Hypoxanthine-aminopterin-thymidine
Her-2	Human epidermal growth factor receptor 2
Ig	Immunoglobulin
IL	Interleukin
INFγ	Interferon gamma
iNOS	Inducible nitric oxide
LPS	Lipopolysaccharide
M-CSF	Macrophage colony stimulating factor
MHC II	Major histocompatibility complex
MS4A	Membrane spanning 4A
NK	Natural killer cells
PAMP	Pathogen associated molecular pattern
TAM	Tumor associated macrophages
TLR	Tol-like receptor
Th1	T-helper cell type I
Th2	T-helper cell type II
TNFα	Tumor necrosis factor alpha
V_H	Variable heavy chain
V_L	Variable light chain

Chapter I
Introduction

A. Antibodies

Antibodies are immunoglobulin molecules that are important mediators of the innate and adaptive immune response. They are produced by B-cells and when secreted help identify and target foreign as well as particulate matter. By doing so they are able to opsonize, neutralize, and target foreign material for phagocytosis. These abilities are attributed to various defining characteristics such as their exceptional ligand specificity, ability to induce cytotoxic responses, and relative stability. Consequently, antibodies form an essential component of the innate and adaptive immune response (Murphy K., 2008).

Antibodies can be classified as members of one of five immunoglobulin classes, IgG, IgM, IgA, IgE, and IgD. Crystallography and biochemical studies indicate that antibodies adopt a "Y" shaped morphology and consist of four polypeptide chains (Figure 1.1). These include two identical heavy chains (H) and two identical light chains (L). Each chain consists of a series of immunoglobulin domains. The number of immunoglobulin domains in the light chain remains consistent between immunoglobulin classes but the number of immunoglobulin domains in the heavy chain varies. For instance, the heavy chain of human IgM and IgE contains five immunoglobulin domains while human IgG contains four. In IgG, these include a single variable domain, V_H, and three constant domains: C_{H1}, C_{H2} and C_{H3}. In contrast, each light chain consists of two immunoglobulin domains: a single variable domain, V_L and a single constant domain, C_{L1}.

In an immunoglobulin molecule, the V_L and C_{L1} domains of a single light chain will associate with the N-terminal half of a single heavy chain (V_H, C_{H1}) and form one "arm" of the "Y" shaped antibody molecule. In a given immunoglobulin molecule the two "arms" are connected to one another by disulfide linkages (Murphy K, 2008; Schroeder & Cavacini, 2010). In IgG, IgA, and IgD the immunoglobulin molecule also contains a hinge region which helps provide flexibility to the arms of the immunoglobulin molecule and also contains disulfide linkages (Schroeder & Cavacini, 2010). In contrast, the "trunk" of the antibody is formed by the pairing of the carboxyl terminal halves of the two heavy chains. The variable domains of the immunoglobulin molecule are located at the N-terminal region of each antibody "arm" and confer to it the ability to bind a specific antigen. The constant domains form the remainder of the antibody and do not show considerable variability within an antibody class. However the constant domains display considerable diversity between immunoglobulin classes (IgA, IgM, IgE, IgD, and IgG). This portion of the antibody binds a family of receptors known as Fc receptors. (Murphy K, 2008; Schroeder & Cavacini, 2010).

B. The Family of Fc Receptors

B.1. Fc Receptor Classes

The Fc receptors are a family of cell surface membrane proteins that recognize and bind the Fc region of an immunoglobulin molecule (Falk, 2007; Murphy K, 2008; Schroeder & Cavacini, 2010). Fc receptors have been categorized into three distinct classes, Fcε, Fcα, and the Fcγ. Each class is characterized by the ability of its members to

preferentially bind a specific class of immunoglobulin molecules (IgA, IgE, or IgG). For instance, the Fcε class of Fc receptors binds IgE and the Fcα class of Fc receptors bind IgA and IgM. The Fcε class of receptors consists of two members, the FcεRI and FcεRII (Schroeder & Cavacini, 2010). The Fcα family of receptors also consists of two members, FcαRI and Fcα/μR (Murphy K, 2008; Schroeder & Cavacini, 2010) . The Fcγ class of receptors binds the most abundant serum immunoglobulin class, IgG, and is characterized by six family members: FcγRI (CD64), FcγRIIA (CD32A), FcγRIIB (CD32B), FcγRIIC (CD32C), FcγRIIIA (CD16A), and the FcγRIIIB (CD16B). All of these Fcγ receptors are involved in cellular activation with the exception of the FcγRIIb which inhibits cellular activation (Falk, 2007; Gillis, Gouel-Cheron, Jonsson, & Bruhns, 2014). The FcγRII and FcγRIII family members exist in multiple isoforms due to gene polymorphisms and display different patterns of expression and different affinities for IgG subclasses (IgG1, IgG2, IgG3, and IgG4) (Gillis et al., 2014). Many Fc receptors exist as a multi-subunit complex. Here, they contain a ligand binding α chain that is required for the recognition and binding to the immunoglobulin Fc region and may also contain a γ subunit that mediates signal transduction. Some Fc receptor complexes, such as the FcεRI, also contain a β subunit, which in this case is implicated in receptor stability and signal transduction (Gillis et al., 2014; Murphy K, 2008). As will be discussed later, the β subunit of the FcεRI is a member of the MS4A family of membrane proteins. To date, crystal structures and atomic level data are available for select Fc receptors (FcγRI, FcγRIIa, FcγRIIb, FcγRIIIb, FcεRI, and FcαRI).

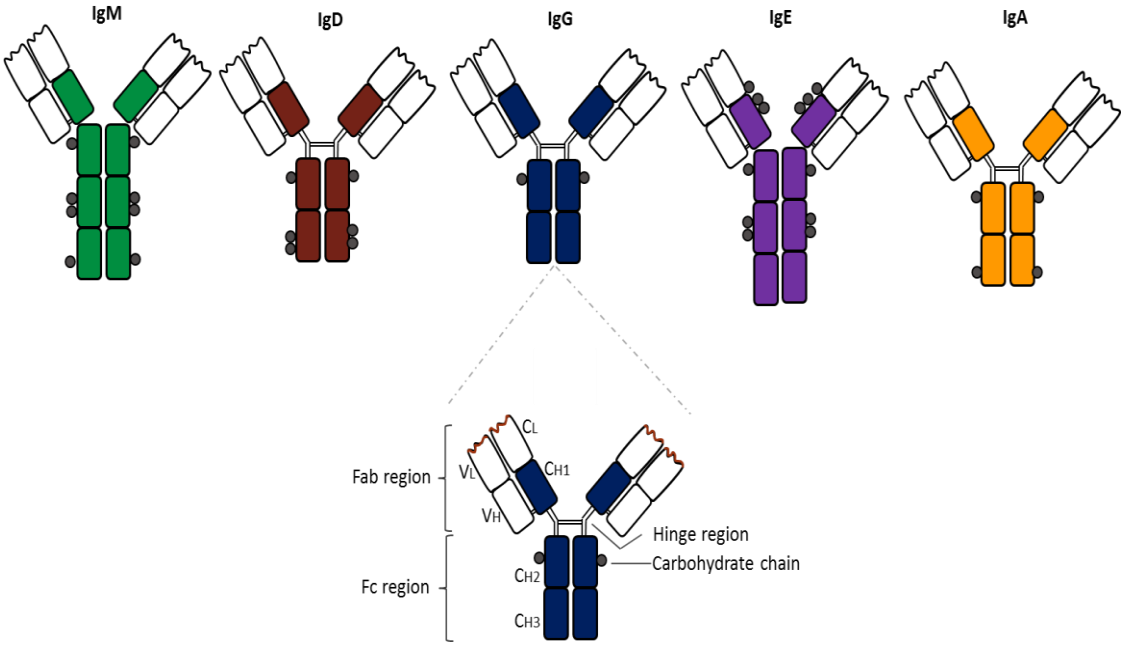

Figure 1.1. Human Immunoglobulin Classes and the Structure of IgG. There are five human immunoglobulin classes: IgM, IgD, IgG, IgE, and IgA. Each immunoglobulin class forms a "Y" shaped molecule and contains two identical heavy and two identical light chains that consist of a series of immunoglobulin domains. The heavy chains of IgM and IgE contain four immunoglobulin domains (C_{H1}, C_{H2}, C_{H3}, and C_{H4}) and the antibodies are not characterized by a flexible hinge region. In contrast, the heavy chains of IgD, IgA and IgG all contain three immunoglobulin domains (C_{H1}, C_{H2}, and C_{H3}) and are characterized by a flexible hinge region. In each immunoglobulin class the N- terminal regions of the heavy and light chain associate so as to form a Fab region, which contains antigen binding capability, while the remaining portion of the heavy chains associate to form the Fc region.

In most cases, the extracellular regions of the Fc receptor ligand binding α chain consists of two immunoglobulin domains that are known as D1 (membrane distal) and D2 (membrane proximal). Due to the orientation of the D1 and D2 domains at acute angles and the presence of beta-sheets, the extracellular regions of the Fc receptor α chains are commonly described as heart-shaped (Woof & Burton, 2004). A notable exception is the high affinity FcγRI, in which the ligand binding α chain contains three immunoglobulin domains (D1, D2, and D3) and forms a hook-like structure (Lu, Ellsworth, Hamacher, Oak, & Sun, 2011).

B.2. Fc Receptor Expression and Ligand Affinity

Many of the human Fc receptors display different patterns of cellular expression and different binding affinities for their immunoglobulin classes and subclasses (Table 1.1) (Falk, 2007; Gillis et al., 2014; Murphy K, 2008). For instance, within the Fcε class of Fc receptors, the FcεRI is expressed in mast cells, eosinophils, and basophils and binds human IgE with high affinity. In contrast, within the Fcα class of Fc receptors, the FcαRI binds IgA with low affinity and is expressed in macrophages, eosinophils, mast cells, and neutrophils (Murphy K, 2008). The Fcγ class of receptors contains six members which all bind IgG. Most of the members of the Fcγ class of Fc receptors can only bind IgG immune complexes and show no detectable affinity for monomeric IgG. The FcγRI is unique in its ability to bind IgG monomerically and with high affinity (Falk, 2007; Murphy K, 2008).

Table 1.1 Human Fc receptor expression and ligand affinity

Fc Receptors	Expression	Immunoglobulin Affinity
FcγRI (CD64)	Activated neutrophils monocytes, macrophages, and DC	1) IgG1 = IgG3 2) IgG4 3) IgG2
FcγRIIA (CD32A)	All myeloid cells, no expression in lymphocytes	1) IgG1 2) IgG3 = IgG2 3) IgG4
FcγRIIB (CD32B)	B cells, basophils DC, macrophages, monocytes, and neutrophils	1) IgG1 = IgG3 2) IgG4 3) IgG2
FcγRIIC (CD32C)	NK cells, neutrophils, and monocytes	1) IgG1 = IgG3 2) IgG4 3) IgG2
FcγRIIIA (CD16A)	Macrophages, monocytes, and NK cells	1) IgG1 = IgG3
FcγRIIIB (CD16B)	Neutrophils and basophils	1) IgG1 = IgG3
FcεRI	Activated eosinophils, basophils, and mast cells	1) IgE
FcεRII	Activated Eosinophils basophils, B-cells, NK cells, and mast cells	1) IgE
FcαRI	Eosinophils, mast cells, macrophages, and neutrophils	1) IgA1 = IgA2
Fcα/μR	B cells and macrophages	1) IgM 2) IgA

This ability is conserved in the mouse homolog of the human FcγRI (Falk, 2007; Mancardi et al., 2013). The FcγRI exists as a multimeric complex with a ligand binding α chain and two associated γ subunits. In humans, the FcγRI is expressed on the surface of monocytes, macrophages, and dendritic cells (DC). It also displays inducible expression in neutrophils (Murphy K, 2008; van der Poel, Spaapen, van de Winkel, & Leusen, 2011). In the mouse, the FcγRI is expressed in macrophages and dendritic cells but is not expressed in either monocytes or activated neutrophils (van der Poel et al., 2011). The human FcγRI preferentially binds to the human IgG1 and IgG3 subclass. The murine homolog preferentially binds mouse IgG2a and IgG2b. In the murine system IgG2a and IgG2b are also the chief immunoglobulin based mediators of the inflammatory response while in humans this is restricted to the IgG1 and IgG3 immunoglobulin subclass (Falk, 2007). The human FcγRI shares considerable sequence similarity with its mouse homolog and also binds with high affinity to mouse IgG2a and IgG2b but not mouse IgG1 (Mancardi et al., 2013). None of the remaining human Fcγ receptors is capable of binding monomeric mouse IgG1, IgG2a, or IgG2b (Gillis et al., 2014).

B.3. Antibody-Fc Receptor Mediated Interactions and their Immunological Importance

Human Fc receptors recognize and bind the Fc portion of an antibody. By doing so immune cells are able to identify antibody-antigen immune complexes and initiate the appropriate effector response (Murphy K., 2008). The precise effector function varies with respect to the cell type and as illustrated in Figure 1.2, these include a number of immune functions such as the initiation of phagocytosis, antibody dependent

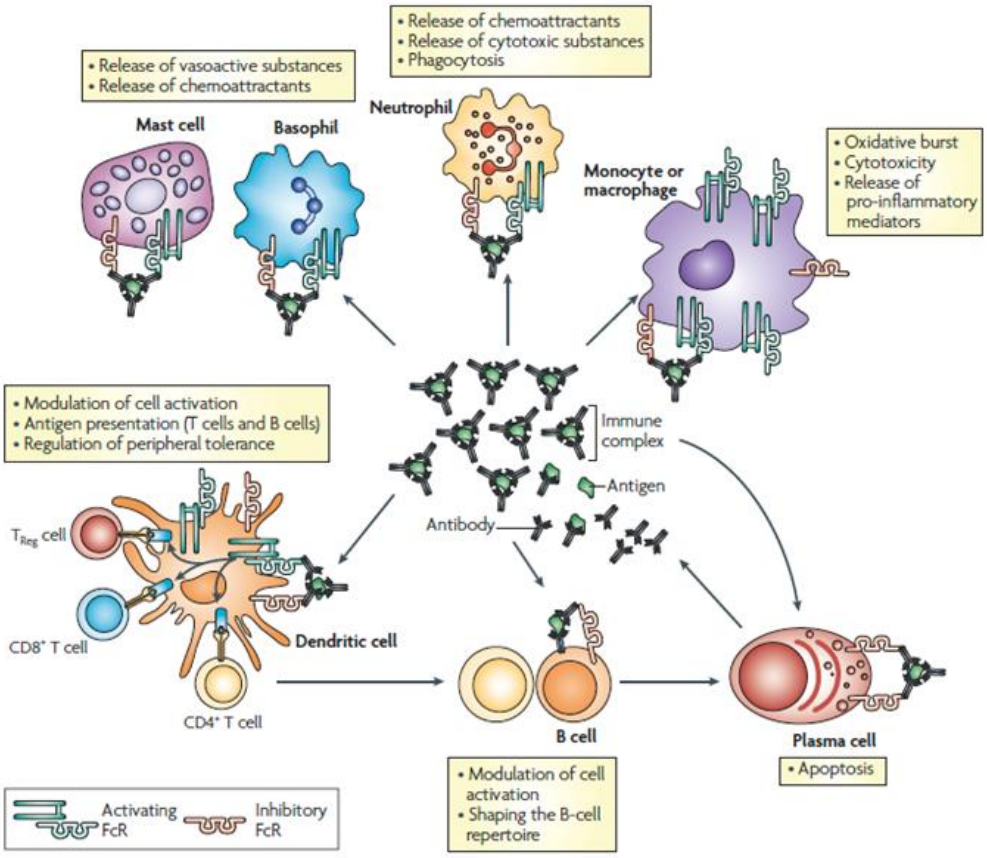

Figure 1.2. Fc receptors as regulators of the immune response. Immune complexes bind the Fc receptors of innate and adaptive immune effector cells. Upon Fc-immune complex binding, immune cells initiate the indicated effector functions. The ability of Fc receptors to trigger a variety of effector functions make them potent regulators of immunity. Adapted by permission from Macmillan Publisher Ltd: [Nature Reviews Immunology] (Nimmerjahn & Ravetch, 2008), copyright (2008).

cytotoxicity (ADCC), as well as the release of pro-inflammatory mediators, chemoattractants, and cytotoxic molecules (Falk, 2007). The aforementioned roles are regulated by activating Fc receptors and are relevant to cells of the early immune response such as neutrophils, monocytes, macrophages, and dendritic cells. The inhibitory Fc receptor, FcγRIIb, down-modulates the activity of cells in the adaptive immune system, namely B-lymphocytes and plasma cells. Collectively, Fc receptors and antibodies interact specifically to regulate the effector functions and activity of cells within the innate and adaptive immune systems (Falk, 2007; Murphy K, 2008). This ability is reflected in their diverse expression within hematopoietic but not non-hematopoietic cell subsets. However, there is an important exception. The Fc receptor neonatal (FcRn) is expressed within hematopoietic and non-hematopoietic cells and does not regulate immune effector functions. Rather the FcRn is expressed on the surface of monocytes and macrophages as well as on the surface of epithelial cells comprising the vasculature, gut, and kidney where it is responsible for binding and recycling human IgG (Roopenian & Akilesh, 2007). Collectively, the ability of Fc receptors to regulate immune responses and recycle immunoglobulin molecules depends upon immunoglobulin-Fc receptor interactions. The crystallography analyses of human FcγR and IgG receptor-ligand interactions indicate that various amino acid residues in the Fc region of IgG molecules bind to the D2 domain (membrane proximal) of the Fc receptor α chain at a 1:1 ratio (Woof & Burton, 2004). In contrast the FcRn consists of an MHC class I like heavy chain and an associated β_2-microglobulin light chain which collectively

bind human IgG at the CH2-CH3 hinge region with a 2:1 receptor to ligand ratio (Roopenian & Akilesh, 2007).

Human Fc receptors display different patterns of expression within the various hematopoietic cell types (Table 1.1). In this thesis we will focus on characterizing the expression of two cell surface proteins which span the plasma membrane four times in hematopoietic cell subsets. Here, particular emphasis will be applied to evaluating their expression in human monocytes and their subsets as well as human macrophages and their subsets. Consequently, herein, a literature review of monocytes and macrophage subsets is provided.

B.3.1 Monocytes and Macrophages

B.3.1.1 Monocytes and their Subsets

Monocytes and macrophages are mononuclear phagocytic cells. However their functional roles and importance in innate as well as adaptive immunity extend beyond phagocytosis. Monocytes, macrophages, and their various subsets, are found in most tissues of the human body and originate in the bone marrow from hematopoietic stem cell derived progenitor cells (Murphy K, 2008; Murray & Wynn, 2011).

In the bone marrow, hematopoietic stem cells differentiate to myeloid progenitor cells, continue with differentiation to monoblasts and pro-monoblasts and end with their differentiation to monocytes, which are released into the blood for circulation. Previously, monocytes were believed to form a homogenous population, however, circulating monocytes can actually be classified into three distinct populations

that may demonstrate considerable heterogeneity with respect to function, phenotype, and turnover (Grage-Griebenow, Flad, & Ernst, 2001; Jaipersad, Lip, Silverman, & Shantsila, 2014; Tallone et al., 2011). Specifically, they can be classified as either classical, alternative or intermediate monocytes based upon the expression of human CD14 and CD16 as well as additional cell surface markers (Grage-Griebenow et al., 2001; Tallone et al., 2011). Classical monocytes comprise 90-95% of circulating monocytes and are $CD14^{high}$ and $CD16^{low}$. Classical monocytes also express Toll-like receptors (TLRs) as well as scavenger receptors, allowing them to recognize and phagocytose pathogens and dying cells. The intermediate population is characterized as both $CD14^{high}$ and $CD16^{high}$ and displays pro-inflammatory functions. Specifically, intermediate monocytes have limited phagocytic activity but have a greater capacity to produce pro-inflammatory cytokines such as Il-1β and TNFα in response to LPS and other pathogen associated molecular patterns (PAMPs). Finally, non-classical (alternative) monocytes are characterized as $CD14^{low}$ and $CD16^{high}$ and are involved in patrolling functions around vessel walls (Grage-Griebenow et al., 2001; Tallone et al., 2011). In the mouse system, non-classical (alternative) monocytes are characterized as anti-inflammatory, however in humans, non-classical monocytes are involved in the release of cytokines such as IL-1β and TNFα in response to DNA and RNA particles, implicating them in pro-inflammatory functions and auto-immune disorders (Grage-Griebenow et al., 2001; Jaipersad et al., 2014; Tallone et al., 2011).

B.3.1.2 Macrophages and their Subsets

Though monocytes form a heterogeneous population, an important function among them is their ability to differentiate into macrophages (Grage-Griebenow et al., 2001; Jaipersad et al., 2014; Tallone et al., 2011). When monocytes are released into the circulatory system, they circulate for several minutes to days before entering the surrounding tissue (Jaipersad et al., 2014). Depending upon the cytokine milieu and environmental signals present, monocytes can differentiate into tissue resident, pro-inflammatory (M1) or anti-inflammatory (M2) macrophages (Mantovani et al., 2004; Murray & Wynn, 2011; Verreck, de Boer, Langenberg, van der Zanden, & Ottenhoff, 2006). Tissue resident macrophages perform specialized functions depending upon their anatomical location. For instance, Kupffer cells, which line the liver sinusoids, are involved in the clearance of blood-borne pathogens, toxins and red-blood cell turnover in the spleen; alveolar macrophages in the lung are responsible for the removal of particulate matter and clearance of air-borne pathogen and; osteoclasts in the bone are responsible for the turn-over of bone tissue (Murphy K, 2008).

Monocytes can differentiate to M1 and M2 macrophages (Mantovani et al., 2004; Murray & Wynn, 2011; Verreck et al., 2006). These subsets perform specialized functions and are instrumental to the immune response and tissue recovery. M1 macrophages are categorized as pro-inflammatory and are predominately involved in the phagocytosis and removal of pathogens, recruitment of immune effector cells, and propagation of the inflammatory response. M1 macrophages have also been shown to

be associated with tissue damage. In contrast M2 macrophages have been traditionally categorized as anti-inflammatory and are involved in subduing the inflammatory response, tissue repair, matrix remodeling and parasite clearance (Mantovani et al., 2004; Murray & Wynn, 2011).

Macrophages can be classified as members of either the M1 or M2 subsets based upon cell-surface protein expression and cytokine production. M1 macrophages synthesize and release elevated levels of the pro-inflammatory cytokines IL-12, IL-23, TNFα, and limited amounts of IL-10. They also produce elevated levels of nitric oxide and reactive oxygen species. Many of these agents contribute to the increased cytotoxic capabilities of M1 macrophages (Mantovani et al., 2004; Murray & Wynn, 2011). Additionally, M1 macrophages express, up-regulate, or lose the expression of a variety of cell surface markers. These include the up-regulation of CD80, MHC II, CD32, and the absence of CD206 and CD14 (Rey-Giraud, Hafner, & Ries, 2012). Finally, M1 macrophages arise from stimulation with Th1 cytokines such as INFγ, in the presence of granulocyte macrophage colony stimulating factor (GM-CSF) and microbial signals such as lipopolysaccharide (LPS). In contrast M2 macrophages arise from stimulation with Th2 cytokines such as IL-4 and IL-13 in the presence of macrophage colony stimulating factor (M-CSF). Similar to the M1 subset, M2 macrophages can also be classified based upon their expression of cell surface markers and cytokine production profile. With respect to cytokine production, M2 macrophages synthesize and release elevated levels of anti-inflammatory cytokines such as IL-10 but low levels of IL-23. The M2 macrophage

subset also expresses, CD14, CD206 (the mannose receptor) and the scavenger receptor on its cell surface (Mantovani et al., 2004; Murray & Wynn, 2011;. However, it lacks CD80 expression and expresses CD32 at levels greater than M1 macrophages (Rey-Giraud et al., 2012). Although the different cytokine profiles and cell surface markers in M1 and M2 macrophages are important for their classification, they also help define the role of the macrophage subsets in the immune response. For instance M2 macrophages produce elevated levels of IL-10, which can promote the production of IL-4 and IL-13 by Th2 cells. Therefore M2 macrophages are implicated in wound healing, since IL-4 activates arginase synthesis, which is important for the production of the extra-cellular matrix and consequently tissue remodeling (Mantovani et al., 2004).

In the mouse system, macrophages can be clearly classified as M1 or M2 based upon differential metabolism of L-arginine. Specifically, M2 macrophages synthesize arginase I, which metabolizes arginine to ornithine and polyamines. M1 macrophages however increase the production of inducible nitric oxide synthase (iNOS), which breaks down arginine to citrulline and nitric oxide. Consequently, mouse M2 macrophages are classified as arginase I^{high} and $iNOS^{low}$ while the converse is true for mouse M1 macrophages (Mantovani et al., 2004; Murray & Wynn, 2011).

C. Immunotherapeutic Antibodies

C.1. The History of Immunotherapy

With advances in molecular biology as well as the identification of tumor specific proteins and survival factors, the concept of targeted therapy for cancer received considerable attention. The concept was first limited to the use of low weight molecular inhibitors, which when given orally are capable of targeting cell specific proteins through membrane diffusion (Sliwkowski & Mellman, 2013). The concept of targeted therapy was later extended to use of anti-tumor antibodies but until relatively recently eluded successful implementation. This was likely due to limitations in antibody humanization and the use of immunoglobulins against antigens not sufficiently restricted to tumor cells. However, within the last two decades, immunoglobulin based therapies have emerged as effective modulators of disease (Sliwkowski & Mellman, 2013). Their utility has been attributed to their antigen specificity and their ability to initiate one or more of many effector functions in order to deplete target cells: antibody dependent cytotoxicity, complement dependent killing, phagocytosis, and direct killing (Figure 1.3) (Clynes, Towers, Presta, & Ravetch, 2000; Sliwkowski & Mellman, 2013; Teicher, 2009). Currently there are more than 14 FDA approved antibodies for the detection and treatment of various cancers and many more for the treatment of other disorders. As shown in Table 1.2, among them are antibodies which can directly target tumor cells and induce their depletion (Rituximab, Ofatumumab, Centuximab, and I^{131}-tositumomab). Many of these antibodies vary in their method of cellular depletion. For

instance, Rituximab, Ofatumumab, and I^{131} – tositumomab are all capable of depleting CD20+ B cells by the induction of Fc mediated effector functions such as CDC and ADCC. However, unlike Rituximab and Ofatumumab, I^{131} – tositumomab mediated CD20+ B cell depletion is also attributed to its ability to be readily internalized and transport a cytotoxic agent (Carter, 2006). In addition, not all monoclonal antibodies function by inducing CDC or ADCC. Monoclonal antibodies can also be used to target soluble factors present in the tumor microenvironment so as to limit their availability.

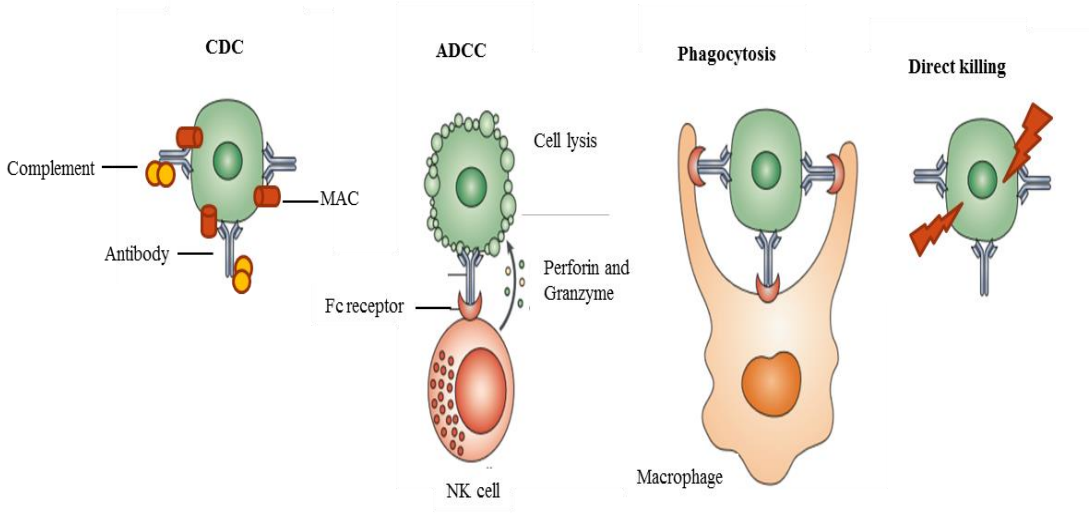

Figure 1.3. Mechanisms of antibody mediated cellular depletion

Immunotherapeutic antibodies are capable of depleting target cells by a variety of mechanisms. They can interact with NK cells so as to induce ADCC via the release of perforin and Granzyme B, they can interact with complement proteins in order to induce CDC via the formation of the membrane attack complex (MAC) or they can induce macrophages to phagocytose the target cells. In addition, antibodies can also deplete target cells by directly inducing cellular apoptosis. Adapted by permission from Macmillan Publisher Ltd: [Nature Reviews Immunology] (Weiner, et al, 2010), copyright 2010.

Table 1.2. Immunotherapeutic antibodies

Antibody Name	Antibody Format	Target	Mechanism of Action	Approved Indications
Rituximab	Chimeric IgG1	CD20	Sensitization to chemotherapy, ADCC, CDC, phagocytosis, and induction of apoptosis	Non-Hodgkin's lymphoma, rheumatoid arthritis, and multiple sclerosis
Ofatumumab	Human IgG1	CD20	Sensitization to chemotherapy, ADCC, CDC and induction of apoptosis	Non-Hodgkin's lymphoma, rheumatoid arthritis, and multiple sclerosis
I^{131}-tositumomab	Mouse IgG2a	CD20	I^{131} induced cytotoxicity, ADCC, CDC and induction of apoptosis	Non-Hodgkin's lymphoma
Bevacizumab	Humanized IgG1	VEGF	Binding of soluble VEGF and inhibition of angiogenesis	Colorectal, breast and lung cancer
Infliximab	Chimeric IgG1	TNFα	Binding of soluble TNFα	Rheumatoid arthritis, Chron's Disease, and ulcerative colitis
Cetuximab	Chimeric IgG1	EGFR	Inhibition of receptor activation, CDC, ADCC, induction of apoptosis, inhibition of cellular proliferation, angiogenesis and sensitization to chemotherapy	Head and neck cancer and metastatic colorectal cancer
Trasutzumab	Humanized IgG1	HER2	Inhibition of receptor activation, CDC, ADCC, and inhibition of cellular proliferation	HER2+ breast cancer
Ipilimumab	Humanized IgG1	CTLA4	Prevents CTLA4 interaction with CD80 or CD86	Unrespectable and metastatic melanoma

For example, vascular endothelial growth factor (VEGF) is a key regulator of angiogenesis released by tumor cells in order to facilitate their growth and metastasis (Carter, 2006; Weiner, Surana, & Wang, 2010). Bevacizumab, is a monoclonal antibody that is capable of binding and depleting VEGF, therefore preventing angiogenesis within the tumor microenvironment (Carter, 2006; Weiner et al., 2010). Recently, there has also been considerable interest in monoclonal antibodies that are capable of modulating the immune response. Among these is Ipilimumab, which was recently approved for the treatment of metastatic and unresectable melanoma (Sliwkowski & Mellman, 2013). Ipilimumab is capable of binding to cytotoxic T-lymphocyte associated protein 4 (CTLA4). CTLA4 is a glycoprotein which is expressed on the surface of regulatory T-cells. When bound by CD80 or CD86, CTLA4 signals for T-cell anergy and the release of immunosuppressive cytokines such as IL-10 and transforming growth factor β, which inactivate the cytotoxic activity of surrounding immune effector cells such as macrophages. The binding of Ipilimumab to CTLA4 prevents its interaction with CD80 and therefore T-regulatory cell deactivation. Clinical studies have shown that by modulating the immune response, Ipilimumab can provide long term benefits or cure patients with metastatic melanoma who have no other available treatment options (Sliwkowski & Mellman, 2013). As shown in Table 1.2, it is clear immunotherapeutic antibodies are important clinical tools. In the next section, immunotherapeutics which target HER2 and CD20 are discussed in detail so as to further demonstrate how immunoglobulins can function as therapeutic tools for modulating disease.

C.2. HER2 Targeting Antibodies—Inhibition of Cellular Proliferation and Antibody Drug Conjugates

Human epidermal growth factor receptor 2 has been an important immunotherapeutic target for breast cancer. Currently, the FDA has approved three monoclonal antibodies for the treatment of Her-2 positive breast cancer: Ado-trastuzumab, Pertuzumab, and Trastuzumab (Sliwkowski & Mellman, 2013). Trastuzumab and Pertuzumab are especially interesting considering that binding of the antibody to Her-2 positive breast cancer cells directly inhibits cellular proliferation and signaling activity (Lewis et al., 1993). By blocking signaling and cellular proliferation it has been proposed that such antibodies may also affect cellular differentiation. Though there is considerable debate as to their ability to induce antibody dependent cytotoxicity, their favorable tolerability profiles allow Trastuzumab and Pertuzumab to be used in conjunction with conventional chemotherapy (Baselga et al., 2012).

Antibody drug conjugation has also been proposed to be a possible method of targeting and depleting Her-2 positive breast cancer cells. Until recently, antibody drug conjugation has eluded successful implementation due to inadequate linker chemistry. The linker is required to attach a cytotoxic compound to a tumor-restricted antibody. If the linker is highly stable it will lead to proteolytic digestion of the antibody drug conjugate and if too labile it will result in premature toxin release (Sliwkowski & Mellman, 2013; Teicher, 2009). However, recent advances have allowed for the development of Her-2 antibody drug conjugates such as T-DM1, which is conjugated to

a maytanisine derivative (DM1) (Lewis Phillips et al., 2008). Other such immunotherapeutics include Brentuximab Vedotin, an anti-CD30 antibody conjugated to monomethyl auristatin E (MMAE), which like DM1 is a microtubule antagonist (Okeley et al., 2010). When internalized, the linkers attaching the MMAE or DM1 toxins to the immunoglobulin molecules are degraded via the lysosomal pathway. MMAE or DM1 subsequently diffuse into the cytoplasm where they induce their cytotoxic effects (Sliwkowski & Mellman, 2013; Teicher, 2009).

C.3. Rituxumab and Ofatumumab

Rituximab is a monoclonal IgG1 chimeric antibody (Cragg, 2005). It contains murine variable sequences directed against CD20 and a human IgG1 backbone. Since the approval of Rituximab in 1997, it has been successfully used for the treatment of patients with non-Hodgkin`s lymphoma, chronic lymphocytic leukemia, and autoimmune disorders such as multiple sclerosis and rheumatoid arthritis (Cragg, 2005; Robak & Robak, 2011). The ability of Rituximab to function as an immunotherapeutic has been attributed to its capability to induce several Fc mediated and non-Fc mediated cellular effects. These include: I) antibody-dependent cytotoxicity, which is mediated by the release of toxic granules containing perforin and granzyme B by natural killer cells and the activity of macrophages or II) complement dependent killing, which is mediated by the complement cascade and eventual lysis of CD20+ cells, or III) cellular apoptosis (Robak & Robak, 2011; Taylor & Lindorfer, 2008). Among these, complement dependent killing and antibody mediated cytotoxicity are believed to be the principal mediators of

CD20+ B-cell depletion (Robak & Robak, 2011). In addition, it has also been demonstrated that Rituximab opsonized cells can be depleted by macrophages via phagocytosis (Lefebvre, Krause, Salcedo, & Nardin, 2006). Recently, Ofatumumab, anti-CD20 human IgG1 antibody, was approved for the treatment of B-cell lymphomas and autoimmune disorders such as rheumatoid arthritis and multiple sclerosis (Coiffier et al., 2008). Ofatumumab binds an epitope at the extracellular region of CD20 which is distinct from that recognized by Rituximab (Cragg, 2005; Robak & Robak, 2011; Teeling et al., 2006). Like Rituximab, Ofatumumab has favorable tolerability profiles (Coiffier et al., 2008). However, Ofatumumab has the ability to initiate complement dependent killing of CD20+ cells at levels that are considerably greater the Rituximab (Reff et al., 1994; Teeling et al., 2004). This may explain why patients who were refractory to Rituximab immunotherapy have been shown to respond positively to Ofatumumab treatment (Coiffier et al., 2008).

C.4. Immunotherapeutic Limitations and Antibody Engineering

Long before the development of the first therapeutic antibodies, there had been considerable doubt about their ability to be used safely as immunotherapeutics. Among the most important limitations were those that suggested that since most anti-human antibodies are produced in mice they would provoke an immune response in humans. However, with the discovery that complementarity-determining or variable regions from mouse antibodies could be grafted onto human IgG, the murine antibodies could be “humanized” (Sliwkowski and Mellman 2013).

Humanization processes have now become more advanced and antibodies are being further modified through immunoglobulin engineering to overcome their various limitations. For one, mutations to the Fc domain and glycosylation patterns are being tested to enhance or reduce immunoglobulin interactions with the FcRn. The FcRn is responsible for returning IgG antibodies to circulation. Consequently, modifying FcRn-immunoglobulin interactions can impact the pharmacokinetic properties of an antibody (Olafsen, 2012). This can prove important in the case of immunoglobulin-antibody drug conjugates, where potential cytotoxicity of the antibody may be mitigated by increased clearance rates. Fc domains are also being modified to enhance complement dependent cytotoxicity. Current developments also extend outside of Fc domain modification. They include the development of bispecific and "one-armed" antibodies that can avoid crosslinking (Jin et al., 2008). Multi-armed antibodies are also in development and genetically fused immunoglobulins with mediators such as cytokines, hormones, and toxins are becoming promising immunotherapeutic candidates, as evidenced by their recent surge in clinical trials (Teicher, 2009). Nonetheless, an important stimulus for the development and modification of immunotherapeutics has been Rituximab. Rituximab, which has been characterized as the most effective immunoglobulin based anti-cancer therapy, demonstrated that immunoglobulin molecules can be successfully and economically used to target disease. Rituximab targets CD20, a plasma membrane protein that belongs to the MS4A family (Cragg, 2005).

D. The MS4A Family of Proteins and the MS4A Family Members

D.1. Overview

MS4A is defined as the membrane spanning 4A family of proteins. The members of the MS4A family are characterized by four transmembrane domains (tetraspanning) that extend across the membrane with two short connecting loops. The structure of the various human MS4A family members is shown in Figure 1.4. Based upon phylogenetic analysis, the MS4A family members first appeared in early vertebrates and then rapidly diversified. As a result homologs of some human MS4A genes are not found in the mouse and vice versa (J. Zuccolo et al., 2010). Currently, there are over 26 identified MS4A members, among which 15 are human (Figure 1.4): MS4A1-3, MS4A4A, MS4A4E, MS4A5, MS4A6A, MS4A6E, MS4A7, MS4A8B, MS4A10, MS4A12-15, and MS4A18 (Ishibashi, Suzuki, Sasaki, & Imai, 2001; Liang, Buckley, Tu, Langdon, & Tedder, 2001; J. Zuccolo et al., 2010). The various members are classified as part of the MS4A family based upon sequence identity with its founding member, MS4A1 (CD20). Sequence similarity between CD20 and the various MS4A family members falls between 20-30%, with the highest degree of similarity found among the first three transmembrane domains. For instance, though CD20 and MS4A8B share 25% overall sequence similarity, their first and second transmembrane domains are 46% identical. Mouse and human MS4A orthologs also share considerable amino acid identity (40-63%) (Liang & Tedder, 2001).

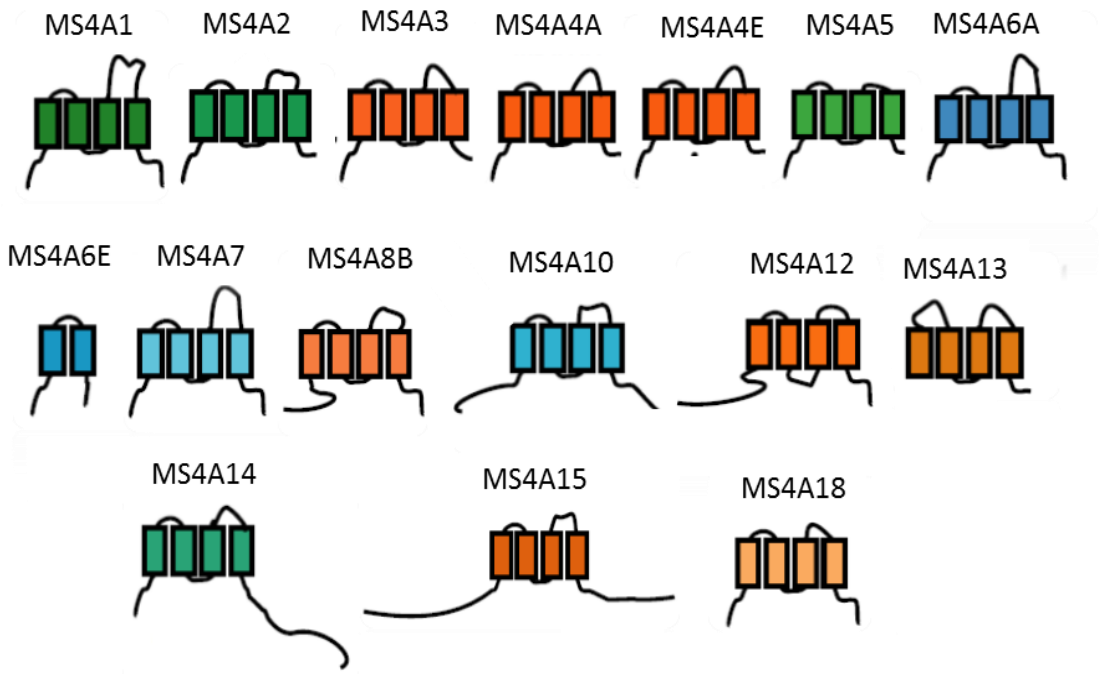

Figure 1.4. Human MS4A Family Members. There are 15 human MS4A family members, most of which are approximately 300 amino acids in length and characterized by four membrane spanning regions. Members of the MS4A family also contain two short connecting loops and N- and C- terminal regions. Members which deviate from the typical structure include: I) MS4A4E, which is characterized by only two transmembrane domains, II) MS4A13 which contains a truncated N- terminal region, III) MS4A14 which contains an elongated C-terminal region and IV) MS4A15 which is characterized by elongated N- and C-terminal region. Modified with permission from Jonathan Zuccolo.

However, it is important to note that the intracellular and extracellular domains are considerably divergent in both species and may contribute to differences in their functional roles. Most MS4A members are also 200 to 300 amino acids in length (Liang & Tedder, 2001) and characterized by three defining similarities: 1) two short extra-cellular loops 2) four transmembrane domains and 3) intracellular cytoplasmic N and C terminal regions (Ishibashi et al., 2001; Liang & Tedder, 2001).

Most of the MS4A family members are uncharacterized (Table 1.3), with their patterns of expression and functional roles unknown. Notable exceptions include MS4A1, MS4A2, and MS4A3. Therefore in the remainder of Chapter I, a literature review of the human MS4A1, MS4A2, and MS4A3 is provided. Since this thesis will focus on the characterization of MS4A4A and MS4A8B expression, a literature review of human MS4A4A, MS4A8B, and their mouse homologs is also provided.

D.2. MS4A1 (CD20)

D.2.1 MS4A1 Expression and Function

MS4A1 (CD20) is a plasma membrane protein that displays restricted protein expression in normal and malignant B-lymphocytes. Expression analysis indicates that MS4A1 maintains elevated expression in B-lymphocytes from the pre-B cell to the mature B-cell stages of development. However, MS4A1 is not expressed in pro-B cells or terminally differentiated plasma B-cells (Cragg, 2005).

Table 1.3. Expression and function of human MS4A family members

MS4A Members	Protein Expression	Function	References
MS4A1 (CD20)	All B-lymphocytes with the exception of pro-B cells and plasma B-cells	Mediation of B-cell receptor signaling extracellular calcium entry	Cragg, 2005; Li et al., 2004; Polyak et al., 2008; Deans, Li, &, Polyak, 2002.
MS4A2 (FcεRI β)	Eosinophils, basophils, and mast cells	Amplification of FcεRI and FcγRIII cell signaling.	David Dombrowicz 1988;Kuster, Zhang et al. 1992;Matsuda, Okayama et al. 2008
MS4A3 (HTm4)	Basophils, CD4- T-lymphocytes, and select epithelial cells	Regulation G1 to S phase cell cycle progression and cell differentiation	Kutok, Yang et al. 2011; Donato, et al. 2002
MS4A4	Unknown	Unknown	
MS4A4A	Unknown	Unknown	
MS4A5	Unknown	Unknown	
MS4A6A	Unknown	Unknown	
MS4A6E	Unknown	Unknown	
MS4A7	Unknown	Unknown	
MS4A8B	Small cell lung carcinoma	Unknown	Bangur et al., 2004
MS4A10	Unknown	Unknown	
MS4A12	Colonic epithelium	Modulation of extracellular calcium entry	Koslowski, Sahin et al. 2008
MS4A13	Unknown	Unknown	
MS4A14	Unknown	Unknown	
MS4A15	Unknown	Unknown	

MS4A1 is a cell surface protein which spans the plasma membrane four times (Liang & Tedder, 2001; Polyak, Tailor, & Deans, 1998). It has a molecular mass of approximately 33,000 and is 297 amino acids in length (Deans, Li, & Polyak, 2002). Structural and biochemical analysis indicates that MS4A1 exists as part of an oligomeric complex and associates with the B-cell receptor (Polyak, Li, Shariat, & Deans, 2008). MS4A1 is also constitutively associated with lipid rafts (Li et al., 2004).

Despite extensive study, the functional role of MS4A1 is not clearly known. *In vitro* studies suggest that MS4A1 may modulate B-cell development, activation, and differentiation (Clark & Shu, 1987; Golay, Clark, & Beverley, 1985). In addition, there is also evidence that MS4A1 is implicated in humoral immunity. Recently, Morsy and colleagues (2013) demonstrated that homozygous CD20 knock-out mice displayed a significantly reduced humoral response to T-cell dependent immunogens such as the adeno-associated virus (AAV). Here, they demonstrated that neutralizing antibodies developed by B-cells against AAV antigens were reduced significantly in CD20 knockout mice (Morsy et al., 2013). The data were consistent with a recent case report of reduced serum IgG levels, suggesting limited T-cell dependent immunity, in a child with a homozygous CD20 mutation that resulted in the absence of protein expression (Kuijpers et al., 2010). Evidence also suggests that MS4A1 is involved in B-cell receptor mediated calcium entry. Specifically, it is believed that MS4A1 may function as a store operated calcium channel that increases calcium conductance following ligation of the B-cell receptor with its antigen (Cragg, 2005). Interestingly, at least one other MS4A family

member has also been identified to function as a store operated calcium channel which has the ability to regulate calcium conductance (Koslowski, Sahin, Dhaene, Huber, & Tureci, 2008).

D.2.2 MS4A1 is the Immunotherapeutic Target of Rituximab

D.2.2.1 A history of MS4A1 as an Immunotherapeutic Target

Given the exceptional ligand specificity of antibody molecules and their capability to induce immune effector functions, the concept of immunotherapy has long received considerable attention (Sliwkowski & Mellman, 2013). However, it was not until the development of hybridoma technology in 1975 by Kohler and Milstein (Kohler & Milstein, 1975) that investigators could develop a monoclonal antibody against a given cell surface protein. Following the introduction of hybridoma technology, investigators began developing antibodies against various human cell surface proteins. Many of these antibodies were evaluated for their ability to deplete cancer cells, induce immune effector functions such as CDC or ADCC, or modulate disease (Nissim & Chernajovsky, 2008). Among the most successful antibodies were those that were developed against CD20. Anti-CD20 antibodies were capable of inducing CDC and lysing human B-lymphocyte cell lines in vitro (Kiesel et al., 1987). Subsequent studies demonstrated that infusion of anti-CD20 to macaque Cynomolgus monkeys successfully depleted 98% of peripheral blood B cells while small scale clinical trials with mouse anti-CD20 (Press et al., 1987) and large scale clinical trials with chimeric anti-CD20 (Maloney

et al., 1997) also indicated that anti-CD20 could be used to deplete B-lymphocytes and provide treatment for patients with non-Hodgkin's B cell lymphoma.

D.2.2.2 Features that Contribute to MS4A1 as an Immunotherapeutic Target

There are multiple features that have contributed to the effectiveness of CD20 as an immunotherapeutic target. First, CD20 displays highly restricted, stable, and elevated expression on the surface of normal and malignant B-lymphocytes. In addition CD20 is not readily shed from the surface of B-lymphocytes. Collectively, these features allow Rituximab and other anti-CD20 antibodies to reliably target malignant B-lymphocytes for depletion (Cragg, 2005). Finally, recent investigations indicate that the structure of CD20 is also believed to contribute to its effectiveness as an immunotherapeutic target. Specifically, the presence of the short transmembrane loops against which Rituximab binds presumably allows for more efficient engagement of Fc-mediated effector functions. It is also believed to influence the low rate of CD20-Rituximab internalization (Lim et al., 2010). The limited internalization of CD20 following Rituximab binding is essential to its role as an immunotherapeutic target since it allows for prolonged exposure of the immunoglobulin Fc domain to Fc targeting effector cells (Lim et al., 2010). The short extracellular loops which contribute to the effectiveness of CD20 as an immunotherapeutic target are found in all members of the MS4A family (Liang & Tedder, 2001), consequently, it is conceivable that those which also display restricted patterns of expression in hematopoietic cells may also form potential immunotherapeutic targets.

D.3 MS4A2 (FcεRI β)

The FcεRI is a high affinity Fc receptor for human IgE. It is a heterotrimeric receptor complex which consists of a single ligand binding α chain and associated γ and β chains (Kuster, Zhang, Brini, MacGlashan, & Kinet, 1992). The β chain of the FcεRI shares 20% amino acid identity with MS4A1 and is the second member of the MS4A family, MS4A2 (Liang & Tedder, 2001). Functional analysis indicates that MS4A2 enhances the cell surface expression of the FcεRI α chain and amplifies FcεRI mediated cellular signalling. MS4A2 is also expressed in the FcγRIII, which is a low affinity Fc receptor for human IgG (Dombrowicz et al, 1988). However, in both cases MS4A2 not essential for human FcεRI or FcγRIII cell surface expression. Gene profiling and protein analysis indicates MS4A2 only displays expressions alongside the FcεRI and FcγRIII in mast cells, basophils, and eosinophils (Kuster et al., 1992). Consequently, MS4A2 is similar to CD20 with respect to its restricted expression in hematopoietic cells. Its expression in mast cells and its role in FcεRI-IgE signalling has suggested that MS4A2 may participate and contribute to the pathogenesis of human allergic disease (Dombrowicz et al, 1988). Indeed, in a study by Dombrowicz and colleagues (2008), MS4A2 was shown to have the capacity to affect the intensity of IgE mediated allergic responses via the amplification of FcεRI signalling. Meta-analysis of MS4A2 gene expression studies have also suggested that polymorphisms in the MS4A2 promoter and 7th exon, may be associated with the risk of developing asthma (Yang, Zheng, Zhang, Yang, & Huang, 2014).

D.4 MS4A3 (HTm4)

MS4A3 is a 217 amino acid intracellular membrane protein. Immunohistochemical analysis indicates that MS4A3 is expressed in hematopoietic tissues such as the lymph nodes (Kutok, Yang, Folkerth, & Adra, 2011). Analysis of MS4A3 expression among hematopoietic cell populations also indicates MS4A3 displays elevated protein expression in basophils and low level expression in activated CD4- T-lymphocytes (Adra et al., 1994; Kutok et al., 2011). In addition MS4A3 expression has also been identified in the spleen. However, in contrast to initial reports, MS4A3 is expressed in the epithelial cells of select non-hematopoietic tissues, including the ductal epithelium in the breast, pancreas, testis, prostate, thymus, and stomach (Kutok et al., 2011). In contrast to many of the MS4A family members, the functional role of MS4A3 has been partially elucidated. Specifically, Kutok and colleagues (2005) previously demonstrated that MS4A3 is an adaptor protein that is capable of regulating G1 to S phase cell cycle progression. Its capacity to influence cell cycle progression was further shown to be a linked to the ability of MS4A3 to regulate the activity of kinase-associated phosphatase, cyclin-dependent kinase 2, and cyclin A (Donato et al., 2002).

D.5 MS4A4A

D.5.1 Overview

Human MS4A4A is a 24 kDa plasma membrane protein. As a member of the MS4A family, MS4A4A is characterized by four transmembrane domains, intracellular N- and C- terminal regions, and two short extracellular loops (Figure 1.5) (Ishibashi et al., 2001). The first transmembrane loop is approximately 13 amino acids in length while the second transmembrane loop is approximately 26 amino acids in length. Overall, MS4A4A shows approximately 25% amino acid sequence identity with previously defined MS4A family members such as MS4A1 (CD20) and MS4A2 (FcεRI β subunit). Further analysis indicates MS4A4A is most homologous in the first and second transmembrane domains with previously characterized human MS4A family members, such as MS4A2, where there is above 37% amino acid sequence identity (Ishibashi et al., 2001; Liang et al., 2001).

D.5.2 MS4A4A cDNA and mRNA Expression

As an uncharacterized member of the MS4A family, knowledge of MS4A4A expression is limited. To date, MS4A4A protein expression has not been evaluated in the literature. Database analysis of MS4A4A cDNA expression suggests a restricted pattern of expression in cells of hematopoietic origin. Specifically, global gene profiling from several microarray datasets indicates that MS4A4A may be expressed in monocytes, monocyte derived macrophages, dendritic cells, and alveolar macrophages (Lu et al., 2011; Shin et al., 2011).

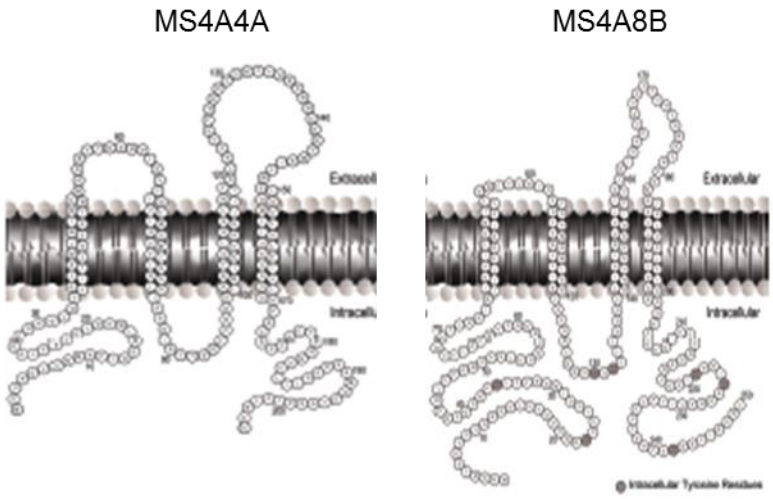

Figure 1.5. The predicted structure of two MS4A family members: MS4A4A and MS4A8B. MS4A4A and MS4A8B are members of the MS4A family of proteins. As such, they are characterized by four trans-membrane domains, two short extra-cellular loops, and intracellular C- and N- terminal domains. Modified with permission from Jonathan Zuccolo.

Furthermore, studies investigating differences in gene expression between monocyte derived M1 and M2 macrophages have identified elevated MS4A4A cDNA expression in the M2 subset (Krausgruber et al., 2011; Martinez, Gordon, Locati, & Mantovani, 2006). Previously, our lab evaluated the expression of MS4A4A mRNA in a panel of human tissues and identified MS4A4A mRNA expression in the lung but not in the trachea, prostate, adrenal gland, liver, testis, uterus, brain, cerebellum, heart, kidney, placenta, skeletal muscle or spinal cord (J. Zuccolo et al., 2013).The tissue mRNA expression and gene database analysis of MS4A4A indicates that it displays a restricted pattern of expression.

D.5.3 MS4A4E

MS4A4E is a human homolog of MS4A4A. Sequence analysis and structural modeling predicts that the *MS4A4E* gene codes for a protein of 220 amino acids and a molecular weight of 23 kDa. It shares approximately 76% overall sequence identity with human MS4A4A and is predicted to display a structure typical of most MS4A family members (Liang et al., 2001). MS4A4A shares considerable amino acid sequence identity with MS4A4E in the transmembrane and intracellular but not extracellular domains (Liang et al., 2001). To date, MS4A4E protein expression has not been evaluated. However, during its initial identification, the mRNA expression of MS4A4E in select human tissues and hematopoietic cell lines was evaluated. Here, Liang and colleagues (2001) could not identify MS4A4E mRNA expression in any of the tissues evaluated (colon, small-intestines, spleen, ovary, prostate, testes, thymus, and peripheral blood

leukocytes). They were also unable to identify MS4A4E expression in cells of B-cell, T-cell, and monocytic origin and MS4A4E cDNA analysis via gene database search could not identify MS4A4A expression in normal or cancerous tissue, suggesting that expression of the gene is either rare or occurs transiently (Liang et al., 2001).

D.5.4 The Mouse Homologs of MS4A4A

MS4 followed by a lowercase "a" (MS4a) indicates the mouse family members. The Sequence and structural analysis of human MS4A4A has identified 3 mouse homologs: MS4a4B, MS4a4C, and MS4a4D. Each of the mouse homologs has a predicted molecular weight of 24 kDa and shares between 40-45% amino acid sequence identity with human MS4A4A. However, the mouse homologs share between 70% and 84% amino acid sequence identity with one another and are predicted to have a structure typical of MS4A family members (Liang & Tedder, 2001).

D.5.4.1 MS4a4B

MS4a4B displays restricted mRNA and protein expression in hematopoietic cell populations. In a study by Xu and Colleagues (2006), RT-PCR amplification of MS4a4B mRNA identified its restricted tissue expression in the mouse thymus, spleen, and bone marrow but not the kidney, brain, liver, or lung. Among these, mRNA expression was greatest in the thymus and spleen. Its mRNA as well as protein expression were subsequently shown to be differentially expressed during thymic development, with initial expression in uncommitted thymocyte progenitor cells, loss of expression in lineage committed thymocytes, and followed by high level re-expression in mature

CD4+ T-lymphocytes. In peripheral whole white blood cells, MS4Aa4B protein was also expressed at high levels in circulating CD4+ T-lymphocytes as well as NK cells but not in B-lymphocytes. Minor expression was identified in cells of myeloid origin such as monocytes and macrophages isolated from the spleen however expression was rapidly lost during cell culture (Xu, Williams, & Spain, 2006). Among T cells, MS4a4B was differentially expressed on Th1 mouse T-lymphocytes and down-regulated in Th2 mouse T-lymphocytes (Venkataraman, Schaefer, & Schindler, 2000; Xu et al., 2010). However, in malignant T-lymphocytes MS4a4B expression was silenced. This was attributed to the ability of MS4A4B to act as a negative regulator of mouse T-cell proliferation. Specifically, MS4A4B is capable of regulating cellular entry from the S phase to the G2 phase of the cell cycle (Xu et al., 2010). Interestingly, not only can MS4a4B act as a negative regulator of T-cell proliferation, but it can also regulate cell apoptosis. Recently, Yan and colleagues (2013) demonstrated that knockdown of MS4a4B via MS4a4B –siRNA or –shRNA promoted apoptosis in primary mouse T cells. Remarkably, treatment of MS4a4B expressing cells with anti-MS4a4B also induced cellular apoptosis (Yan et al., 2013).

D.5.4.2 MS4a4C

MS4a4C has a molecular weight of 24 kDa and shares approximately 41% sequence identity with human MS4A4A. Sequence analysis and protein modeling predicts that MS4a4C displays a structure typical of most MS4A family members with an intracellular N- and C- terminal region (Liang & Tedder, 2001). Tissue mRNA analysis also

indicates that MSaA4c displays widespread expression among hematopoietic and non-hematopoietic tissues. Notably, an investigation by Xu and colleagues (2006), identified MS4a4C mRNA expression in the bone marrow, spleen, kidney, liver, lung, brain and bone marrow. Similar to MS4a4B, the greatest level of tissue mRNA was amplified from the spleen. MS4a4C RT-PCR analysis of select hematopoietic cellular populations further identified MS4a4C mRNA in CD4+ T-lymphocytes and NK cells (Xu et al., 2006).

D.5.4.3 MS4a4D

MS4a4D shares 41% amino acid sequence identity with human MS4A4A (Liang & Tedder, 2001). Tissue mRNA analysis indicates MS4a4D displays restricted patterns of expression. Specifically, in an investigation by Xu and colleagues (2006), MS4a4D expression was identified in the lung and liver but was absent from the spleen, kidney, brain, and bone marrow. MS4a4D RT-PCR analysis of select hematopoietic cell populations further identified the absence of MS4a4D mRNA expression in CD4+ T-lymphocytes, macrophages, and NK cells (Xu et al., 2006).

Among the mouse MS4a4B, MS4a4C, and MS4a4D (Xu et al., 2006), none of the mouse homologs display an expression pattern consistent with the cDNA analysis of MS4A4A expression (Lu et al., 2011; Shin et al., 2011). However, MS4a4B displays restricted patterns of expression in hematopoietic cells (Xu et al., 2006). As previously mentioned, gene global database analysis of human MS4A4A expression suggests it also displays restricted expression in hematopoietic cell subsets (Lu et al., 2011; Shin et al., 2011).

D.6 MS4A8B

D.6.1 Overview

Human MS4A8B is a 24 kDa plasma membrane protein (Bangur et al., 2004). As a member of the MS4A family, MS4A8B is characterized by four-transmembrane domains with two extra-cellular loops as well as intracellular N- and C-terminal tails (Figure 1.5) (Bangur et al., 2004; Ishibashi et al., 2001). The extracellular loops of MS4A8B are relatively small, with the first and second loop consisting of 8 and 24 amino acids. However, MS4A8B is characterized by larger intracellular N- and C-terminal regions (Liang & Tedder, 2001), which contain two tyrosine residues, one of which is part of the consensus PPXY tyrosine phosphorylation motif (Dinkel et al., 2014). Lastly, the transmembrane domains of MS4A8B consist of hydrophobic amino acids and display homology with the previously defined members of the MS4A family members such as MS4A1 (CD20) and MS4A2 (FcεRI β subunit) . The first and second transmembrane domains of MS4A8B are 46% identical to human MS4A1 (CD20) and 41% identical to human MS4A2 (FcεRI β subunit) (Liang & Tedder, 2001).

D.6.2. MS4A8B cDNA and mRNA Expression in Human Tissues and Cell Populations

As an uncharacterized member of the MS4A family, knowledge of MS4A8B expression is limited. *MS4A8B* gene database expression analysis indicates that MS4A8B may be expressed in tissues such as the lung, intestines, colon, and uterus. Further analysis suggests no differences in cDNA expression of MS4A8B among cancerous and non-cancerous cells in the aforementioned tissues. However, gene database analysis

does indicate that MS4A8B cDNA expression is not widespread but rather restricted among the various tissues (Shin et al., 2011). To evaluate and further investigate MS4A8B expression, our lab tested a panel of human tissues and identified restricted patterns of MS4A8B mRNA expression. Specifically, MS4A8B displayed mRNA expression in the lung, trachea, prostate, adrenal gland, testis, uterus and brain but not the cerebellum, heart, kidney, placenta, skeletal muscle or spinal cord (J. Zuccolo et al., 2013). Here, the greatest level of MS4A8B mRNA expression was found in the lung (J. Zuccolo et al., 2013). Despite cDNA and mRNA analysis the investigation of MS4A8B protein expression is limited. However, a study by Bangur and Colleagues (2004) previously identified MS4A8B protein expression in the lung (Bangur et al., 2004).

D.6.3 MS4A8B cDNA, mRNA, and Protein Expression in the Small Cell Lung Carcinoma

In the study by Bangur and colleagues (2004), microarray analysis of select tissue indicated that MS4A8B is over-expressed in primary small cell lung carcinoma cells at levels that are 2 fold greater than the normal tissue sample controls. Analysis of other tissues such as adeno- and squamous- lung carcinoma, the heart, spleen, liver, kidney, thymus and bone marrow showed limited to no detectable expression of MS4A8B (28). Therefore, Bangur and colleagues (2004) focused on MS4A8B expression analysis within primary small cell lung carcinoma tissues, normal lung tissue controls, and the small cell lung cancer (SCLC) cell lines: HTB-171, HTB-175, DMS-78, NCI-H128, and NCI-H69. Here, Bangur and colleagues (2004) identified MS4A8B cDNA expression in the NCI-H69 SCLC cell line and in primary SCLC but not the HTB-171, HTB-175, DMS-78, NCI-H128 SCLC cell

lines and normal lung tissue. Real time PCR analysis confirmed MS4A8B mRNA expression in primary SCLC samples, its absence in normal lung tissues and identified MS4A8B mRNA expression in the NCI-H69, HTB-173, and HTB-172 cell lines. However, mRNA expression, as identified by real time PCR, was greatest in the NCI-H69 cell line. Finally, they confirmed protein expression in the MS4A8B mRNA expressing SCLC cell lines by staining cells with affinity purified polyclonal anti-MS4A8B and analyzing samples by flow cytometry. Primary SCLC tissue and normal lung control samples were also evaluated for protein expression by immunohistochemistry. Collectively, they demonstrated MS4A8B protein expression in the NCI-H69 and HTB-173 SCLC cells and in 2 out of 7 primary SCLC tumor samples (Bangur et al., 2004). Interestingly Bangur and colleagues (2004) identified limited to no MS4A8B mRNA expression in normal lung tissue samples while our lab (J. Zuccolo et al., 2013) and others (Shin et al., 2011) detected elevated expression of MS4A8B mRNA from normal lung and trachea tissue samples. In addition, though Bungur and Colleagues (2004) only identified MS4A8B mRNA in the lung tissue our lab identified mRNA expression in additional tissues (J. Zuccolo et al., 2013).

D.6.4 MS4a8A is the Mouse Homolog of MS4A8B

MS4a8A is a 26 kDa plasma membrane protein and the mouse homolog of human MS4A8B. As a member of the MS4A family, MS4a8A is characterized by four transmembrane domains. Similar to MS4A8B, MS4a8A has two short extra-cellular loops and relatively larger intracellular N- and C-terminal regions (Liang & Tedder, 2001;

Schmieder et al., 2012; Schmieder et al., 2011). The extracellular loops and intracellular N- and C-terminal regions of MS4a8A and MS4A8B show considerable sequence variability (Liang & Tedder, 2001) and may contribute to potential differences in its function. However, the transmembrane domains of MS4a8A and MS4A8B share substantial sequence similarity. Specifically, MS4A8B shares 78% sequence identity with mouse MS4a8A in the first three transmembrane domains and 68% identity in domain 4 (Liang & Tedder, 2001).

D.6.4.1 MS4a8A Expression in M2 Macrophages

As an uncharacterized member of the MS4A family, knowledge of MS4A8B expression is limited. However, the expression of the mouse homolog, MS4a8A, has been evaluated. In 2012, Schmeider and colleagues evaluated the gene expression profiles of a newly identified subset of tumor associated macrophages (TAM). The subset was characterized by the expression of the cell surface proteins stabilin-1 and lymphatic endothelium specific hyaluronan receptor (LYVE-I). Both are proteins which have been suggested to play a role in tumor lymphangiogenesis. Gene profiling and RT-PCR analysis identified the novel expression of MS4a8A. Protein analysis of TAM within murine mammary adencarinoma, confirmed MS4a8A protein expression (Schmieder et al., 2011). In general, TAMs have been found to represent a special subset of alternatively activated, M2 macrophages (Liu, Zou, Chai, & Yao, 2014). Consequently, it is not surprising that Schmeider and colleagues (2012) identified MS4a8A expression in monocyte derived M2 but not M1 macrophages. Recently, in vitro expression of

MS4a8A was confirmed in murine M2 macrophages using the in vivo C57BL/6 mouse parasitic infection model (Schmieder et al., 2012). Parasitic infection of C57BL/6 mice with *Trypanosoma congolense* and *Taenia crassiceps* has been the most commonly used and well characterized model for studying M2 macrophages. Here, macrophages isolated from *Trypanosoma congolense* and *Taenia crassiceps* infected C57BL/6 mice, clearly transition from an early (M1 predominance) to late phase of infection (M2 predominance) (Schmieder et al., 2012). Expression analysis indicated that MS4a8A is not expressed in murine M1 macrophages during early stage *Trypanosoma congolense* and *Taenia crassiceps* infections but was expressed in approximately 30% of M2 macrophages during late stage infection (Schmieder et al., 2012).

E. The Evaluation of MS4A mRNA Expression and the Generation of Monoclonal Antibodies against MS4A4A and MS4A8B

Members of the MS4A family are characterized by transmembrane domains which span the plasma membrane four times (Kutok et al., 2011; Liang et al., 2001). They also contain two short extracellular loops, which in the case of MS4A1, has been shown to contribute to its ability to function as an immunotherapeutic (Cragg, 2005). However, many MS4A family members remain uncharacterized. Consequently, in an effort to further characterize MS4A family members that may also serve as immunotherapeutic targets, our lab searched for MS4A family members that like MS4A1 (CD20) may display restricted patterns of expression. Our lab identified the restricted tissue mRNA expression of MS4A4A and MS4A8B (J. Zuccolo et al., 2013) and

subsequently generated monoclonal antibodies against their extracellular epitopes. In order to generate antibodies against MS4A8B and MS4A4A, human MS4A8B-GFP or MS4A4A-GFP was ectopically expressed in the 300.1 pre-B cell line and used to immunize C57BL/6 mice that had been tolerized. The spleen from each mouse was collected and the splenocytes were fused with myeloma cells in the presence of HAT medium (Figure 1.6). Collectively, hundreds of hybridoma clones were obtained, but only one produced antibody that was specific against MS4A8B (3E2), and three that produced antibody specifically against MS4A4A (3F2, 4H2, and 5C12). The process by which specific clones were selected is illustrated in Figure 1.7. Antibody produced from each clone was isotyped by the SACRI Antibody Services (University of Calgary). Here, the 3E2 anti-MS4A8B and the 3F2, 4H2, and 5C12 anti-MS4A4A antibodies were all isotyped as mouse IgG1.

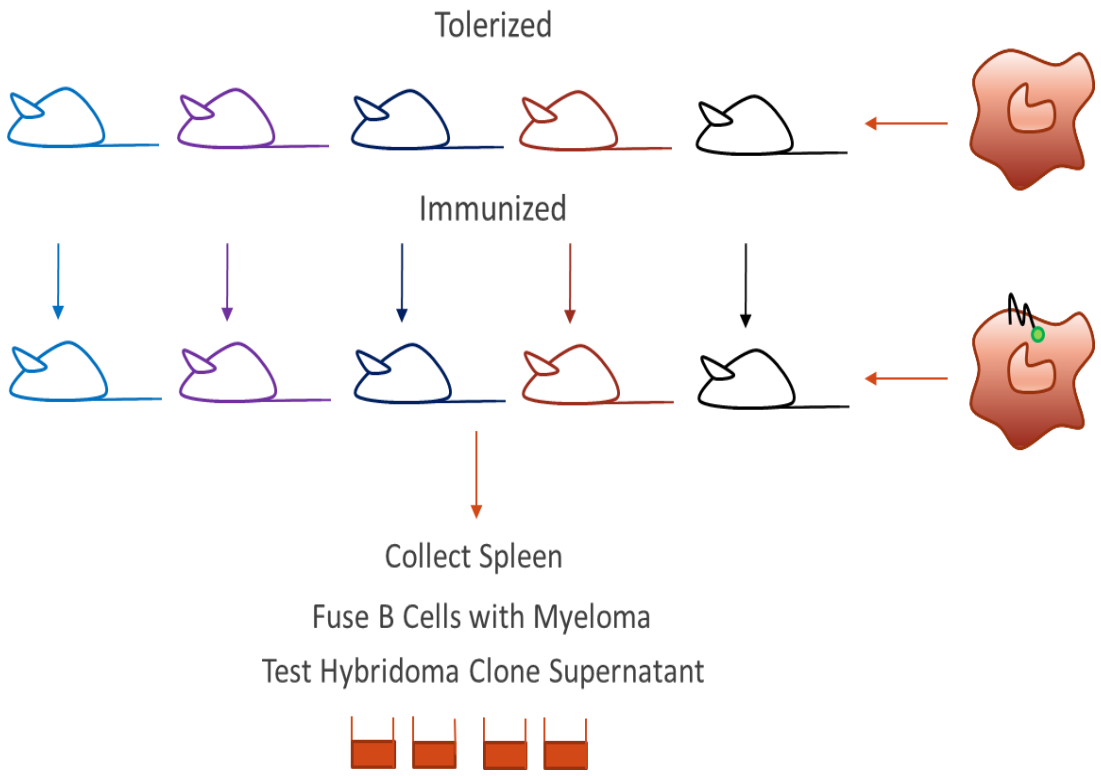

Figure 1.6. Anti-MS4A4A and Anti-MS4A8B antibody production. Anti-MS4A4A and Anti-MS48B monoclonal antibodies were produced by tolerizing multiple mice with 300.19 B-cells followed by repeated immunizations of the same mice with 300.19-MS4A8B-GFP or 300.1-MS4A4A-GFP cells. Mouse spleens were subsequently collected, fused with myeloma cells, and cultured in HAT medium. Antibody producing hybridoma clones were subsequently evaluated for specific binding. Modified with permission from Jonathan Zuccolo.

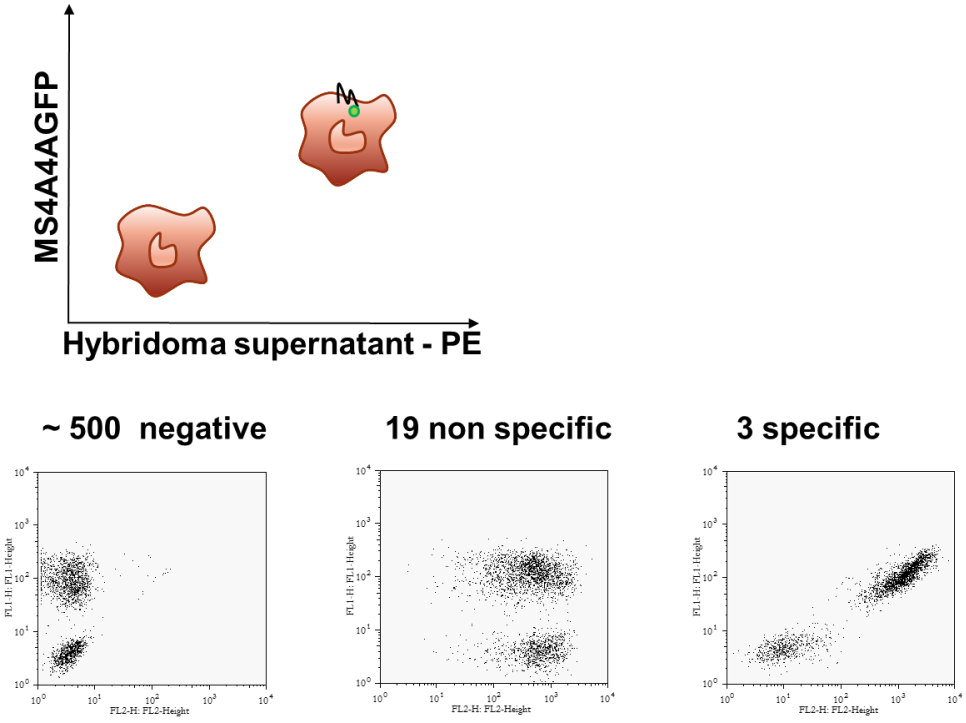

Figure 1.7. Identification of anti-MS4A4A specific hybridoma clones. In order to identify hybridoma clones which produced antibody against MS4A4A, equal amounts of 300.1 and 300.1-MS4A4A-GFP cells were combined into a single sample and incubated with supernatant produced from a hybridoma clone. Cells were subsequently incubated with a goat-anti-mouse IgG-PE antibody and evaluated by flow cytometry. Clones which produced antibody against 300.1-MS4A4A-GFP cells but not 300.1 cells were considered specific for MS4A4A. Modified with permission from (Jonathan Zuccolo, 2010).

F. Hypothesis and Objectives

F.1 Hypothesis I: MS4A8B is expressed in hematopoietic cell populations.

F.1.1 Rationale

Messenger RNA studies suggested that MS4A8B displayed restricted expression among various tissues (J. Zuccolo et al., 2013). The mouse homolog of human MS4A8B, MS4a8A, displays restricted expression in hematopoietic cell subset, M2 macrophages (Schmieder et al., 2012; Schmieder et al., 2011). Due to the considerable sequence and structural similarity of MS4a8A with human MS4A8B (Ishibashi et al., 2001), as well as its restricted tissue expression (J. Zuccolo et al., 2013), MS4A8B may also be expressed on M2 macrophages or other hematopoietic cell populations.

F.2 Hypothesis II: MS4A4A is expressed on human monocytes as well as M2 macrophages and is a potential immunotherapeutic target.

F.2.2 Rationale:

Microarray and gene database analyses suggest MS4A4A is preferentially expressed on human monocytes and M2 macrophages (Krausgruber et al., 2011; Martinez et al., 2006). MS4A4A mRNA is not expressed on other hematopoietic cells such as B- and T- lymphocytes and presents highly restricted patterns of tissue mRNA expression (lung) (J. Zuccolo et al., 2013). Furthermore, one of the most closely related mouse paralogs, MS4a4B, is known to regulate cellular apoptosis and antibodies generated against its extracellular epitope are known to, like Rituximab, induce cellular apoptosis (Yan et al., 2013). Given its restricted tissue mRNA expression and the

structural similarity of MS4A4A with the mouse homolog, MS4a4B, and with CD20, as well as the presence of small extracellular loops (Liang & Tedder, 2001), human MS4A4A may be a potential target for immunotherapy.

G. Objectives:

1. Confirm the specificities of anti-MS4A4A and anti-MS4A8B and evaluate the protein expression of both MS4A4A and MS4A8B in hematopoietic cells.
2. Investigate the ability of anti-MS4A4A to induce cellular apoptosis and non-Fc mediated effects *in vitro.*

Chapter II
Materials and Methods

A. Antibodies and Reagents

Antibodies and reagents used to perform the experiments described herein are listed in Table 2.1 and Table 2.2.

Table 2.1. Antibodies

Antibody	Source
Anti-CD3-PE	BD Pharmingen
Anti-CD14-FITC	BD Pharmingen
Anti-CD16-FITC	BD Pharmingen
Anti-CD19-PE	BD Pharmingen
Anti-CD27-PE	BD Pharmingen
Anti-CD32-FITC	BD Bioscience
Anti-CD45-PE	Sigma Aldrich
Anti-CD56-FITC	BD Pharmingen
Anti-CD64-APC	Biolegend
Anti-CD64	ATCC (hybridoma)
Anti-CD80-FITC	BD Pharmingen
Anti-CD206-FITC	BD Pharmingen
Anti-HA	Sigma Aldrich
Anti-MS4A4A-Alexa 647 (4H2, 5C12, 3F2)	Deans Lab
Anti-MS4A4A (4H2, 5C12, 3F2)	Deans Lab
Anti-MS4A8B (monoclonal)	Deans Lab
Anti-MS4A8B (polyclonal)	Deans Lab
Anti-MS4A8B-Fab	Deans Lab
Anti-MS4A8B-FITC	Deans Lab
Goat anti mouse IgG	Jackson Immuno Research
Goat anti mouse IgG PE	Jackson Immuno Research
Goat anti mouse IgG1-PE	Santa Cruz Biotechnology
Goat anti mouse IgG2a-PE	Santa Crus Biotechnology
mIgG1	Southern Biotech
mIgG1-Alexa-647	Invitrogen
mIgG1-Alexa-488	MBL technologies
mIgG1-FITC	Invitrogen
mIgG2a	Southern Biotech

mIgG2a-FITC	BD Pharmingen
Rituximab (CD20)	Genentech

Table 2.2. Reagents

Reagents	Source
Cell Culture	
Antibiotic & Antimycotic	GIBCO
Fetal Bovine Serum	GIBCO
G418	GIBCO
Glutamax	GIBCO
GM-CSF	R&D Systems
IL-4	R&D Systems
IFNγ	R&D Systems
LPS	R&D Systems
Lymphocyte Separation Medium	GE Healthcare
M-CSF	R&D Systems
MEM Media	GIBCO
Optimem Media	Life-Technologies
RPMI-1640	GIBCO
Serum Free Media	GIBCO
Molecular Biology Reagents	
5X First Strand Buffer	Invitrogen
Chloroform	ACS
dNTP Mix	Invitrogen
DTT	Invitrogen
Nuclease and Ribonuclease Free Water	Life Technologies
Molecular Grade Isopropanol	Electron Microscopy Science
Superscript II RT	Invitrogen
Miscellaneous	
30,000 MWCO Filter	Amicon
Annexin V-FITC	Invitrogen
Digitonin	Sigma Aldrich
DTT	Invitrogen
EDTA	Millipore
Fab and F(ab')$_2$ Isolation Kit	Invitrogen
Immobilin P Membranes	Millipore
Maltoside	Sigma Aldrich

Propidium Iodide	Invitrogen
Triton X-100	Millipore
Trizol Reagent	Invitrogen

B. Cell Culture and Cells

Primary cells and established cell lines (Table 2.3) were grown and maintained in culture using RPMI-1640 (GIBCO) growth medium supplemented with 10% fetal bovine serum (FBS) (GIBCO), 1% antimycotic and antibiotic (A-A) (GIBCO), as well as 1% Glutamax (GIBCO). The BJAB cell lines that ectopically expressed either the GFP- or HA-tagged MS4A4A or MS4A8B protein constructs were further supplemented with the G418 antibiotic (GIBCO) at a concentration of 100ug per ml of media to maintain selection. All cells were grown and cultured at 37°C in the presence of 5% CO_2.

Table 2.3: Cultured Human Cells

Cell Name	Cell Description	Source
U937	A promonocytic cell line	ATCC
THP-1	A promonocytic cell line	ATCC
BJAB	Burkitt B cell line	ATCC
BJAB-MS4A4A –HA or –GFP	Burkitt B cell line transfected with HA- or GFP- tagged human MS4A4A	Derived in-house (Deans Lab)
BJAB-MS48B –HA or –GFP	Burkitt B cell line transfected with HA- or GFP- tagged human MS4A8B	Derived in-house (Deans Lab)
NCI-H69	A small cell lung cancer cell line	Dr. Donald Morris
Whole blood derived monocytes	Primary monocytes isolated from whole blood	Derived from donated human blood
M1 and M2 macrophages	M1 and M2 macrophages differentiated from whole blood derived primary monocytes	Differentiated from donated human blood monocytes

C. Hybridoma Expansion and Antibody Isolation

Hybridomas were thawed into a single 75ml flask and grown in 40ml of RPMI-1640 supplemented with 10%FBS,1%AA, and 1% Glutamax until 40% confluent. The cells were then expanded into 2 additional flasks with fresh medium and the process was repeated until ten 75ml-sized flasks were obtained. The cells were subsequently grown to 90% confluency and switched to 50ml of serum free media (Life Technologies) for 8 days. The supernatant from each flask was then collected and centrifuged at 3500g for 20 minutes to remove suspended cells. To evaluate anti-MS4A4A production, BJAB-MS4A4A-GFP cells were stained with 50ul of MS4A4A hybridoma supernatant followed by detection with goat-anti-mIgG-PE (Jackson Immuno Research Laboratories) and analyzed via the Attune Flow Cytometer (Refer to Materials and Methods: Flow Cytometry). Antibody was subsequently isolated using column chromatography with immobilized protein G beads and concentrated using a 30,000 MWCO filter (Amicon).

D. Mononuclear Cell Isolation

Approval was obtained from the Conjoint Health Research Ethics Board (CHREB) for the collection of peripheral blood from healthy volunteers (Ethics ID# E-24776). For this study, 30 ml of blood was collected from over 5 independent blood donors into collection tubes coated with heparin to prevent blood clotting. White blood cells were isolated by aseptically transferring 30 ml of whole blood into sterile 50 ml conical tubes, diluting 1:1 with sterile PBS, and under-layering 6 ml of LSM Lymphocyte Separation Media (GE Healthcare). The LSM-blood mixture was centrifuged at 400g for 20 minutes

at room temperature with no brake and the mononuclear cell layer was removed and transferred to a sterile 15 ml conical tube. The mononuclear cell layer was washed with PBS (260g for 10 minutes) and re-suspended in complete growth medium (RPMI-1640/10%FBS/1%AA and Glutamax) so as to achieve a mononuclear cell density of $2.0x10^6$ cells per ml.

E. Monocyte Isolation

To isolate primary human monocytes, 1ml of $2.0x10^6$ mononuclear cells per ml of growth medium (RPMI-1640/10%FBS/1%AA and Glutamax) was added to a sterile, 24 well, polyethylene plate (COSTAR) and incubated for 4 hours. After incubation, monocytes became tightly adherent while granulocytes and lymphocytes were non-adherent. To remove the non-adherent cells, the media in each well was gently removed and fresh culture medium (RPMI-1640/10%FBS/1%AA and Glutamax) was added drop wise 4-6 times and replaced with 1 ml of final culture medium (RPMI-1640/10%FBS/1%AA and Glutamax). The wells were then assessed by phase-contrast microscopy for the presence of adherent cells.

F. Monocyte Derived M1 and M2 Macrophages

In order to derive human M1 and M2 macrophages, primary adherent monocytes were maintained for 3 days in culture at 37°C with 5% CO_2, in 24 well sterile polyethylene plates, with 1 ml of M1 (RPMI-1640/10% FBS/1%A-A/1% Glutamax/40ng per ml GM-CSF [R&D Systems]) or M2 (RPMI-1640/10% FBS/1%A-A/1% Glutamax/25ng per ml M-CSF[(R&D Systems]) culture medium. At day 3 the culture medium was

removed from each well and 1 ml of fresh M1 or M2 culture medium was added. Special care was made to thaw GM-CSF and M-CSF only once and immediately before use so as to prevent loss of its activity. Upon day 5, the medium overlaying the cells from each well was removed and Day 5 M1 (RPMI-1640/10% FBS/1%A-A/1% Glutamax/100ng of LPS [R&D Systems] per ml/20ng of INFγ [R&D Systems] per ml) or Day 5 M2 (RPMI-1640/10% FBS/1%A-A/1% Glutamax/15ng per ml IL-4) differentiation medium was added. The cells were then incubated for an additional 2 days at 37°C with 5% CO_2 and evaluated for M1 and M2 differentiation via cell surface markers using flow cytometry. Note, the M1 and M2 differentiation experiments were performed using primary monocytes obtained from over 5 independent blood donors.

G. Flow Cytometry

Cultured cells were centrifuged at 500g (1230 RPM) for 7 minutes and washed with RPMI-1640. Cells were pelleted, re-washed with cold FACS Buffer (4°C) (PBS [Lonza]/2% FBS/0.5mmol EDTA [Millipore]) and suspended at a density of $1x10^6$ cells per 50ul of cold FACS Buffer, per sample, in a sterile 96 well polyethylene plate. The final volume was then adjusted to 100ul by the addition of primary antibody diluted in 50ul of cold FACS Buffer. For direct staining, samples were incubated with 1ug of directly conjugated primary antibody or the appropriate isotype control for 30 minutes on ice at 4°C. Samples were then washed twice with 100ul of cold FACS Buffer and transferred to FACS Tubes for analysis. For experiments requiring indirect staining, samples were incubated with 1ug of unconjugated primary antibody or the appropriate isotype

control for 30 minutes on ice at 4°C. Samples were washed twice with a 100ul of cold FACS Buffer and re-incubated with a 1:100 dilution of goat anti-mouse IgG-PE on ice and 4°C for 30 minutes. After incubation, samples were washed once with 100ul of cold FACS Buffer and transferred to FACS Tubes for analysis. Flow cytometry analysis was performed using the Attune Flow Cytometer.

H. Total RNA Extraction

RNA was extracted from primary or cultured cell lines (Table 2.3) for complementary DNA (cDNA) synthesis and polymerase chain reaction (PCR) analysis. In order to isolate RNA, 5 x 10^6 cultured or primary cells were suspended in 500ul of Trizol Reagent (Invitrogen), at room temperature for 5 minutes. Phase separation of the Trizol-cell mixture was induced by the addition of 200ul of chloroform (ACS) and the subsequent centrifugation of the samples at 15000g, at 4°C, for 15 minutes. The resultant mixture contained two phases: an organic DNA containing phase and an aqueous RNA containing phase. The aqueous, RNA containing phase was transferred to a sterile 1.5 ml tube, precipitated with molecular grade isopropanol (Electron Microscopy Science) and washed twice. The final sample was re-suspended in 20ul of nuclease and ribonuclease free water (Life Technologies) and RNA was quantified using Nanodrop.

I. Complementary-DNA Synthesis

Complementary DNA was synthesized by first diluting 1ug of total RNA in 12ul of nuclease and ribonuclease free water, containing Oligo (dt) (1ul of 500ug/ml)

(Invitrogen) and dNTP Mix (1ul of a 10mM) (Invitrogen). The resultant mixture was heated at 65°C for 5 minutes using the Eppendorf Mastercycler and subsequently chilled on ice. Upon chilling, 8ul of a cDNA Master Mix (5X First Strand Buffer [Invitrogen], 0.1M DTT [Invitrogen], 40 units of RNase OUT [Invitrogen] and 4000 units of Superscript II RT [Invitrogen]) was added to each sample. The samples were then incubated for an additional 50 minutes at 42°C and the resultant cDNA samples were stored -20°C or used immediately for PCR amplification.

J. Polymerase Chain Reaction

Qualitative PCR amplification was performed by adding 200ng of template cDNA to 25ul of PCR Mastermix (Qiagen) supplemented with 50pmol of the appropriate forward and reverse primers (Table 2.4). The mixture was then diluted to a final volume of 50ul by the addition of nuclease and ribonuclease free water and subsequently amplified for 36 cycles using the Eppendorf Mastercycler on Standard setting (Table 2.5)

Table 2.4. HPRT, MS4A4A, and MS4A8B Amplification Primers

Primer	Sequence
HPRT	F: 5’ CACAGGACTAGAACACCTGC 3’ R: 5’ GCTGGTGAAAAGGACCTCT 3’
MS4A4A	F: 5’ AGTCCTGCAGTCAAACCTCATTAAGTGG 3’ R: 5’ GACTAGATCTATGCATCAGACCTACAGC 3’
MS4A8B	F: 5’ GACTCTCGAGGCATGAATTCGATGACTTCA 3’ R: 5’ AGTCGGTACCTTACTTATTTGCTTGGAT 3’

Table 2.5 Standard Setting for PCR Amplification of cDNA using the Eppendorf Mastercycler

Temperature (°C)	Time (minutes)	Cycles
95	5.00	1
94→55→72	1.00 at each temperature	34
72	10	1
4	∞	-

K. Immunoprecipitation

In order to perform immunoprecipitations, $1.0x10^7$ cells per sample were washed, pelleted, and lysed in 1% Triton X-100 or Digitonin lysing buffer containing the protease inhibitors: leupeptin (1ul/ml), aprotinin (1ug/ml), phenylmethylsulfonyl fluoride (1 mM; PMSF) and EDTA (1mM). Cell lysis was performed for 15 minutes on ice and the resultant mixture was centrifuged at 13,000g for 15 minutes at 4°C to remove detergent insoluble material. Soluble lysates were subsequently incubated with antibody and mixed with protein A- or protein G- coated beads as appropriate. The samples were then rotated, pelleted and washed in lysis buffer, while rotating between 150mM NaCl (low salt) containing and 500mM NaCl (high salt) containing buffers. Once immunoprecipitated, the proteins were solubilized in 2X sodium dodecyl sulfate sample buffer. Immunoprecipitation experiments, as described, were performed by Maria Polyak and Ratna Sanyal.

L. Western Blotting

For western blot analysis, protein samples were prepared and denatured under reducing conditions using SDS. Samples were loaded into polyacrylamide gels alongside

a prestained MW marker and transferred to Immobilin P membranes. Blocking of the membranes was achieved by incubation with 5% BSA/TTBS (0.05% Tween-20, 20 mM TRIS-HCL [pH 7.5], 150 mM NaCl) for 1 hour. Upon blocking membranes were blotted with a unlabelled antibody diluted in the 5% BSA/TTBS blocking buffer and binding was detected using the appropriate secondary antibody. Samples were evaluated for chemiluminescence using the Fluor-S Max Imager. Western Blot analysis, as described, was performed by Maria Polyak and Ratna Sanyal.

M. Antibody Plating

Antibody coating was achieved by incubating polystyrene plates with 300ul of PBS-diluted antibody stock solution (20ug of antibody diluted in 1 ml of PBS), for 3 hours, at 37°C in the presence of 5% CO_2. The antibody solution was then removed and the plates were washed with sterile PBS.

N. Cell Apoptosis

In order to evaluate cellular apoptosis, $1.0x10^6$ cells per sample were harvested and washed with 1ml of Ca^{2+} and Mg^{2+} free PBS. The cells were then re-pelleted (500g for 5 minutes), suspended in 100ul of Annexin V Binding Buffer (10mM HEPES, 140mM NaCl, 2.5mM CaCl, pH 7.4) (Invitrogen) and stained with 3ul of Annexin-V-FITC (Invitrogen) for 30 minutes at room temperature. In order to differentiate between dead and live cells 50ng of propidium iodide was subsequently added to each sample for 2 minutes. Once stained with Annexin V-FITC and propidium iodide the samples were immediately analyzed by flow cytometry.

O. Cell cycle analysis

Cell cycle analysis was performed by first harvesting $1.0x10^6$ cells per sample and washing them with 1ml of Ca^{2+} and Mg^{2+} free PBS. The cells were subsequently re-suspended in 500ul of Ca^{2+} and Mg^{2+} free PBS, after which 500ul of absolute ethanol was slowly added. The cell suspension was then gently mixed and incubated at 4°C for 6 hours. Upon incubation the cells were washed with Ca^{2+} and Mg^{2+} free PBS and re-suspended in 300ul of the Cell Cycle Staining Solution (0.1% Triton X-100 [Millipore], 20ug/ml propidium iodide [Invitrogen] and 200ug/ml RNAse A) for 45 minutes at room temperature. The cells were then immediately analyzed by flow cytometry.

P. Antibody Digestion

Mouse IgG1 $F(ab')_2$ fragments were isolated from whole antibody by digestion with Ficin in the presence of cysteine (4mM). Ficin, when accompanied by 1-4mM of cysteine, is known to predominantly generate $F(ab')_2$ fragments from mouse IgG1. As outlined in the Pierce Mouse IgG1 Fab and $F(ab')_2$ Preparation Kit, this required the completion of three independent steps. The first step involved the preparation and equilibration of the Pierce Desalting Column. This involved washing the supplied desalting columns with Pierce Digestion Buffer via centrifugation (500g for 5 minutes) 3 times. Upon which, 500mg of antibody, in a 200ul volume, was added to the column and desalted via centrifugation (1500g for 2 minutes). The second step involved the digestion of whole antibody in the presence of cysteine (4mM). Here, the desalted antibody was added to the 0.8ml Pierce Immobilized Ficin Column and incubated in a

table-top rocker for 18 hours at 37°C. The digested antibody was removed via centrifugation (5000g for 1 minute) and 3 wash products were obtained using Pierce Protein A Binding Buffer (5000g for 1 minute). Finally, the digested antibody was isolated using an equilibrated NAb Protein A Plus Spin Column (Pierce). This involved adding 500ul of the digested antibody fraction to the NAb Protein A Plus Spin Column (Pierce), re-suspending the mixture within the resin by gentle inversion and subsequently incubating the column in a table top mixer at 37°C. The resultant Fab and $F(ab')_2$ was removed via centrifugation (5000g for 1 minute) alongside 3 wash products using Pierce Protein A Binding Buffer. The presence of Fab and $F(ab')_2$ antibody fragments was subsequently evaluated using coomassie blue staining under reducing and non-reducing conditions while the concentration of the Fab and $(Fab')_2$ fragments was determined by measuring absorbance at 280nm with Nanodrop.

Q. Transfections

HEK293 cells were transfected with MS4A8B-GFP or CD64 plasmid DNA using Lipofectamine 2000 (Invitrogen). Here, $5.0x10^5$ cells per well were first grown to 90% confluency in a 48 well polyethylene plate, using MEM media (Life Technologies). The media overlaying the cells was then removed and replaced with 900ul of Optimem Media. The transfection reagents were subsequently prepared as follows. First, 600ng of MS4A8B or CD64 plasmid DNA was diluted in Optimem Media to a final volume of 37.5ul. Then, 2ul of Lipofectamine 2000 was diluted to a final volume of 37.5ul, with Optimem Media. Both diluted reagents were equilibrated at 37°C for 5 minutes. The

Lipofectamine 2000 was subsequently added to the plasmid mixture and allowed to incubate at 37°C for 30 minutes. This allowed for Lipofectamine 2000-plasmid DNA complexes to form. The resultant mixture was adjusted to a volume of 100ul via the addition of Optimem Media and was subsequently added to each well containing HEK293 cells. The transfected cells were then incubated at 37°C for 48 hours to allow for recovery. The MS4A8B-GFP or CD64 expressing HEK293 cells were subsequently selected by incubating with 1mg of G418 antibiotic per ml of growth media. Since the MS4A8B-GFP or CD64 transfected cells express the *neor* resistance gene, cells that were successfully transfected were resistant to G418. MS4A8B-GFP and CD64 expression in HEK293 transfected cells was subsequently confirmed by flow cytometry. Specifically, MS4A8B-GFP expressing HEK293 cells were evaluated for GFP expression and anti-MS4A8B + goat-anti-mouse IgG-PE binding while HEK293 CD64 transfected cells were evaluated for anti-CD64-APC binding.

R. Statistical Analysis

In order to determine statistical significance, the two tailed unpaired Students T-Test analysis was performed. Data were predicted to follow a Gaussian curve and analysis was performed between control and treatment samples with statistically significant events having a *p* value equal to or less than 0.05.

Chapter III
MS4A8B Expression and the Critical Importance of Isotype Controls

A. Introduction

Several members of the MS4A family, whose expression has been evaluated, display relatively constrained patterns of expression in hematopoietic cells. Consider: I) MS4A1, which exhibits restricted expression in B cells (Cragg, 2005), II) MS4A2, which is expressed in basophils as well as mast cells (Matsuda et al., 2008) and III) MS4A3, whose expression is restricted to basophils, activated CD4-T-lymphocytes, and certain epithelial cells (Kutok et al., 2011). However, unlike MS4A1, MS4A2, and MS4A3 many of the remaining 15+ MS4A family members have not been characterized with respect to their mRNA or protein expression (Ishibashi et al., 2001; Liang & Tedder, 2001). In an effort to further characterize the expression of the MS4A family, our lab evaluated the mRNA expression of select human MS4A family members within a panel of tissues. The lab was also interested in identifying MS4A family members that may, like MS4A1, act as immunotherapeutic targets. Consequently, our search was restricted to MS4A family members that like CD20 are: I) expressed in hematopoietic cells of human origin and II) display restricted patterns of expression. Among the 15+ MS4A family members the lab identified 4 human members whose expression was either unknown or believed to be restricted to hematopoietic tissue (MS4A4A, MS4A6A, MS4A7, and MS4A8B) (Liang & Tedder, 2001). Among these, the lab identified widespread expression of MS4A6A and MS4A7 but relatively constrained patterns of expression for MS4A8B and MS4A4A.

Specifically, MS4A4A mRNA was detected within the lung tissue while MS4A8B displayed mRNA expression in the lung, trachea, prostate, adrenal gland, liver, testis, uterus and brain but not the cerebellum, heart, kidney, placenta, skeletal muscle or spinal cord (J. Zuccolo et al., 2013). Given that the mouse homologs of these members are expressed in hematopoietic cells (Schmieder et al., 2011; Xu et al., 2006; Xu et al., 2010), MS4A4A and MS4A8B may also be expressed in hematopoietic cells. For MS4A4A, restricted mRNA expression in the lung could be explained by the presence of the large number of alveolar macrophages and hematopoietic cells lining the alveolar walls. For MS4A8B, expression in hematopoietic cells could also explain its patterns of its mRNA expression: since its mouse homolog, MS4a8A, is expressed in M2 macrophages (Schmieder et al., 2011), MS4A8B expression among tissue macrophages could explain why its mRNA expression was found in only certain tissues. Therefore, to further investigate the expression of MS4A8B and MS4A4A our lab developed a unique set of mouse monoclonal antibodies against their extracellular epitopes. We were able to generate 1 antibody against MS4A8B (3E2) and 3 antibodies against MS4A4A (3F2, 4H2 and 5C12). The antibodies were all isotyped as mouse IgG1 by The SACRI Antibody Services (University of Calgary). This chapter describes the results of characterizing the protein expression of MS4A8B using the mouse monoclonal anti-MS4A8B (3E2) antibody. Using anti-MS4A8B, which we believed to be of the mouse IgG1 isotype, we obtained data suggesting MS4A8B was expressed in monocytes and associates with the human FcγRI α and γ subunits. However, based upon a series of investigations described

below, we subsequently determined that the initial isotyping of MS4A8B was incorrect. Re-evaluation using the correct isotype control (mouse IgG2a) indicated that MS4A8B was not expressed in monocytes after all. Unlike, the mouse homolog MS4a8A, MS4A8B was also not found to be expressed in the M2 macrophage subset but was expressed at the mRNA and protein level in the NCI-H69 small cell lung carcinoma cell line, as previously reported (Bangur et al., 2004).

B. Results

B.1 Anti-MS4A8B Specificity

In order to investigate the protein expression of MS4A8B our lab developed a mouse monoclonal antibody against MS4A8B (anti-MS4A8B). The specificity was first evaluated by using parental BJAB cells and MS4A8B-GFP transfected BJAB cells (BJAB-MS4A8B-GFP). Given that anti-MS4A8B was identified as of the mouse IgG1 isotype, parental BJAB and BJAB-MS4A8B-GFP cells were also incubated with the mouse IgG1 isotype control. Anti-MS4A8B and mouse IgG1 binding were detected using the PE-conjugated goat-anti-mouse IgG secondary antibody and the resultant fluorescence was detected using the Attune Flow Cytometer. As shown in Figure 3.IA, anti-MS4A8B bound to the BJAB-MS4A8B-GFP cells but not to parental BJAB cells. In order to further confirm the specificity, we evaluated whether anti-MS4A8B could selectively immunoprecipitate MS4A8B from cell lysates. This was done by immunoprecipitating MS4A8B using our monoclonal anti-MS4A8B antibody from BJAB-MS4A8B-HA cell lysates and as a control parental BJAB cell lysates.

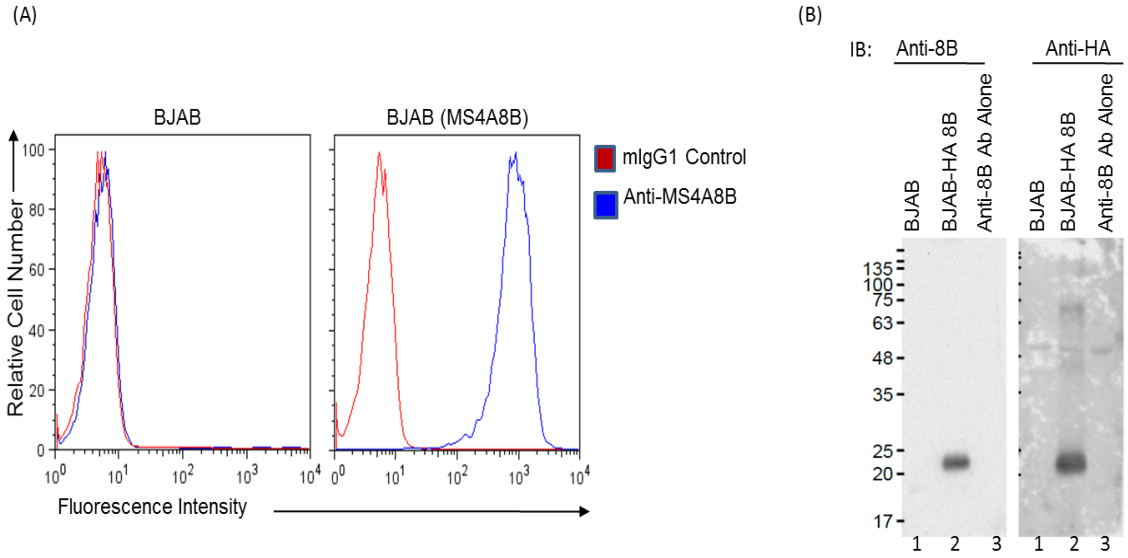

Figure 3.1: Anti-MS4A8B specificity. Anti-MS4A8B specificity was evaluated by (A) staining parental BJAB and BJAB-MS4A8B-GFP cells with either 1ug of anti-MS4A8B (blue) or mIgG1 (red). Stained samples were detected with goat-anti-mouse IgG-PE and and evaluated by flow cytometry. Note, anti-MS4A8B bound to BJAB-MS4A8B-GFP cells but not to parental BJAB cells. (B) Specificity was further evaluated by immunoprecipitating BJAB and BJAB-MS4A8B-HA cell lysates with anti-MS4A8B followed by western blot analysis using rabbit anti-MS4A8B (left panel). The same immunoblot was subsequently stripped and re-blotted with anti-HA (right panel). Note, proteins immunoprecipitated from the BJAB and BJAB-MS4A8B-HA cell lysates are respectively shown in lane 1 and lane 2. In addition, 1ug of the immunoprecipitating antibody, anti-MS4A8B, was run in lane 3. (N>3).

The immunoprecipitated products were then detected by immunoblot using a rabbit anti-MS4A8B antibody directed against an intracellular epitope. The same immunoblot was subsequently stripped and the identity of the detected protein confirmed by re-blotting with anti-HA (right panel). As shown in Figure 3.IB, anti-MS4A8B immunoprecipitated a protein from BJAB-MS4A8B-HA cell lysates but not parental BJAB cell lysates. A single band was detected with its molecular weight consistent with that of MS4A8B (~24kDa). When the MS4A8B immunoblot was stripped and re-probed with anti-HA, the same band was detected, indicating that our mouse monoclonal anti-MS4A8B antibody was indeed specific for MS4A8B.

B.2 Anti-MS4A8B Binds to Human Blood Monocytes but not Resting Lymphocytes or Granulocytes

MS4a8A, the mouse homolog of MS4A8B, is expressed in M2 macrophages (Schmieder et al., 2011). In order to investigate MS4A8B expression among hematopoietic cells, peripheral blood human white blood cells were isolated and incubated with either anti-MS4A8B or mouse IgG1 isotype control and binding was detected via incubation with the goat-anti-mouse IgG-Cy3 secondary antibody and analysis by flow cytometry. Gating based upon forward scatter (FSC) and side scatter (SSC) was used to examine resting granulocytes, lymphocytes, and monocytes. As shown in Figure 3.2A, anti-MS4A8B bound to human peripheral blood monocytes but not to lymphocytes or granulocytes.

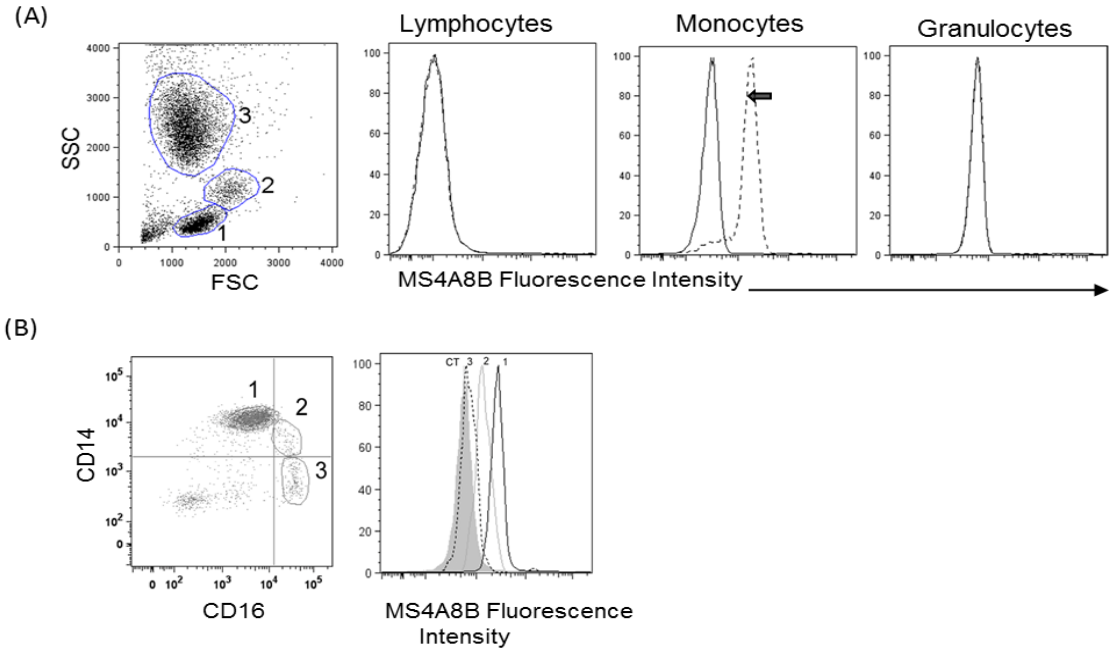

Figure 3.2: Anti-MS4A8B binds to human blood monocytes but not lymphocytes or granulocytes. (A) Human peripheral blood, depleted of red blood cells, was incubated with anti-MS4A8B followed by anti-mIgG-Cy3. Populations defined by FSC and SSC were analyzed for Cy3 fluorescence. As illustrated in panel A, anti-MS4A8B bound to monocytes (dashed line) but overlapped with the mIgG1 isotype control (solid line) in lymphocytes and granulocytes. In panel (B), PBMC's were stained with anti-MS4A8B, detected with anti-mIgG-Cy3 and subsequently stained with CD14-FITC and CD16-PE. FSC and SSC was used to gate monocytes after which CD14 and CD16 were used to gate the 3 monocytic subsets; classical (1), intermediate (2), and alternate (3). Note: anti-MS4A8B bound most strongly to CD14+ CD16- (1) monocytes and the mIgG1 isotype control is shaded (N>3).

Monocytes can be categorized based upon CD14 and CD16 expression, as classical, intermediate, or alternative monocytes (Mantovani et al., 2004; Shi & Pamer, 2011). Classical monocytes comprise 90-95% of circulating monocytes and are characterized as $CD14^{high}$ and $CD16^{low}$. Alternative monocytes are $CD14^{low}$ and $CD16^{high}$, while the intermediate population expresses intermediate levels of both CD14 and CD16 (Shi & Pamer, 2011). Since anti-MS4A8B bound to a greater extent to human peripheral blood monocytes, we evaluated anti-MS4A8B binding to classical, intermediate, and alternative monocyte subsets. Here, peripheral blood mononuclear cells, which are depleted of granulocytes, were incubated with anti-MS4A8B or the mouse IgG1 isotype control, followed by a secondary incubation with goat-anti-mouse IgG-Cy3. The same cells were subsequently incubated with CD14-FITC and CD16-PE and analyzed by flow cytometry. Monocytes were gated based upon FSC and SSC, while monocytic subsets were characterized as classical, intermediate or alternative based upon CD14-FITC and CD16-PE fluorescence as previously discussed. As shown in Figure 3.2B, anti-MS4A8B binding was greatest in classical monocytes ($CD14^{high}$ and $CD16^{low}$), lowest in alternative monocytes ($CD14^{low}$ and $CD16^{high}$) and midway in the intermediate monocytic subset.

B.3 Anti-MS4A8B binding to BJAB, BJAB-MS4A8B, U937, THP-1 and NCI-H69 Cells

Bangur and colleagues (2004) previously evaluated MS4A8B mRNA and protein expression in SCLC tissue samples and cell lines. Among these, MS4A8B protein was shown to be expressed in the NCI-H69 cell line (Bangur et al., 2004). In order to confirm MS4A8B protein expression in SCLC, NCI-H69 cells were incubated with either anti-

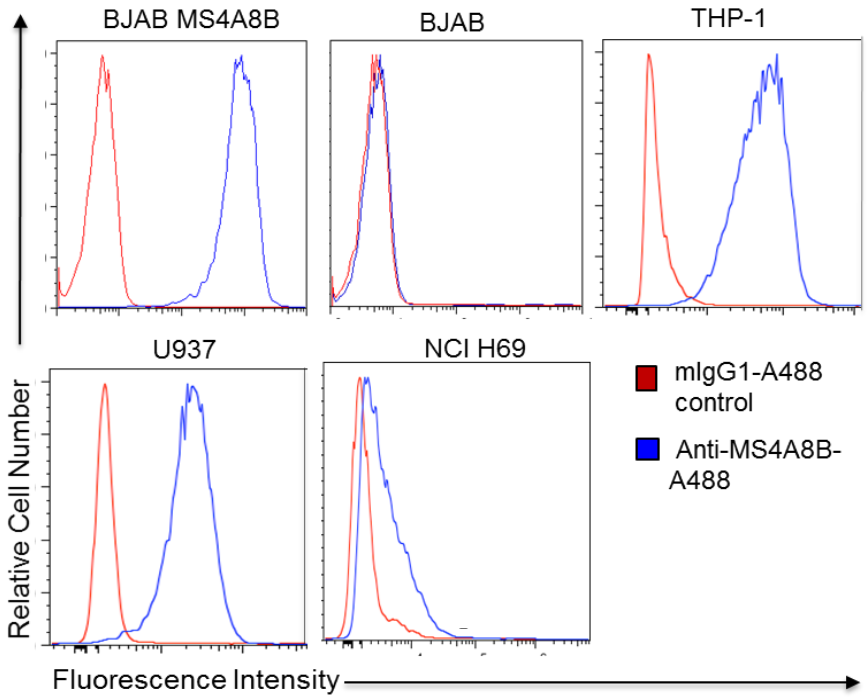

Figure 3.3: Anti-MS4A8B and mouse IgG1 binding to BJAB-MS4A8B, BJAB, U937, THP-1 and NCI-H69 cells. The hematopoietic cell lines, BJAB-MS4A8B, BJAB, U937 and THP-1 as well as the SLCC NCI H69 cell line, were stained with anti-MS4A8B-A488 (blue) or mouse IgG1-A488 isotype control (red). Cells were then analyzed by flow cytometry and gated based upon FSC and SSC (N>3).

MS4A8B-Alexa 488 or mouse IgG1-Alexa 488 isotype control and analyzed by flow cytometry. As shown in Figure 3.3, anti-MS4A8B-Alexa 488 bound to the NCI-H69 cells. Given that anti-MS4A8B binding was detected in peripheral blood gated human monocytes (Figure 3.2) anti-MS4A8B binding was also evaluated in the human THP-1 and U937 monocytic cell lines, using anti-MS4A8B-Alexa 488 or the mouse IgG1-Alexa 488 isotype control. As shown in Figure 3.3, anti-MS4A8B bound to U937 and THP-1 cells at levels that were logarithmically greater that the mouse IgG1-Alexa 488 isotype control. In addition, as previously shown in Figure 3.1, BJAB-MS4A8B-HA cells also bound anti-MS4A8B while parental BJAB cells did not.

B.4 Human IgG Blocks Anti-MS4A8B Binding to U937 and THP-1 but not BJAB-MS4A8B Cells

The experiments shown in Figure 3.2 and Figure 3.3 were performed using indirect and direct staining methods respectively. Both sets of experiments indicated specific binding of anti-MS4A8B to peripheral blood monocytes as well as the monocytic U937 and THP-1 cell lines. However, when we assessed anti-MS4A8B staining in the presence of Fc blocking buffer (human IgG) we found that anti-MS4A8B binding to monocytic U937 and THP-1 cells was blocked (Figure 3.4). The U937 and THP-1 cells express the FcγRI (CD64) and FcγRII (CD32). Since mouse IgG1 antibodies do not bind to human Fc receptors and another mouse IgG1 antibody that our lab had generated against a different protein (anti-MS4A4A) did not bind to U937 or THP-1 (Chapter 4), it appeared that blocking of anti-MS4A8B by human IgG was a specific phenomenon.

Therefore we hypothesized that MS4A8B may be in close proximity to the ligand binding α chain of an Fc receptor (CD32 or CD64) and that due to their proximity, binding of human IgG to the ligand binding α chain of an Fc receptor could have sterically hindered and prevented anti-MS4A8B from binding to its target. When we pre-incubated BJAB-MS4A4A-GFP cells, which express the low affinity FcγRII (CD32) but not the high affinity FcγRI (CD64), human IgG did not block anti-MS4A8B binding (Figure 3.4). Collectively, the data suggested that the blocking of anti-MS4A8B to its target was a specific phenomenon and might be a result of the steric hindrance from human IgG binding to CD64.

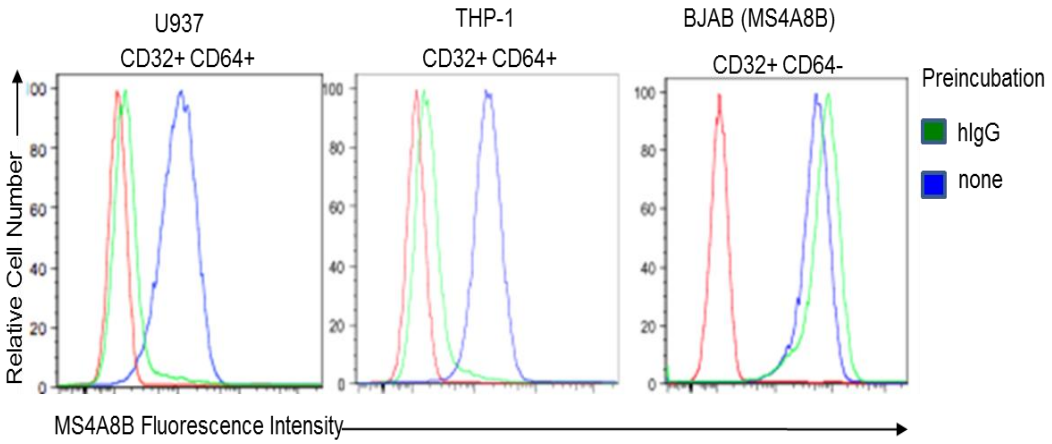

Figure 3.4: Human IgG blocks anti-MS4A8B binding to U937 and THP-1 but not BJAB-MS4A8B cells. The U937 (CD32+/CD64+), THP-1 (CD32+/CD64+) and BJAB-MS4A8B-HA (CD32+/CD64-) cell lines were pre-incubated with either 1ug of human IgG (green) or nothing (blue) for 30 minutes at 4°C. The cells were subsequently stained with 1ug anti-MS4A8B-A488 (blue) or mouse IgG1-A488 isotype control (red) for 30 minutes at 4°C and analyzed by flow cytometry. Note that human IgG blocks binding of anti-MS4A8B to U937 and THP-1 cells but not to BJAB-MS4A8B cells (N=3).

B.5 Anti-MS4A8B Blocks Binding of human IgG to THP-1 and U937 Cells

Human IgG binding to CD64 blocked the binding of anti-MS4A8B to its target in the THP-1 and U937 cell lines (Figure 3.4). Therefore, we questioned whether anti-MS4A8B binding to its target was capable of blocking human IgG binding to CD64. To examine the cross-blocking effect, the CD64 expressing THP-1 and U937 cells were pre-incubated with anti-MS4A8B or mouse IgG1 and evaluated for human IgG-Alexa 488 binding. We predicted that if CD64 is associated with MS4A8B, anti-MS4A8B binding to its epitope may sterically hinder human IgG binding to CD64. As shown in Figure 3.5A, anti-MS4A8B but not mouse IgG1 blocked binding of human IgG-Alexa 488 to the monocytic U937 and THP-1 cell lines. To determine whether blocking was concentration dependent anti-MS4A8B and mouse IgG1 were first titrated logarithmically from 10ug of anti-MS4A8B or mouse IgG1 per $1.0x10^6$ cells to 0.001ug of anti-MS4A8B or mouse IgG1 per $1.0x10^6$ cells. The U937 cells were pre-incubated with the titrated amounts of either anti-MS4A8B or mouse IgG1 and assessed for human IgG- Alexa 488 binding. As shown in Figure 3.5B, the binding of human IgG-Alexa 488 to the monocytic U937 cell line was inversely proportional to the concentration of anti-MS4A8B used to pre-incubate the cells. The cross-blocking experiment suggested that as the concentration of anti-MS4A8B used to pre-incubate the cells increased, the ability of human IgG to bind to its ligand (CD64) was increasingly reduced.

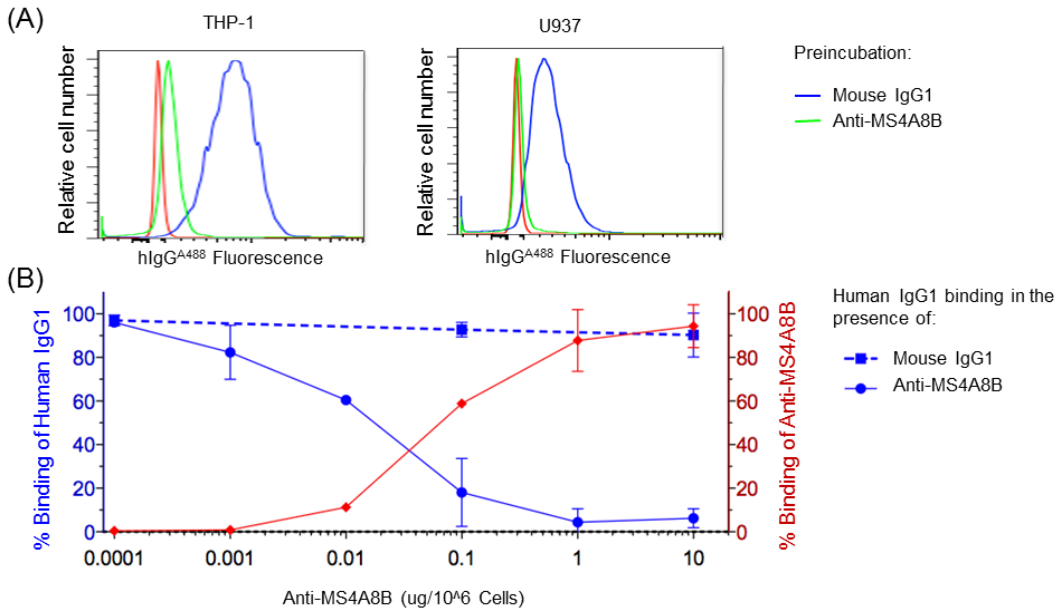

Figure 3.5: Anti-MS4A8B blocks binding of human IgG to THP-1 and U937 cells. (A) The monocytic THP-1 and U937 cell lines were pre-incubated with 1ug of mIgG1 (blue) or anti-MS4A8B (green) and subsequently evaluated for human IgG1-alexa-488 binding. Anti-MS4A8B reduced human IgG1-alexa-488 binding to THP-1 and U937 cells while mIgG1 did not. (B) The effect of anti-MS4A8B concentration on human IgG1-alexa-488 binding was also investigated by titrating anti-MS4A8B logarithmically from 10ug/10^6 cells to 1.0E-4ug/10^6 cells and evaluating human-IgG1-alexa-488 binding via flow cytometry (N=3).

B.6 Coordinate Binding of Anti-MS4A8B and Anti-CD64 to Human U937 Cells

Cross-blocking studies suggested an association between human CD64 and MS4A8B. In many cases the components of receptors and their associated signalling subunits are coordinately expressed (Hupp, Siwarski, Mock, & Kinet, 1989; San Jose, Sahuquillo, Bragado, & Alarcon, 1998). Here, coordinate expression refers to the regulation of protein expression in a manner such that the expression of one protein is related to the expression of another. In order to investigate the coordinate expression between MS4A8B and CD64, monocytic U937 cells were incubated with anti-MS4A8B-Alexa 488 as well as with anti-CD64-APC and evaluated by flow cytometry. As controls, U937 cells were also incubated with anti-MS4A8B-Alexa 488 alongside anti-CD27-PE or anti-CD45-PE, both of which are cell surface proteins expressed on U937 cells. As illustrated in Figure 3.6, anti-MS4A8B-Alexa 488 and anti-CD64-APC bound coordinately to the U937 monocytic cell line while anti-MS4A8B-Alexa 488 and anti-CD27-PE or anti-CD45-PE did not.

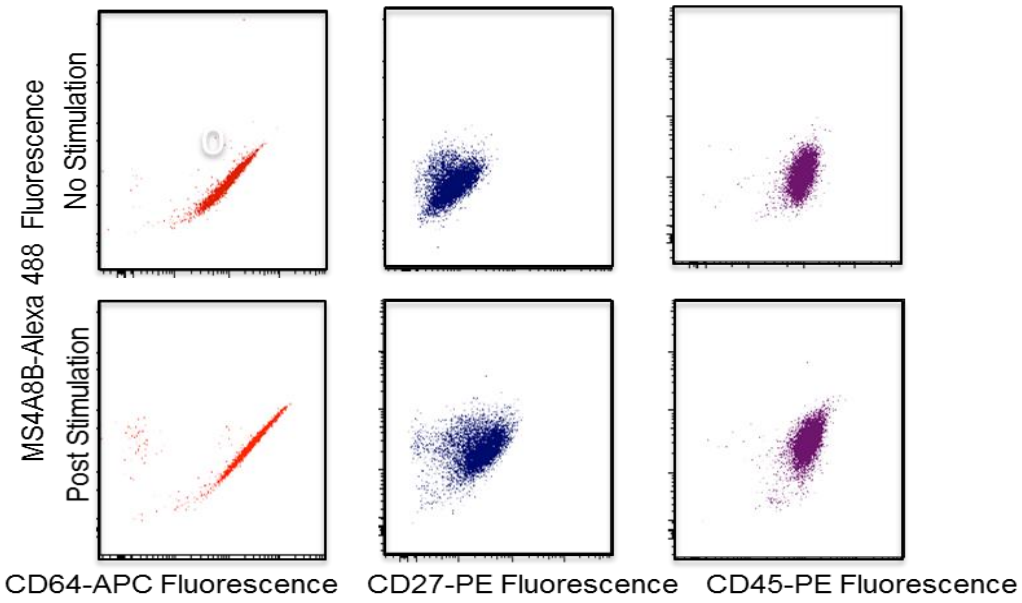

Figure 3.6: Coordinate binding of anti-MS4A8B and anti-CD64 to human U937 cells. U937 cells were stained directly with anti-MS4A8B-alexa 488 and either CD64-APC, CD27-PE or CD45-PE and analyzed by flow cytometry. Anti-MS4A8B-alexa 488 showed random staining with respect to CD27-PE (blue) and CD45-PE (purple) but stained coordinately with anti-CD64-APC (red) (N=3).

B.7 Anti-CD64 Crosslinking Reduces Anti-MS4A8B Binding to U937 Cells and the Converse

The human FcγRI complex consists of 2 γ chains associated with a single ligand binding α chain (CD64) (Falk, 2007; Mancardi et al., 2013). Crosslinking CD64 in U937 cells induces the internalization of the FcγRI complex from the cell surface (Davis, Harrison, Hutchinson, & Allen, 1995; Jones, Nusbacher, & Anderson, 1985). Consequently, extracellular binding of anti-CD64 to the FcγRI α chain is reduced. We postulated that if MS4A8B is associated with CD64, internalization of the FcγRI complex may also reduce anti-MS4A8B-Alexa 488 binding. Internalization of the FcγRI complex was induced by incubating monocytic U937 cells with anti-CD64 followed by crosslinking with goat-anti-mouse IgG (XL). As a control, cells were also incubated with the mouse IgG1 isotype control followed by the addition of the goat-anti-mouse IgG crosslinking agent. The cells were subsequently stained with anti-MS4A8B-Alexa 488 and evaluated via flow cytometry. As shown in Figure 3.7A, anti-MS4A8B-Alexa 488 binding to U937 cells was reduced in samples where the FcγRI complex internalization was believed to be induced. Similarly, we also investigated whether MS4A8B crosslinking in the monocytic U937 cell line influenced anti-CD64 binding to the α chain of the FcγRI complex. MS4A8B internalization was induced by incubating cells with anti-MS4A8B followed by crosslinking with goat-anti mouse IgG. As a control, the monocytic U937 cell line was also incubated with the mouse IgG1 followed by the addition of the goat-anti-mouse IgG crosslinking agent.

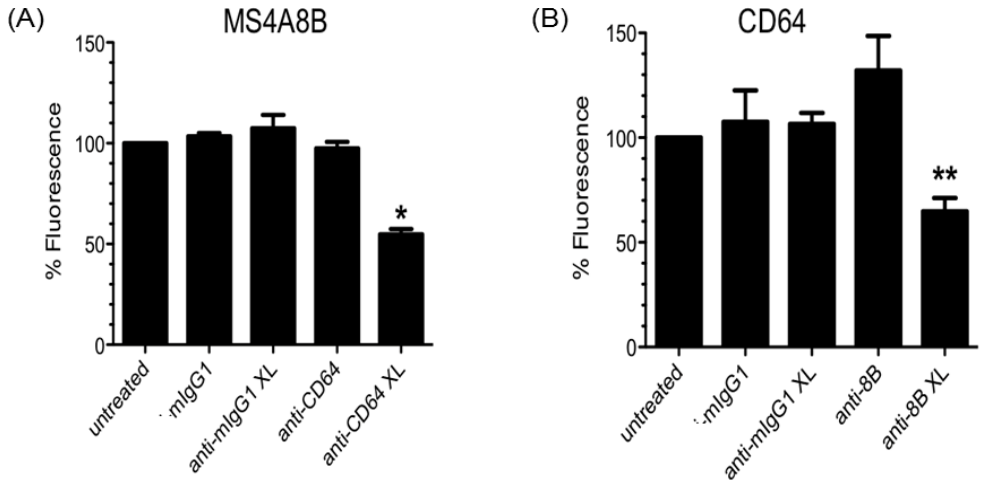

Figure 3.7: Anti-CD64 crosslinking reduces anti-MS4A8B binding and the converse. Crosslinking CD64 induces FcγRI internalization. Consequently we assessed whether crosslinking CD64 affects anti-MS4A8B cell binding. To do so, U937 cells were incubated with mIgG1 or (A) anti-CD64 ± goat-anti-mIgG (XL) to induce crosslinking. Cells were then evaluated for anti-MS4A8B-Alexa488 binding. Similarly, to investigate whether anti-MS4A8B crosslinking affects anti-CD64 binding, U937 cells were incubated with mIgG1 or (B) anti-MS4A8B ± goat-anti-mIgG (XL) and stained with anti-CD64-APC. Cells were analyzed by flow cytometry (N=3).

The cells were subsequently stained with anti-CD64 APC and evaluated for anti-CD64-APC binding via flow cytometry. As shown in Figure 3.7B, anti-CD64 binding was reduced in samples were MS4A8B internalization was believed to be induced. Collectively, the data were consistent with the possibility that MS4A8B associates with FcγRI complex.

B.8 Anti-MS4A8B co-immunoprecipitates the FcR α and γ Subunits

In order to directly evaluate the potential association between MS4A8B and the FcγRI complex, monocytic U937 cells ($1.0x10^7$ cells per sample) were lysed in 1% maltoside. The cell lysates were then divided into two equal samples. The first sample was immunoprecipitated with the mouse IgG1 isotype control, while the second sample was immunoprecipitated using our mouse monoclonal anti-MS4A8B antibody. The samples were analyzed by an anti-FcR γ western blot. As shown in Figure 3.8A, anti-MS4A8B but not mouse IgG1 immunoprecipitated a protein with molecular weight consistent with that of the FcR γ subunit (10kDa). In a second experiment, U937 cells ($1.0x10^7$ cells per sample) were similarly lysed in 1% maltoside and divided into four equal samples. The first sample was immunoprecipitated with the mouse IgG1 isotype control while the second sample was immunoprecipitated using our mouse monoclonal anti-MS4A8B antibody. As controls, the third and fourth samples were immunoprecipitated with anti-CD64 and anti-FcR γ antibodies. When analyzed by an anti-CD64 western blot, a protein with molecular weight consistent with the FcγRI α subunit (75 kDa) was immunoprecipitated with anti-MS4A8B, anti-CD64, and anti-γ chain but not mouse IgG1 (Figure 3.8B).

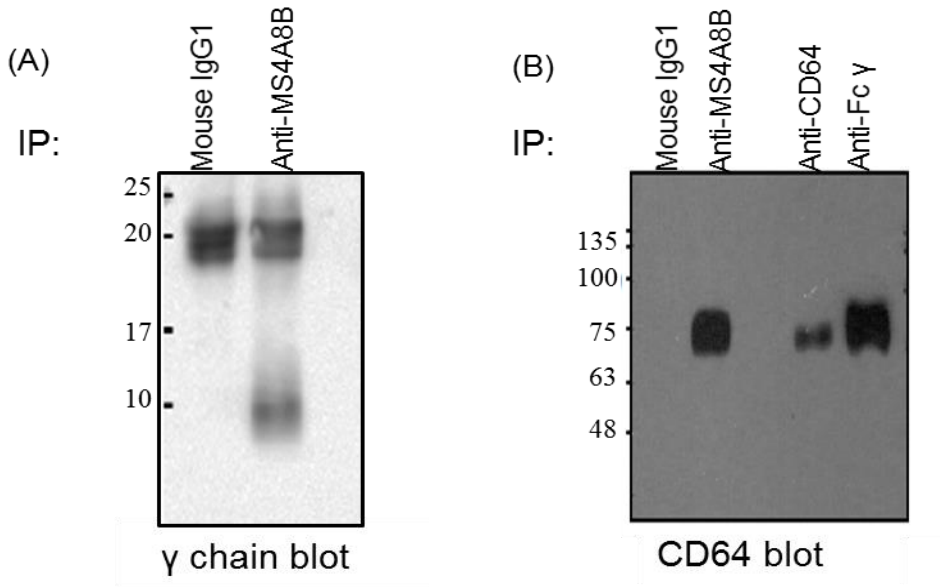

Figure 3.8: Anti-MS4A8B Immunoprecipitates FcR γ and α Subunits. U937 cells were lysed in 1% maltoside and immunoprecipitated with (A) mIgG1 or mouse anti-MS4A8B. Samples were then analyzed by an anti-FcR γ western blot. In a second experiment, U937 lysates were immunoprecipitated with mouse IgG1, anti-MS4A8B, anti-CD64 or anti-Fcγ subunit. Samples were then analyzed by an anti-CD64 western blot. As shown, anti-MS4A8B immunoprecipitates the 12kDa Fcγ subunit (A) and the 75 kDa CD64 α chain (B).

These immunoprecipitation data supported the hypothesis that MS4A8B associates with the FcγRI complex.

B.9 Anti-MS4A8B-Alexa 488 Binds to CD64 expressing IIA1.6 Cells

Immunoprecipitation data suggested an association between MS4A8B and the FcγRI α and γ subunits (Figure 3.8). Consequently, we were interested in identifying whether MS4A8B was required for FcγRI mediated cellular functions. In order to investigate the potential role of MS4A8B within the receptor complex, we required a cell line that expressed the human FcγRI α and γ subunits without MS4A8B. The objective was to ectopically express MS4A8B alongside the FcγRI α and γ subunits and evaluate FcγRI mediated functions in the presence and absence of MS4A8B. Therefore, we obtained the IIA1.6 cell line (University Hospital Utrecht, Netherlands) that ectopically expressed the human FcγRI α and γ subunits. The IIA1.6 cell line is thought to be of B-cell origin and is a mouse cell line. Therefore the IIA1.6 cell line not expected to express human MS4A8B, however, unexpected binding of anti-MS4A8B-Alexa 488 to the IIA1.6 B cell line was later observed (Figure 3.9). Anti-MS4A8B-Alexa 488 binding was unexpected for several reasons: I) the IIA1.6 B cell line is of mouse origin and ectopically expressed the FcγRI α and γ subunits but was not transfected with MS4A8B and II) previous staining experiments indicated that anti-MS4A8B did not bind to peripheral blood gated lymphocytes (Figure 3.3). Nonetheless, the binding was clear. Therefore, we considered the possibility that anti-MS4A8B may be binding directly to the FcγRI ligand binding α chain (CD64) ectopically expressed in the IIA1.6 B cell line.

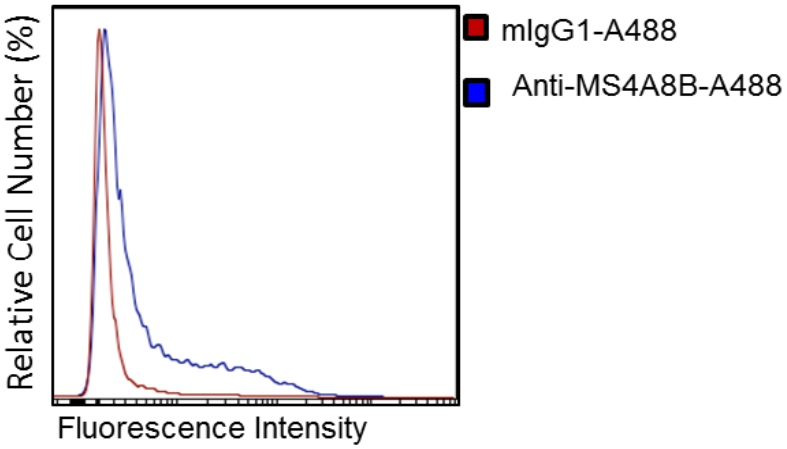

Figure 3.9: Anti-MS4A8B-A488 binding to CD64 expressing IIA1.6. As shown in the left panel, IIA1.6 B cells ectopically expressing CD64 were stained with anti-MS4A8B-A488 (blue) and mIgG1-A88 isotype control (red). Cells were subsequently analyzed via flow cytometry. Note, IIA1.6-CD64 cells bound to anti-MS4A8B-A488 (N=2).

B.10 Anti-MS4A8B Binds to Human CD64 Transfected HEK293 Cells

To evaluate potential binding of anti-MS4A8B to human CD64, HEK293 cells were transfected with either a CD64 plasmid or an empty vector control (mock) using Lipofectamine 2000. Two days post transfection, the CD64 and mock transfected samples were stained with anti-CD64 APC or the corresponding mouse IgG1-APC isotype control. As shown in Figure 3.10A (left panel), anti-CD64-APC bound to HEK293 cells transfected with the CD64 plasmid but not the mock transfected cells, indicating that CD64 was successfully expressed. In the same experiment, a second set of CD64 and mock transfected cells were incubated with anti-MS4A8B or the mouse IgG1 isotype control and detected via a secondary incubation with the goat anti-mouse IgG-PE antibody and analysis by flow cytometry. As shown in Figure 3.10A (right panel), anti-MS4A8B bound to CD64 transfected cells, but not to mock transfected cells. The data indicated anti-MS4A8B binds to human CD64. In a subsequent experiment, we evaluated whether anti-CD64 binds to MS4A8B. Here, HEK293 cells were transfected with an MS4A8B plasmid or an empty vector (mock). Two days post transfection, the MS4A8B and mock transfected samples were incubated with anti-MS4A8B or the mouse IgG1 isotype control followed by secondary staining with the goat-anti-mouse IgG-PE and analysis via flow cytometry.

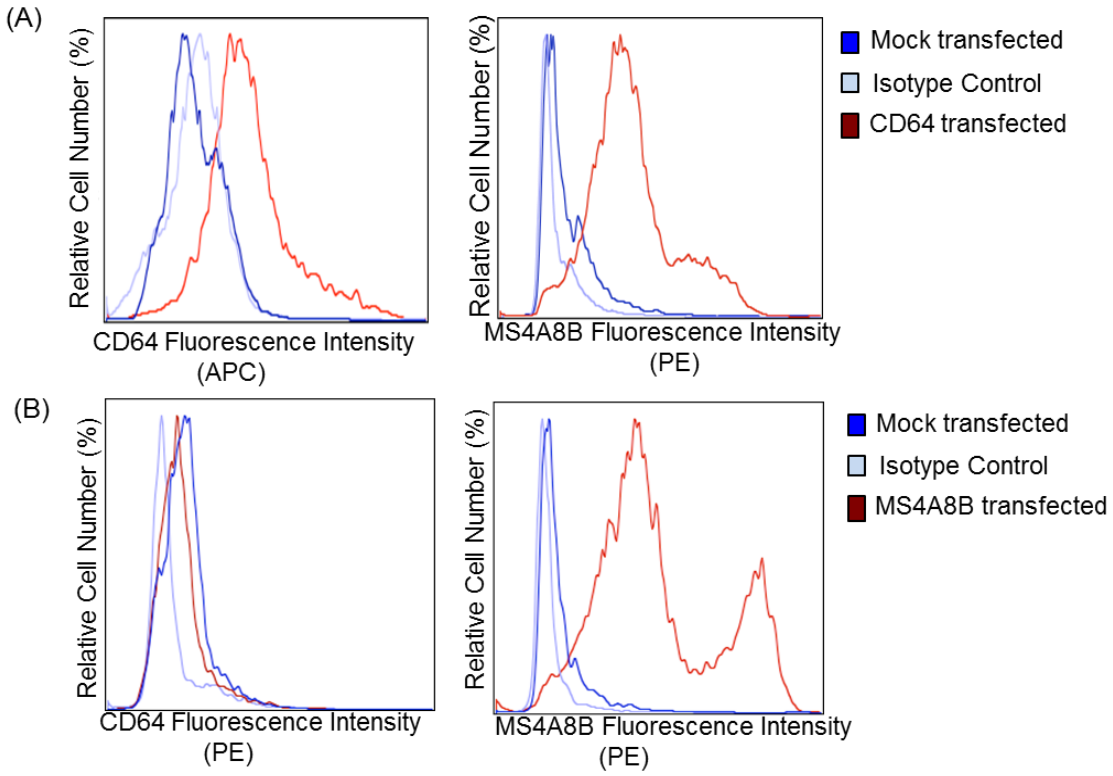

Figure 3.10: Anti-MS4A8B binds to human CD64 transfected HEK293 cells. (A) HEK293 cells were transfected using 2ul of Lipofectamine 2000 and either 2ug of CD64 plasmid or no vector (mock). Two days post transfection, CD64 and mock transfected cells were stained directly with mIgG1-APC, anti-CD64-APC (left) or indirectly with mIgG1 or anti-MS4A8B + goat-anti-mIgG-PE (right), as indicated. Cells were then immediately analyzed by flow-cytometry. As illustrated in the right panel, anti-MS4A8B bound to HEK293 cells ectopically expressing CD64 but not to mock transfected cells. (B) HEK293 cells were also transfected with MS4A8B and stained with anti-MS4A8B and anti-CD64. As shown in the left panel, CD64 did not bind to HEK293 cells ectopically expressing MS4A8B (N=3).

As shown in Figure 3.10B (left panel), anti-MS4A8B bound to HEK293 cells transfected with the MS4A8B plasmid but not to mock transfected cells, indicating that MS4A8B was successfully expressed. In the same experiment, a second set of MS4A8B and mock transfected cells were incubated with anti-CD64 or the mouse IgG1 isotype control and similarly detected via a secondary incubation with the goat anti-mouse IgG-PE antibody and analysis via flow cytometry. As shown in Figure 3.10B (right panel), anti-CD64 did not bind to MS4A8B transfected cells. Collectively, the data indicated that anti-MS4A8B bound to the ligand binding α chain of the FcγRI complex (CD64).

3.11 Anti-MS4A8B Fab' Binding to the FcγRI Expressing U937 Cell Line

Anti-MS4A8B binding to human CD64 was unexpected given that it was believed to be of the mouse IgG1 isotype. Nonetheless, anti-MS4A8B binding could have been occurring through either Fc mediated interactions or as a consequence of anti-MS4A8B variable domain interactions with human CD64 (off-target). In order to evaluate both possibilities, anti-MS4A8B-fab fragments were generated. Anti-MS4A8B-fab fragments were generated by cleavage of whole anti-MS4A8B with Ficin, in the presence of 4mM cysteine. U937 cells, which natively express the FcγRI complex, were then incubated with whole anti-MS4A8B, mouse IgG1 isotype control, or anti-MS4A8B-fab fragments and detected by secondary incubation with goat-anti-mouse IgG-PE and flow cytometric analysis. As shown in Figure 3.11 (left panel), anti-MS4A8B-fab fragments had limited binding to U937 cells.

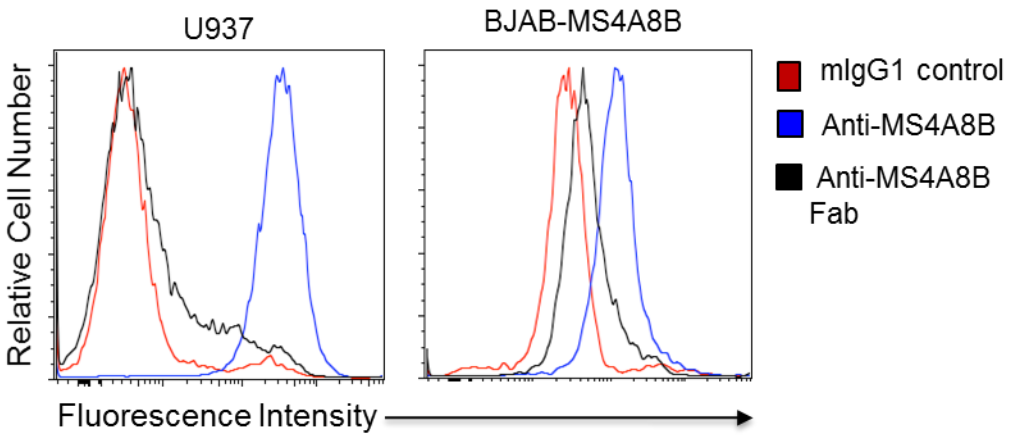

Figure 3.11: Anti-MS4A8B Fab' displays limited to no binding to the FcγRI expressing U937 cells. FcγRI expressing U937 cells were stained with whole anti-MS4A8B and an Fab' anti-MS4A8B fragment, which lacks the Fc region. As demonstrated in the left panel, whole anti-MS4A8B (blue) binds to U937 cells while the Fab' fragments displayed limited to no binding (black). To ensure the immunoreactivity of the anti-MS4A8B Fab' fragment BJAB-MS4A8B cells were stained with whole anti-MS4A8B and anti-MS4A8B Fab' (left panel) (N=2).

In the same experiment, the immunoreactivity of the anti-MS4A8B-fab fragment was confirmed by incubating BJAB-MS4A8B-GFP cells, which do not express the FcγRI complex but ectopically express MS4A8B, with whole anti-MS4A8B, anti-MS4A8B-fab or mouse IgG1 isotype control. Antibody binding was detected by incubation with goat anti-mouse IgG-PE and flow cytometric analysis. As shown in Figure 3.11 (right panel), anti-MS4A8B-fab bound to BJAB-MS4A8B-GFP cells at levels greater than the isotype control, indicating specific reactivity. Collectively, the data suggested that anti-MS4A8B, isotyped as a mouse IgG1 antibody, was binding to human CD64 by Fc mediated interactions.

3.12 MS4A8B mRNA Expression in Hematopoietic Cells and the NCI-H69 Cell Line

The Fc mediated binding of anti-MS4A8B to human CD64 led us to question MS4A8B expression in previously evaluated cells. As a result, we performed a series of investigations which included the analysis of MS4A8B mRNA expression. The objective was to determine whether MS4A8B mRNA was expressed in cells where anti-MS4A8B binding was previously identified. In order to accomplish this, MS4A8B mRNA was reverse transcribed and amplified for a total of 36 cycles from the monocytic U937 and THP-1 cells, the BJAB and BJAB-MS4A8B-GFP cells, and the small cell lung carcinoma, NCI-H69 cell line. As shown in Figure 3.13B MS4A8B mRNA was detected at elevated levels in BJAB cells ectopically expressing MS4A8B-GFP and in the NCI-H69 SCLC cell line.

The presence of mRNA in both cell lines was consistent with anti-MS4A8B binding (Figure 3.12A). The parental BJAB cell line expressed relatively low levels of MS4A8B mRNA (Figure 3.12B) consistent with a previous report (Liang & Tedder, 2001) but did not bind to anti-MS4A8B (Figure 3.12A). In contrast, MS4A8B mRNA could not be detected in the CD64 expressing U937 and THP-1 cell lines (Figure 3.12B).

3.13 Anti-MS4A8B is of the Mouse IgG2a Isotype

Anti-MS4A8B was initially identified as a mouse IgG1 isotype. Literature analysis indicates that mouse IgG1 antibodies do not bind to human Fc receptors. Consequently, the Fc mediated binding of anti-MS4A8B to human CD64 was puzzling. As a result, the isotype of anti-MS4A8B was re-evaluated. The isotype was first re-evaluated by flow cytometric analysis using a cell line which natively expressed MS4A8B (NCI-H69). The objective was to incubate NCI-H69 cells with our monoclonal mouse anti-MS4A8B antibody and determine whether the goat-anti-mouse IgG1-PE or the goat-anti-mouse IgG2a-PE antibodies were capable of detecting it. As shown in Figure 3.13A, anti-MS4A8B binding was detected following incubation with the goat-anti-mouse IgG2a-PE antibody but not following incubation with the goat anti-mouse IgG1-PE antibody. Anti-MS4A8B was then sent for re-isotyping by an independent commercial facility, Green Mountain Antibody Services. Using the MAGPIX Mouse Isotyping Assay, Green Mountain Antibody Services identified anti-MS4A8B to react as a mouse IgG2a isotype and not a mouse IgG1 (Figure 3.13B).

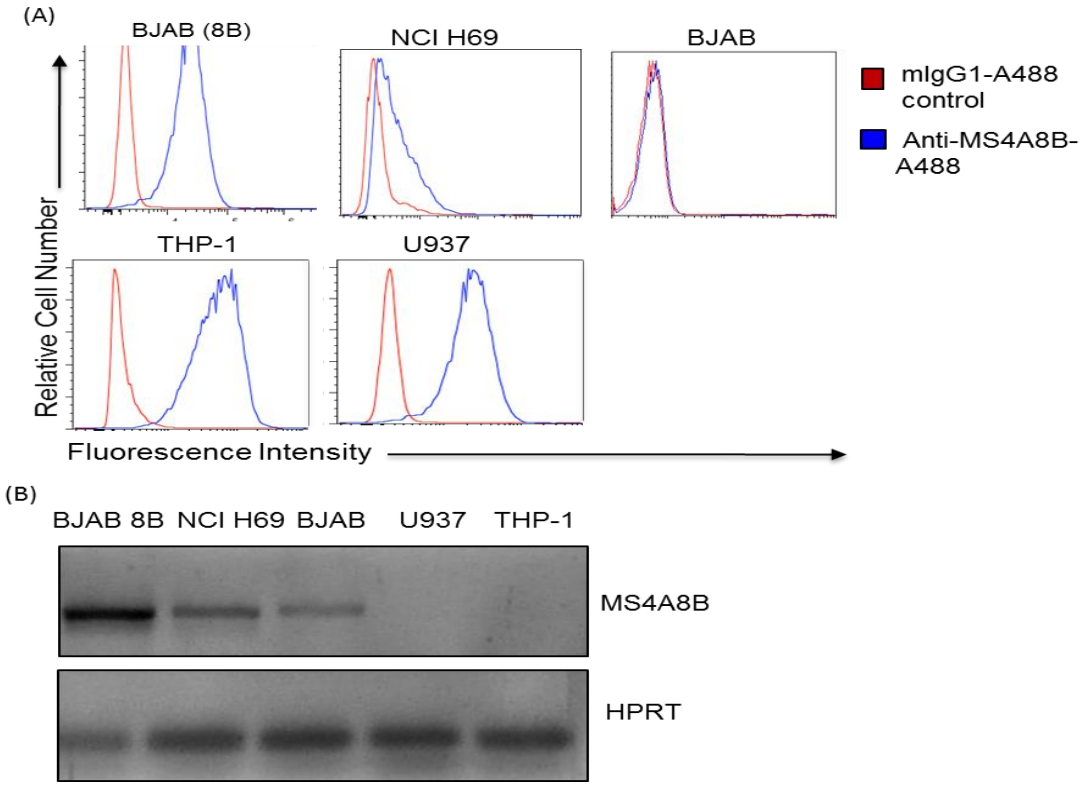

Figure 3.12: Anti-MS4A8B binding and mRNA expression in hematopoietic and NCI-H69 cell lines. (A) Four hematopoietic cell lines (U937, THP-1, BJAB-MS4A8B-GFP and parental BJAB) as well as the NCI-H69 SCLC cell line were stained with anti-MS4A8B-alexa 488 (blue) or the mouse IgG1-Alexa 488 isotype control (red). Cells were gated based upon FSC and SSC and analyzed by flow cytometry. Note, parental BJAB cells show no observable MS4A8B staining, NCI-H69 show moderate staining, while the remaining cells present high anti-MS4A8B staining. Also note that the data shown in (A) is repeated from Figure 3.3 to facilitate comparison with mRNA expression as shown by PCR in (B). The same cell lines when analyzed by PCR for MS4A8B mRNA expression show that U937 and THP-1 cells do not express MS4A8B mRNA while the remaining cells do (N=3).

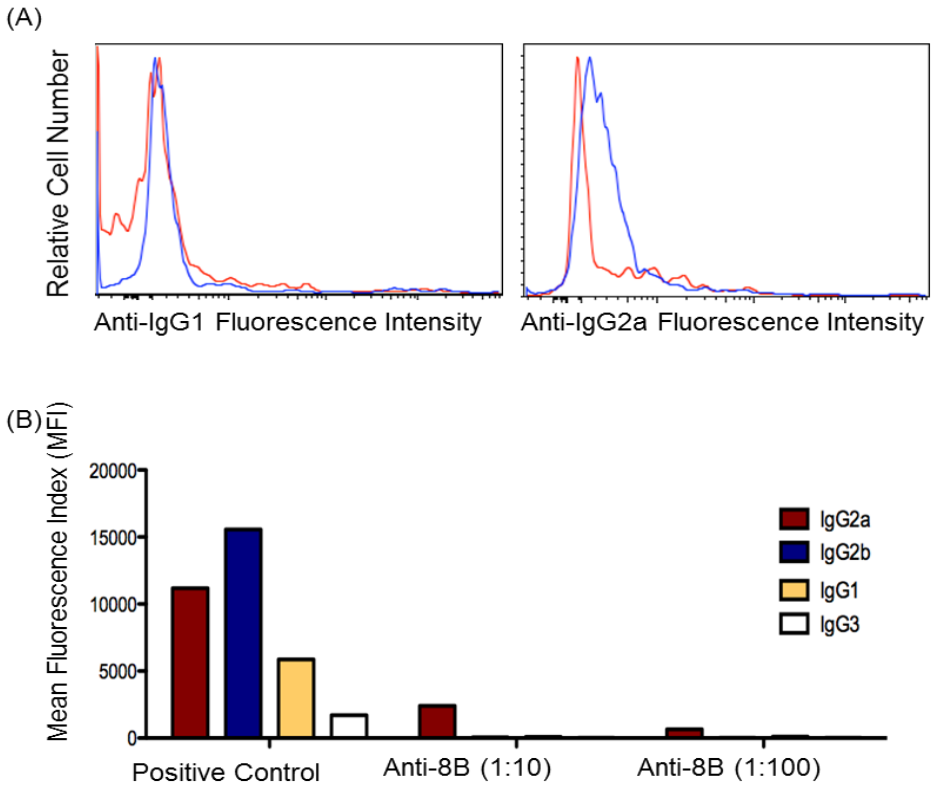

Figure 3.13: Anti-MS4A8B is of the mouse IgG2a isotype. A) The SCLC NCI-H69 cell line was stained with anti-MS4A8B or mouse IgG1 isotype control and detected with either goat-anti-mouse-IgG1-PE (left) or goat-anti-mouse-IgG2a-PE (right). Anti-MS4A8B binding was detected with goat-anti-mouse IgG2a (right) but not goat-anti-mouse IgG1 (left). B) The isotype of anti-MS4A8B was confirmed via the MAGPIX Mouse Isotyping Assay (Green Mountain Antibody Services). As shown, anti-MS4A8B stained positive for mIgG2a (1:10 and 1:100) but for anti-IgG1.

3.14 Anti-MS4A8B and Mouse IgG2a Binding to BJAB, U937, THP-1 and NCI-H69 Cells

With the identification that anti-MS4A8B was not of the mouse IgG1 subclass, protein expression was re-evaluated using the correct isotype control. The hematopoietic cell lines, BJAB, BJAB-MS4A8B, U937 and the small lung cell carcinoma, NCI H69 cell line, were all incubated with anti-MS4A8B or mouse IgG2a isotype control. Antibody binding was then detected by a secondary incubation with goat-anti-mouse IgG-PE and analysis by flow cytometry. MS4A8B was not detected in the monocytic U937 cell-line (Figure 3.14), consistent with mRNA analysis (Figure 3.12B). Anti-MS4A8B binding to the FcγRI negative BJAB, BJAB-MS4A8B-GFP, and NCI-H69 was consistent with previous antibody binding experiments. Specifically, BJAB cells did not express MS4A8B, while the BJAB-MS4A8B-GFP and NCI-H69 cell line both expressed MS4A8B. This is expected since BJAB, BJAB-MS4A8B-GFP and NCI-H69 cells do not express human CD64.

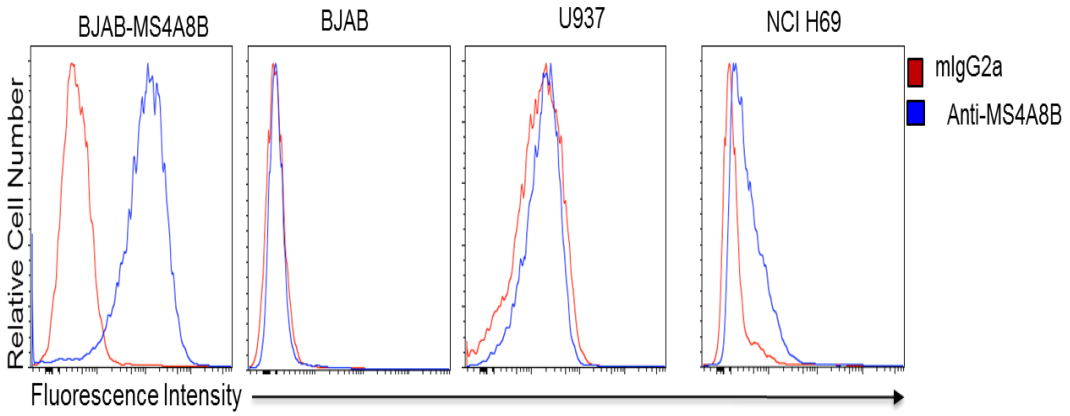

Figure 3.14: Anti-MS4A8B and mouse IgG2a binding to BJAB-MS4A8B, BJAB, U937, and NCI-H69 cells. The hematopoietic cell lines, BJAB-MS4A8B, BJAB, U937 and the SLCC NCI H69 cell line were stained with anti-MS4A8B (blue) or mouse IgG2a isotype control (red). Live cells were gated based upon FSC and SSC and then analyzed by flow cytometry. Note, anti-MS4A8B bound to BJAB cells ectopically expressing MS4A8B (BJAB-MS4A8B) and NCI-H69 cells but not to parental BJAB or U937 cells.

3.15 MS4A8B is not expressed in M1 and M2 Monocyte Derived Macrophages

MS4a8A, is expressed in monocyte derived M2 but not M1 macrophages (Michel et al., 2013). Therefore we first evaluated whether MS4A8B protein was expressed in monocyte derived M1 and M2 macrophages. Here, peripheral blood mononuclear cells were respectively differentiated to M1 or M2 macrophages by treatment with I) 40ng of GM-CSF for 5 days followed by 100ng of LPS and 20ng of IFNγ per ml of growth media for 2 days or II) 25ng M-CSF for 5 days and then 15ng of IL-4 per ml of growth media for 2 days. Cells were then incubated with antibodies directed against cell surface markers of M1 and M2 differentiation (CD14, CD32, and CD80) or with anti-MS4A8B-Alexa 488 or the appropriate isotype control. Literature analysis indicates that M1 macrophages are characterized by the presence of CD80, the absence or limited expression of CD14 and relative to M2 macrophages, reduced expression of CD32 (Verreck et al., 2006). In contrast, in M2 macrophages these include the lack of CD80 expression (Mantovani et al., 2004; Rey-Giraud et al., 2012) and relatively greater levels of CD14 and CD32 (Verreck et al., 2006). As indicated in Figure 3.15, M1 (A) and M2 (B) macrophages expressed the aforementioned differentiation markers at levels described in the literature. However, MS4A8B was not expressed in either subset. To confirm protein expression analysis, MS4A8B mRNA was amplified from M1 and M2 macrophages. We also evaluated MS4A8B mRNA expression in CD14+ monocytes and monocyte derived dendritic cells, donated by the lab of Dr. Christopher Mody. Here, MS4A8B mRNA was not detected in any of the mentioned hematopoietic cell populations (Figure 3.15C)

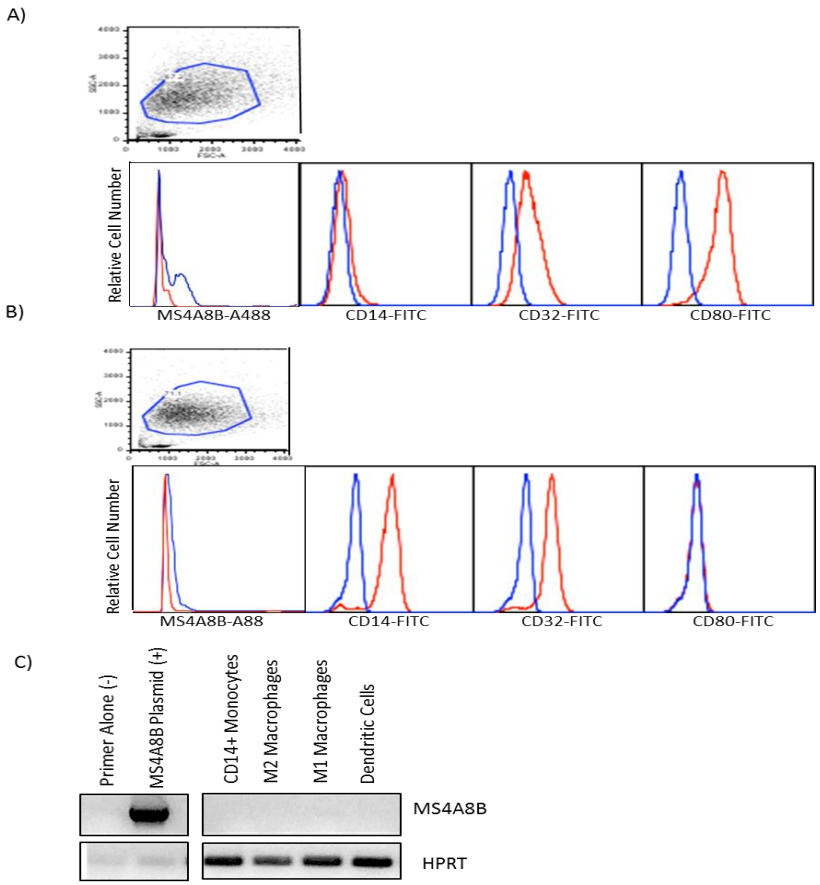

Figure 3.15 MS4A8B is not expressed in M1 and M2 monocyte-derived macrophages. Primary monocytes were differentiated into M1 or M2 subsets by respectively treating monocytes with: I) 40ng/mL GM-CSF 5 for days and then 100ng/ml of LPS plus 20ng/ml of IFNγ for 2 days or II) 25ng/mL M-CSF for 5 days and then 15ng/ml of IL-4 for 2 days. To investigate MS4A8B protein expression M1 (A) and M2 (B) macrophages were stained with anti-MS4A8B-A488, anti-CD14-FITC, anti-CD32-FITC, or anti-CD80-FITC (red) and the appropriate isotype controls (blue) as indicated. Additionally, M1 and M2 macrophages were also evaluated for MS4A8B mRNA expression (C), alongside CD14+ monocytes and monocyte derived dendritic cells that were donated by Dr. Christopher Mody's lab (N=3).

C. Discussion

The results described herein support the absence of human MS4A8B expression in resting whole white blood cell gated monocytes, granulocytes, and lymphocytes. In addition, unlike its mouse homolog, we identified that MS4A8B is not expressed in monocyte derived M2 or M1 macrophage subsets (Figure 3.15). However, we confirmed MS4A8B expression in the human NCI-H69 small cell lung carcinoma cell line. It was interesting that despite sequence and structural homology and considerable amino acid identity with its mouse homolog, MS4A8B was not found to be expressed in any of the evaluated hematopoietic cell populations. Recently, MS4A8B protein expression was identified in epithelial cells comprising the prostate (Ye et al., 2014) and in the luminal side of the colon (Michel et al., 2013). The expression of MS4A8B within the small cell lung carcinoma, prostate, and colonic epithelium, suggests that the previously identified restricted patterns of MS4A8B tissue mRNA expression (J. Zuccolo et al., 2013) may be due to its presence in specific cells of epithelial but not hematopoietic origin.

Anti-MS4A8B was initially identified as of the mouse IgG1 isotype using an ELISA based isotyping assay (Invitrogen). The ELISA based assay provided antigen independent identification of the anti-MS4A8B isotype by using microplates that were pre-coated with class- or subclass- specific antibodies (IgM, IgA, IgG1, IgG2a, IgG2b, or IgG3). The antibodies target the C_{H2} and C_{H3} domains of the immunoglobulin heavy chain, which collectively form part of the Fc region of an antibody and differ between an antibody class and subclass. Since the assay employs anti-class- and anti-subclass specific

antibodies, which do not cross react, it is considered as both a sensitive and specific assay for isotype determination (Arista, Ferraro, Cascio, Vizzi, & di Stefano, 1995; Jonsson, Arnason, & Valdimarsson, 1986; Wild, 2013). In addition, the assay is commonly used for isotype determination and is also considered reliable (Wild, 2013). However, surprisingly, anti-MS4A8B was inaccurately isotyped as of the mouse IgG1 subclass using the ELISA based antibody isotyping assay. The incorrect isotyping could have been due to several reasons. Initially, we questioned whether the anti-MS4A8B producing hybridoma consisted of two distinct clones: one which produced an antibody of the mouse IgG1 subclass and another which produced an antibody of the mouse IgG2a subclass. However, this was questionable for the following reasons: I) a series of limiting dilutions were performed to isolate a single anti-MS4A8B producing hybridoma clone and II) the ELISA based isotyping assay, which was first used to classify the isotype of anti-MS4A8B indicated that it displayed elevated reactivity with only anti-IgG1 but not both anti-IgG1 and anti-IgG2a. Re-isotyping experiments similarly identified elevated anti-MS4A8B reactivity with only a single IgG subclass (Figure 3.13). For similar reasons, it is also unlikely that the anti-MS4A8B producing hybridoma clones spontaneously switched production of a mouse IgG1 antibody to a mouse IgG2a antibody—an effect which is known to occur at low frequency in an exceeding small number of hybridoma cells during culture (Radbruch, Bruggemann, Liesegang, & Rajewsky, 1982; Radbruch, Liesegang, & Rajewsky, 1980).

The isotype of anti-MS4A8B was independently re-evaluated three times. Each experiment employed a different method of isotype detection. The first experiment utilized a cassette method and was performed by The SACRI Antibody Services (University of Calgary). The second method involved the incubation of MS4A8B expressing cells with anti-MS4A8B followed by flow cytometric detection using IgG specific anti-subclass antibodies (Figure 3.13A). In both of these latter cases, the identification methods classified anti-MS4A8B as of the mouse IgG2a isotype. The last re-isotyping experiment was performed by Green Mountain Antibody Services and used the MAGPIX Isotyping Assay. The MAGPIX Isotyping Assay is a quantitative test which employs beads associated with anti-class and anti-subclass specific antibodies to identify an immunoglobulin isotype (Houser, 2012). The MAGPIX isotyping assay also identified anti-MS4A8B as mouse IgG2a and not mouse IgG1 isotype. However, since it is a quantitative assay, it was able to identify that the reactivity of anti-MS4A8B with anti-IgG2a subclass specific antibodies was unusually low (Figure 3.13B). Further clarification with Green Mountain Antibody Services indicated that such limited reactivity is rare. Consequently, it is probable that there are unique features or characteristics pertaining to our mouse monoclonal anti-MS4A8B antibody which may have contributed to the initial mis-isotyping by the SACRI Antibody Services (University of Calgary).

An immunoglobulin molecule consists of two identical heavy and two identical light chains that are linked together by disulfide linkages. The disulfide linkages are not rigid, but rather form a flexible tether, allowing for the antibody molecules to attain

numerous three dimensional configurations (Jimenez, Salazar, Baldridge, & Romesberg, 2003; Murphy K, 2008). Some configurations may result in the presentation of antibody domains that are capable of attracting other antibody molecules via non-covalent interactions and resulting in their aggregation. Indeed, aggregation of immunoglobulin molecules is a well-defined phenomenon and occurs as a result of both Fc and non-Fc mediated antibody-antibody interactions (Correia, 2010; Zhang, Cui, & Gross, 2014). Aggregation of anti-MS4A8B, particularly at the Fc domain, could mask the epitopes that are typically targeted by anti-class and anti-subclass antibodies. In this case, anti-MS4A8B may possess structural or biochemical features that increase its susceptibility to immunoglobulin protein aggregation. Differences in post-translational modifications in immunoglobulin molecules, such as variations in glycosylation and fucosylation, have been recently shown to contribute to their structural stability and susceptibility to aggregation (Correia, 2010; Zhang et al., 2014; Zheng, Bantog, & Bayer, 2011). Specifically, differences in the extent of antibody glycosylation can affect the stability of the Fc containing C_{H2} domain, resulting in its unfolding and eventually the increased aggregation about the Fc region (Zheng et al., 2011). Inhibiting or reversing immunoglobulin aggregation is relatively difficult to achieve. Protein aggregation studies have indicated that the antibody isolation, purification, and freeze thaw processes itself can substantially contribute to immunoglobulin aggregation (Zhang et al., 2014). Recently, a biochemical analysis of human IgG1 and IgG2 molecules documented that human IgG2 is more susceptible than IgG1 to aggregation and unfolding under high salt

and acidic pH conditions (Hari, Lau, Razinkov, Chen, & Latypov, 2010). Consequently, it is possible that anti-MS4A8B possesses unique structural or biochemical features that masked its Fc region and contributed to its initial mis-isotyping as mouse IgG1 and not mouse IgG2a. Aggregation may also account for why the MAGPIX assay identified low reactivity of anti-MS4A8B with anti-IgG2a subclass specific antibodies (Figure 3.13B).

Using anti-MS4A8B, which we initially believed to be of the mouse IgG1 isotype, we obtained data suggesting that MS4A8B was expressed in monocytes (Figure 3.2; Figure 3.3) and associated with the α and γ subunits of the human FcγRI complex (Figure 3.8). It was not until we identified the binding of anti-MS4A8B to the murine IIA1.6 B cell line (Figure 3.9), which ectopically expressed the human FcγRI α and γ subunits that we began to question its non-specific or off-target binding. The IIA1.6 cell line is a murine B-cell line that was transfected to ectopically express the human FcγRI α (CD64) and γ subunits but not MS4A8B (van Vugt et al., 1996). Although the IIA1.6 cell line was not believed to express human MS4A8B it bound anti-MS4A8B-Alexa 488 (Figure 3.9). We considered whether anti-MS4A8B may be binding to human CD64 but at this point we were not convinced for several reasons. First, although the IIA1.6 cell line is a murine B-cell line, it possesses characteristics that resemble a monocytic and macrophage cell line, such as robust phagocytic potential and the presence of monocytic and macrophage cell surface markers (van Vugt et al., 1996). Since MS4a8A, the mouse homolog of MS4A8B, is known to be expressed in macrophage subsets (Schmieder et al., 2011) we questioned whether the mouse homolog was also expressed in the murine

IIA1.6 cell line – which displayed characteristics of mouse monocytes and macrophages. In that case, our monoclonal anti-MS4A8B antibody might have been cross reacting with conserved amino sequences in the extracellular domain of the murine MS4a8A protein. Nevertheless, based upon the aforementioned experiment we evaluated the possibility that anti-MS4A8B may bind to human CD64.

To evaluate the possibility that anti-MS4A8B bound to human CD64 we obtained HEK 293 cells, which do not natively express human CD64. They were subsequently transfected with or without human CD64 and evaluated for anti-MS4A8B binding. Here, anti-MS4A8B bound to Hek-293 cells ectopically expressing CD64 but not to the mock transfected control (Figure 3.10A). The study provided the first clear evidence that anti-MS4A8B was binding directly to human CD64. Since anti-MS4A8B-fab fragments displayed essentially no binding to human CD64 expressing cells (U937) (Figure 3.11), we realized that the intact antibody was binding to human CD64 by Fc mediated interactions.

The identification of anti-MS4A8B as a mouse IgG2a immunoglobulin molecule (Figure 3.13) provided an explanation for I) the Fc mediated interaction of anti-MS4A8B with human CD64 (Figure 3.10A) and consequently II) anti-MS4A8B binding to CD64 expressing cells (Figure 3.2; Figure 3.3). Immunoglobulin and plasmon resonance based studies have repeatedly shown mouse IgG1 is not capable of binding to human CD64. However, mouse IgG2a binds to human CD64 by high affinity Fc mediated interactions

(Falk, 2007; Mancardi et al., 2013). No other human Fc receptor is capable of binding mouse IgG2a (Bruhns, 2012).

Mouse IgG2a-CD64 Fc mediated interactions also provides an explanation for anti-MS4A8B binding to CD64 expressing cells in the absence of MS4A8B mRNA. Expression analysis indicates human CD64 is expressed in monocytes (Falk, 2007; van der Poel et al., 2011). Consequently, despite the absence of MS4A8B mRNA (Figure 3.12), anti-MS4A8B binding to the U937 and THP-1 monocytic cell lines (Figure 3.3) and peripheral blood gated monocytes (Figure 3.2) can be attributed to anti-MS4A8B Fc mediated interactions with human CD64 (Figure 3.10A). Indeed, when human CD64 was saturated with its ligand, human IgG, subsequent binding of anti-MS4A8B was not observed in the monocytic U937 and THP-1 cells lines (Figure 3.4). Similarly, anti-MS4A8B binding among the classical (CD64 high), alternative (CD64 low), and intermediate (CD64 intermediate) monocytes (Figure 3.2B) can also be attributed to differential expression of human CD64 (Tallone et al., 2011). In congruence with mRNA analysis, re-evaluation of anti-MS4A8B binding in the U937 and THP-1 monocytic cell lines with the correct isotype control (mouse IgG2a) identified no specific binding (Figure 3.14). In contrast, in cells where CD64 was not expressed the initial analysis of anti-MS4A8B binding paralleled the patterns of expression identified with the correct isotype Figure 3.14). Consequently, expression analysis indicates MS4A8B is not expressed in monocytes, granulocytes, and lymphocytes and confirmed expression in the NCI-H69 cell line. Interestingly, although we were able to consistently identify

MS4A8B protein and mRNA expression in the NCI-H69 cell line (Figure 3.12; Figure 3.14), our results differed from those published by Bangur and Colleagues (2004). Specifically, Bangur and Colleagues identified MS4A8B protein expression at levels that were at least 2 log-fold greater than the appropriate isotype control (Bangur et al., 2004). However, we consistently identified only low-level anti-MS4A8B binding (Figure 3.3; Figure 3.14). It is possible that MS4A8B expression was reduced during cellular culture or is up-regulated upon exposure to specific environmental signals that may have been present in the study performed by Bangur and colleagues (2004). Finally, the Fc mediated anti-MS4A8B binding to human CD64 also provides an explanation for the initial series of experiments that suggested MS4A8B and human CD64 were associated. Among these was the cross-blocking experiments in U937 cells, which suggested anti-MS4A8B binding to MS4A8B was capable of blocking the binding of human IgG to CD64 (Figure 3.5). However, with the identification that: I) anti-MS4A8B was not a mouse IgG1 but a mouse IgG2a immunoglobulin molecule and II) that the U937 cell line does not actually express MS4A8B (Figure 3.13), it was clear that the cross-blocking effect was a consequence of anti-MS4A8B and human IgG binding to the same cellular target. Similarly, the co-ordinate binding of anti-MS4A8B with human CD64 (Figure 3.6) and its ability to immunoprecipitate human CD64 from monocytic U937 cell lysates (Figure 3.8) can also be attributed to anti-MS4A8B and anti-CD64 both binding the same cellular targets (human CD64).

Interestingly, although the mouse homolog, MS4a8A, shares considerable amino acid and structural similarity with MS4A8B, their patterns of expression differ (Ishibashi et al., 2001). Specifically, MS4a8A is differentially expressed in M2 monocyte derived macrophages (Schmieder et al., 2012). However, we could not identify MS4A8B expression in monocyte derived M2 macrophages (Figure 3.15). The difference in expression pattern may reflect the differential regulation of MS4a8A and MS4A8B genes and may possibly extend to different functional roles. In that respect, MS4A8B may be more similar to members of the MS4A family which are expressed outside of the hematopoietic system such as MS4A12 (Koslowski et al., 2008). Indeed, a recent report showed that MS4A8B, like MS4A12, is expressed in colonic epithelium and linked its function to cell cycle regulation (Michel et al., 2013). The study further demonstrated that MS4A8B is differentially regulated in the epithelial cells comprising the crypt-luminal axis of the colon and that MS4A8B expression is lost in human colon carcinoma (Michel et al., 2013). Recently, a second study by Ye and colleagues (2014) showed that MS4A8B is preferentially over-expressed in prostate cancer cells. Here, human MS4A8B was also linked to cell cycle regulation, with in vitro studies demonstrating that its down-regulation induces G1-S phase cell cycle arrest and reduced cellular vitality (Ye et al., 2014). Collectively, the data suggests MS4A8B is not expressed in hematopoietic cells but is expressed in cells of epithelial origin.

Chapter IV
The Evaluation of MS4A4A Expression in Hematopoietic Cells

A. Introduction

Formerly, we evaluated a panel of 18 distinct human tissues and searched for MS4A family members that, like MS4A1 (CD20), are expressed in hematopoietic cells and display restricted patterns of expression. Unlike any other MS4A gene, among solid tissues MS4A4A mRNA was expressed only in the lung (J. Zuccolo et al., 2013). Given its restricted tissue mRNA expression and sequence homology with MS4A1 our lab generated mouse monoclonal antibodies directed against extracellular epitopes of MS4A4A. Three monoclonal antibodies were obtained (3F2, 4H2, and 5C12) and all were isotyped as mouse IgG1. Given the incorrect initial isotyping of anti-MS4A8B, they were re-isotyped and confirmed as mouse IgG1.

This chapter describes the characterization of MS4A4A expression using our mouse monoclonal anti-MS4A4A antibodies. Notably, we identified the restricted expression of MS4A4A in monocytes and M2 macrophages. Furthermore, unlike the mouse homolog, MS4a4B, MS4A4A was not expressed in resting CD3+ peripheral blood T-lymphocytes. Recently, Yan and colleagues (2013) demonstrated that mouse MS4a4B is capable of regulating cellular apoptosis. The binding of anti-MS4a4B has also been shown to induce mouse T-cells to undergo cellular apoptosis (Yan et al., 2013). Given that MS4A4A shares substantial sequence similarity with its mouse homolog, MS4a4B, as well as with human MS4A1 (CD20) (Liang & Tedder, 2001), and displays restricted

protein expression, we also investigated its potential to induce cellular apoptosis and influence cellular differentiation.

B. Results

4.1 The Specificity of the Monoclonal Anti-MS4A4A 3F2, 4H2, and 5C12 Antibodies

To investigate MS4A4A protein expression our lab generated mouse monoclonal antibodies (IgG1) against extracellular epitopes. These antibodies were designated as anti-MS4A4A 3F2, 4H2 and 5C12. Their specificity was evaluated by incubating parental BJAB and MS4A4A-GFP transfected BJAB cells (BJAB-MS4A4A-GFP) with each of the anti-MS4A4A monoclonal antibodies or the mouse IgG1 isotype control. As an additional negative control, parental BJAB and BJAB-MS4A4A-GFP cells were also incubated with anti-MS4A8B. Binding of the primary antibodies was assessed by secondary incubation with PE-conjugated goat-anti-mouse IgG and flow cytometric analysis. As shown in Figure 4.1A, anti-MS4A4A (3F2, 4H2 and 5C12) bound to BJAB cells ectopically expressing MS4A4A (red), but did not bind to parental BJAB cells (orange). Furthermore, neither the isotype control (green) nor the anti-MS4A8B negative control (blue) bound to parental BJAB or BJAB-MS4A4A-GFP transfected cells. Consequently, flow cytometric data indicated that anti-MS4A4A 3F3, 4H2, and 5C12 were specific for human MS4A4A.

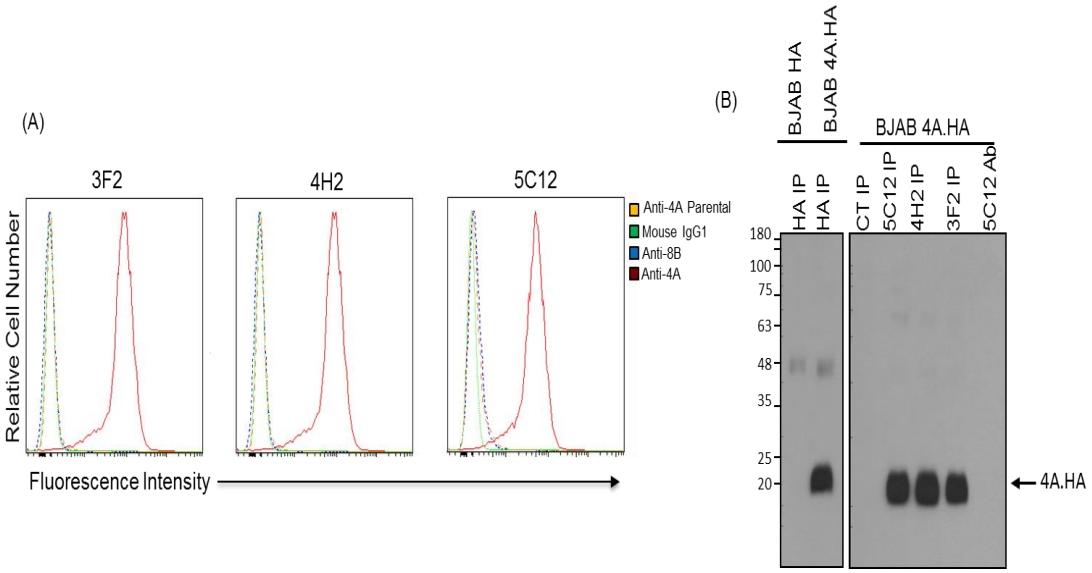

Figure 4.1: The Specificity of the monoclonal Anti-MS4A4A 3F2, 4H2 and 5C12 Antibodies. (A) BJAB-MS4A4A-HA cells were incubated with anti-MS4A4A (3F2, 4H2, or 5C12) (red), the mouse IgG1 isotype control (green) or anti-MS4A8B (blue). Parental BJAB cells were similarly incubated with anti-MS4A4A (3F2, 4H2, or 5C12) (orange), the mouse IgG1 isotype control or anti-MS4A8B. Samples were subsequently incubated with PE--conjugated goat anti-mouse IgG and analyzed by flow cytometry. Mouse IgG1 and anti-MS4A8B binding to parental BJAB cells was not shown to facilitate presentation, however, neither displayed binding to BJAB cells. Note, all three anti-MS4A4A antibodies specifically bound to BJAB-MS4A4A but not BJAB cells. (B) To confirm antibody specificity, BJAB HA and BJAB 4A.HA (2 X 10^7 cells/sample) were lysed in 1% maltoside. Soluble lysates were immunoprecipitated with rabbit anti-HA, isotype control (IgG1; CT) and mouse anti-MS4A4A (5C12, 4H2, 3F2), as indicated, and analyzed by rabbit anti-HA western blot.

In order to confirm their specificity, we investigated whether the antibodies could selectively immunoprecipitate MS4A4A from cell lysates. Using our monoclonal anti-MS4A4A antibodies, MS4A4A was immunoprecipitated from soluble BJAB-MS4A4A-HA cell lysates. As shown in Figure 4.IB, anti-MS4A4A 3F2, 4H2, and 5C12 but not the mouse IgG1 isotype control, immunoprecipitated a protein from BJAB-MS4A4A-HA cell lysates with its molecular weight consistent with MS4A4A (~23 kDa). The same band was identified when soluble lysates were immunoprecipitated with mouse anti-HA and assessed by a rabbit anti-HA western blot. Collectively, the data confirmed that the mouse monoclonal anti-MS4A4A 3F2, 4H2, and 5C12 antibodies were specific for human MS4A4A.

4.2 MS4A4A is Expressed at the Cell Surface of Primary Human Monocytes

MS4a4B, a mouse homolog of human MS4A4A, is expressed in resting T-lymphocytes (Xu et al., 2010; Yan et al., 2013). Consequently, we questioned whether MS4A4A is expressed in hematopoietic cells. MS4A4A expression was first evaluated in the three major hematopoietic cell subsets that comprise whole blood: resting monocytes, granulocytes, and lymphocytes. Here, whole white blood cells were isolated and incubated with anti-MS4A4A-Alexa 647 or mouse IgG1-Alexa 647 isotype control. Analysis by flow cytometry and gating based upon forward and side scatter was used to assess anti-MS4A4A binding in monocytes as well as resting granulocytes and lymphocytes.

As indicated in Figure 4.2A (A), MS4A4A was expressed in monocytes but not in resting lymphocytes or granulocytes. In order to further assess MS4A4A expression, whole white blood cells were also incubated with anti-MS4A4A-Alexa 647 or mouse IgG1-Alexa 647 isotype control, alongside markers of either granulocytes, monocytes, or lymphocytes. Granulocyte subsets were identified with the cell surface marker, CD16. In granulocytes, CD16 is expressed in neutrophils (CD16+) (Falk, 2007) but not eosinophils (CD16-) (Davoine et al., 2002) or basophils (CD16-) (Murphy K, 2008; Takahashi et al., 1993). As shown in Figure 4.2A (B), less than 1% of CD16+ and CD16- granulocytes expressed MS4A4A. Monocytes were identified with the cell surface markers CD14 and CD16 (Grage-Griebenow et al., 2001; Tallone et al., 2011). Here, MS4A4A was expressed in CD14+ and CD14- monocytes as well as CD16+ and CD16- monocytes. Finally, lymphocyte subsets were identified with the cell surface markers, CD3 (T-lymphocytes), CD19 (B-lymphocytes), and CD56 (NK cells) (Murphy K, 2008). Here, MS4A4A was expressed in expressed in approximately 3% of both CD3+ T-lymphocytes and CD19+ B-lymphocytes while less than 1% expression was identified in CD56 NK cells. However, the detection of MS4A4A expression in the minor percentage of B- and T- lymphocytes and NK cells was inconsistent. For example, Figure 4.2B shows an additional experiment in which MS4A4A was not detected in CD3+ T-lymphocytes and was detected in less than 1% of CD3- lymphocytes. However, MS4A4A was consistently identified, at elevated levels, in monocytes.

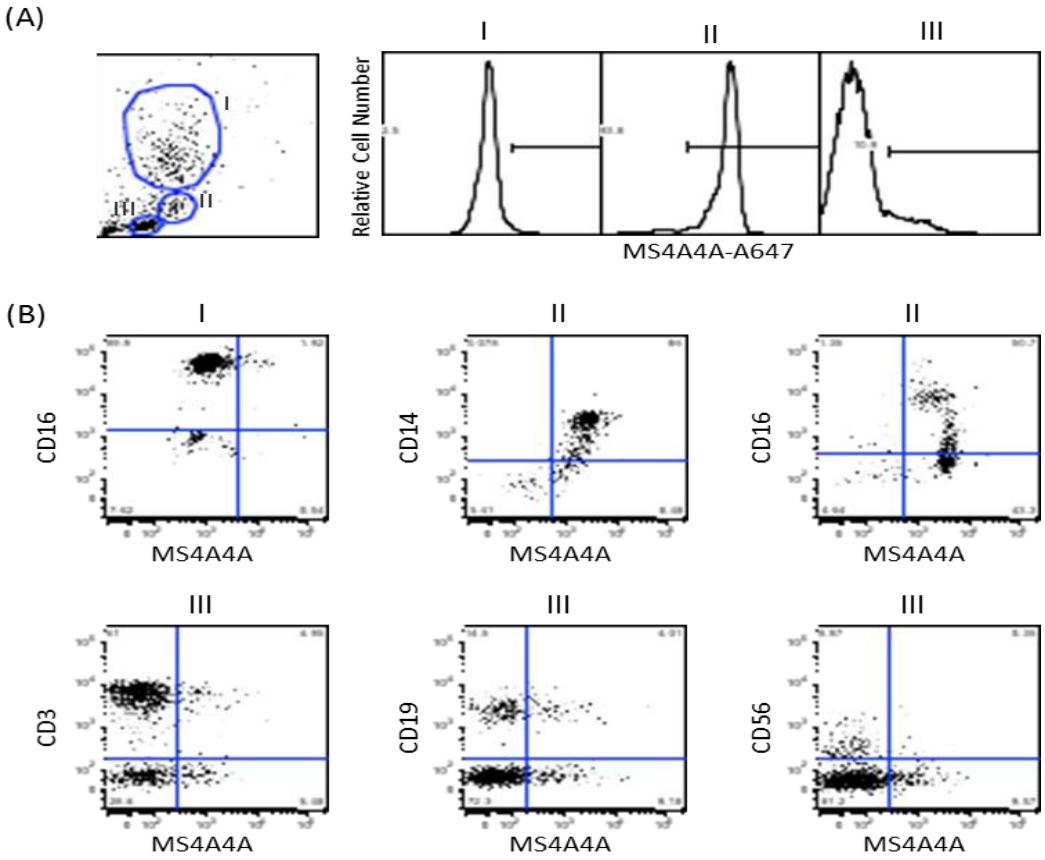

Figure 4.2A: MS4A4A is expressed at the cell surface of primary human monocytes. Peripheral blood leukocytes were isolated from whole blood and then stained with isotype control (mIgG1-A647, mIgG1/mIgG2b-FITC, mIgG1-PE) or anti-MS4A4A-A647. A) Resting granulocytes (I), monocytes (II) and resting lymphocytes (III) were gated based upon FSC and SSC as indicated. Note that the level of isotype staining in *A* is indicated to the left of the black bars (⊢). B) Cells were stained with anti-MS4A4A-A647 as well as either CD14-FITC, CD16-FITC, CD3-PE, CD19-PE or CD56-FITC as indicated by scatter dot plots. Staining of the various leukocyte subsets is indicated.

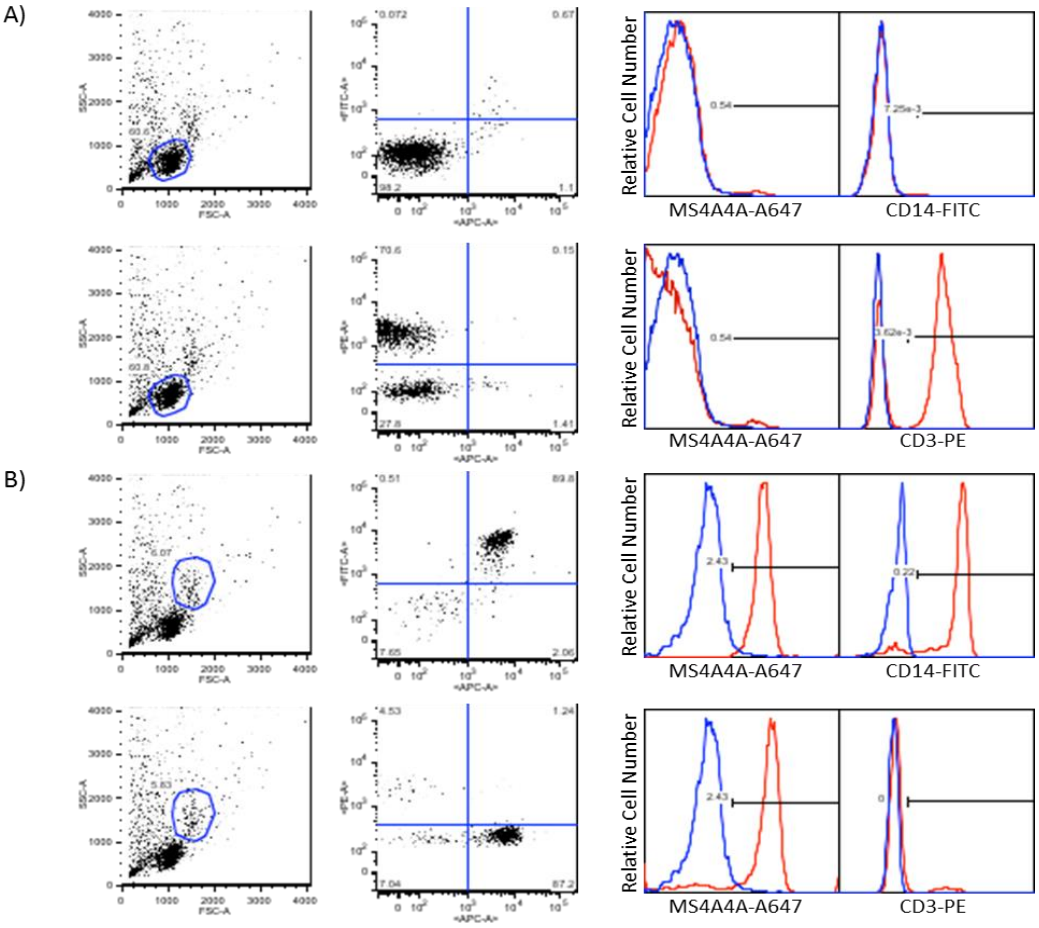

Figure 4.2B: Anti-MS4A4A selectively binds to primary human monocytes.

Peripheral blood mononuclear cells were isolated from whole blood, stained directly with isotype control (mIgG1-A647, mIgG1-FITC, mIgG1-PE; blue), anti-MS4A4A-A647, anti-CD14-FITC, anti-CD3-PE (red) as indicated. Lymphocyte (A) and monocyte (B) populations were gated based on FSC and SSC as shown and analyzed separately.

4.3 Anti-MS4A4A Selectively Binds to the M2 Subset of Monocyte Derived Macrophages

Since MS4A4A was expressed in monocytes we questioned whether it was also expressed in its differentiated progeny. As a result, we evaluated whether MS4A4A was expressed in monocyte derived macrophages. Classically (M1) and alternatively (M2) activated macrophages were attained by incubating peripheral blood mononuclear cells with culture media supplemented with GM-CSF or M-CSF. At day 5, cells were re-incubated with media containing the M1 (LPS and INFγ) or M2 (IL-4) cytokine mixtures. The monocyte derived M1 and M2 macrophages were subsequently incubated with anti-MS4A4A-Alexa 647 or mouse IgG1-Alexa 647. Flow cytometric analysis of the macrophage subsets indicated that MS4A4A was expressed in M2 but not M1 macrophages (Figure 4.3A). In order to confirm M1 and M2 identity and ascertain cellular differentiation, cells were also evaluated for markers of differentiation. As previously discussed, in M1 macrophages, these include the presence of CD80, the absence or limited expression of CD14 and relative to M2 macrophages, reduced expression of CD32 (Verreck et al., 2006). In contrast, in M2 macrophages these include the lack of CD80 expression (Mantovani et al., 2004; Rey-Giraud et al., 2012) and relatively greater levels of CD14 and CD32 (Verreck et al., 2006). As indicated in Figure 4.3, M1 and M2 macrophages expressed all of the aforementioned cellular differentiation markers at levels described within the literature. Consequently, the data demonstrated that the MS4A4A protein is selectively expressed in peripheral blood monocyte derived M2 but not M1 macrophages.

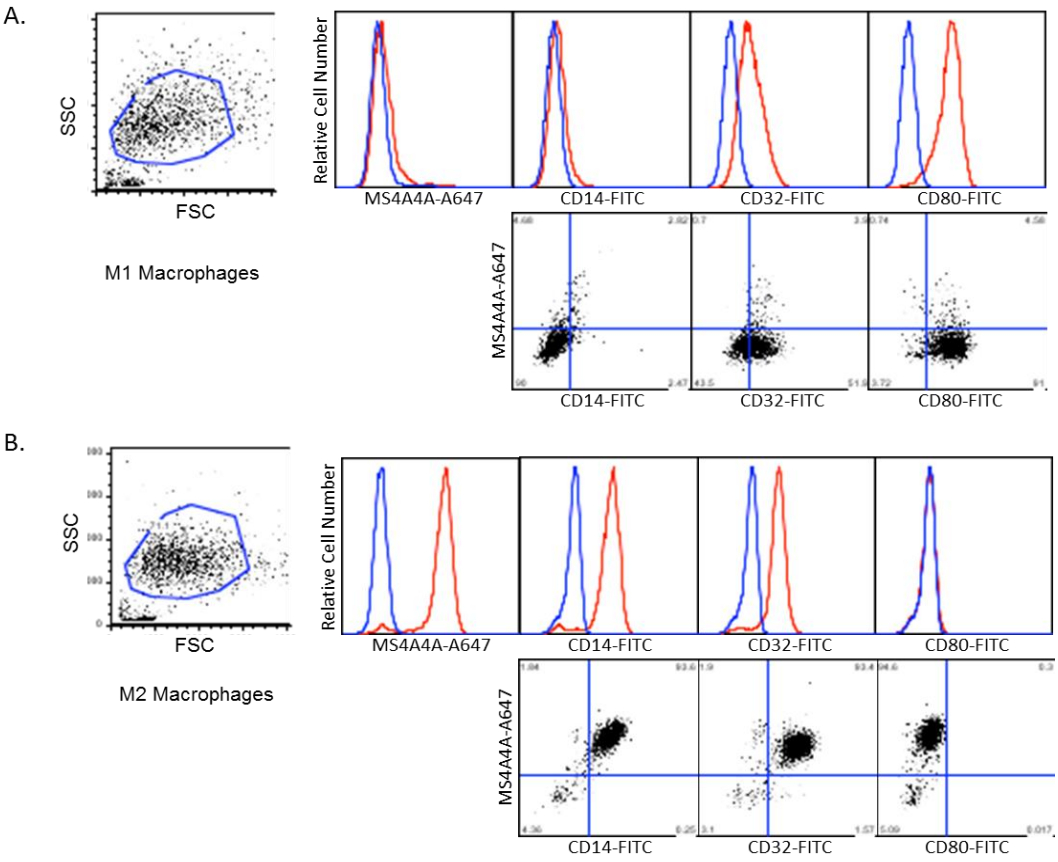

Figure 4.3: MS4A4A is selectively expressed in the M2 subset of monocyte-derived macrophages. Monocytes were isolated by adhesion and differentiated into M1 or M2 subsets. M1 cells were grown in 40ng/mL GM-CSF (5 days) and then in LPS plus IFNγ (2 days), while M2 cells were grown in 25ng/mL M-CSF (5 days) and then in IL-4 (2 days). M1 (A) and M2 (B) cells were collected, stained with isotype control (mIgG1-A647, mIgG1-FITC; blue), anti-MS4A4A-A647, anti-CD14-FITC, anti-CD32-FITC, or anti-CD80-FITC (red) as indicated by histograms. Percent cells in each quadrant is indicated (N=4).

4.4 Anti-MS4A4A Binding to PMA Differentiated U937

U937 cells are characterized as a pro-monocytic cell line and when treated with phorbal myristate acetate (PMA) can be differentiated into macrophages, with a phenotype partially resembling the M2 subset (Minafra, Di Cara, Albanese, & Cancemi, 2011). Given the differential protein expression of MS4A4A in M2 macrophages, we sought to identify whether MS4A4A was also expressed in U937 differentiated macrophages. To investigate expression, U937 cells were differentiated with PMA for 3 days and evaluated for anti-MS4A4A-Alexa 647 or mouse IgG1-Alexa 647 binding. PMA is a hydrophobic reagent and was therefore dissolved in DMSO. Consequently, U937 cells were also treated with DMSO and evaluated for anti-MS4A4A-Alexa 647 or mouse IgG1-Alexa 647 binding by flow cytometry. As illustrated in Figure 4.4, MS4A4A was expressed in PMA but not DMSO treated U937 cells at 24 (day 1), 48 (day 2) and 72 (day 3) hours post treatment. Maximum MS4A4A expression was attained following 48 hours of PMA treatment.

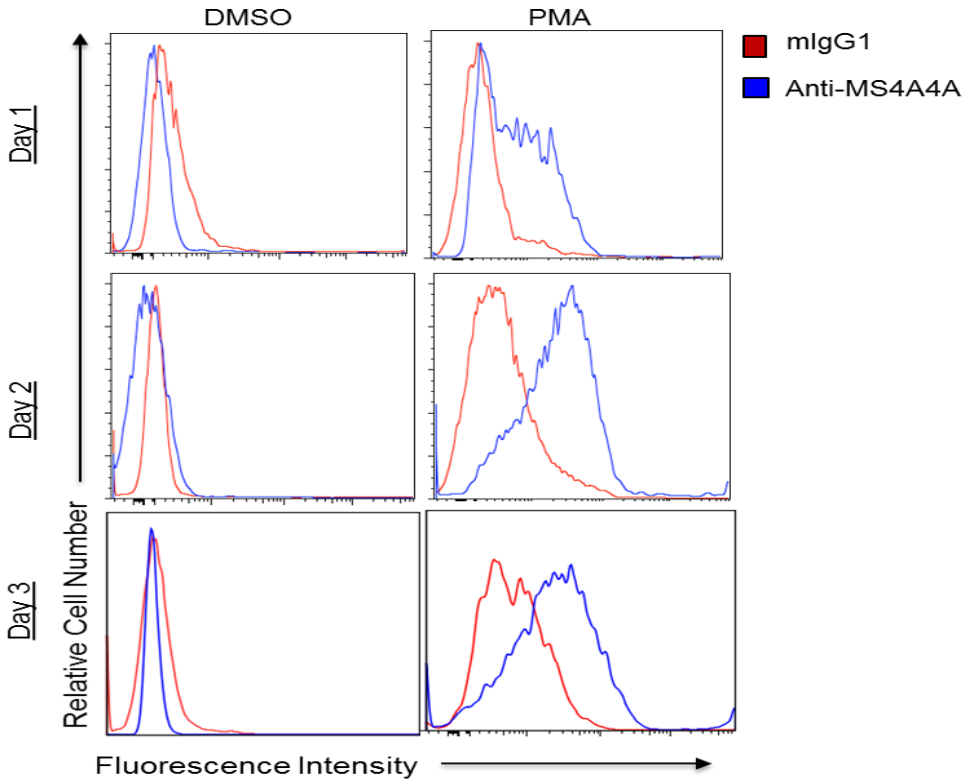

Figure 4.4: Anti-MS4A4A binding to PMA differentiated U937 cells. U937 cells were seeded at a density of $3.0x10^5$ and treated with either 20ng/ml of PMA or DMSO for 24, 48 and 72 hours. At 24, 48 and 72 hours PMA- or DMSO- treated U937 cells were stained with either anti-MS4A4A-alexa-647 (mIgG1) or mouse IgG1-alexa-647 isotype control. Live cells were gated based upon FSC and SSC and then analyzed by flow cytometry (N=3).

4.5 MS4A4A mRNA Expression

Total RNA from monocytes and macrophage subsets was amplified by RT-PCR in order to confirm MS4A4A expression. In a preliminary investigation (Figure 4.6A), total RNA was extracted from primary adherent white blood cells, as a source of monocytes, and from monocyte derived M1 and M2 macrophages. From each sample, MS4A4A mRNA was reverse transcribed and amplified alongside MS4A4A plasmid cDNA (positive control). BJAB RNA was also included as a negative control. As indicated in Figure 4.5A, a faint band was detected in mRNA amplified from adherent white blood cells (monocytes) and M1 macrophages. In contrast, a prominent band was identified in mRNA amplified from M2 macrophages.

The data suggested that MS4A4A mRNA was minimally expressed in monocytes and, following differentiation, was up-regulated in the M2 macrophage subset. However, in the experiment described (Figure 4.5A), MS4A4A mRNA was amplified from adherent white blood cells alongside M1 and M2 monocyte derived macrophages. The M1 and M2 macrophage subsets represent a relatively pure population of cells. However, adherent white blood cells do not consist exclusively of monocytes. Rather, they consist of a heterogeneous population (monocytes, lymphocytes, and granulocytes), in which monocytes are concentrated. As a result, it was not possible to ascertain whether MS4A4A mRNA was inherently low in monocytes or whether it was diluted by non-monocytic cells. Consequently, a pure population of monocytes (CD14+), was attained by selection and MS4A4A mRNA expression was re-evaluated.

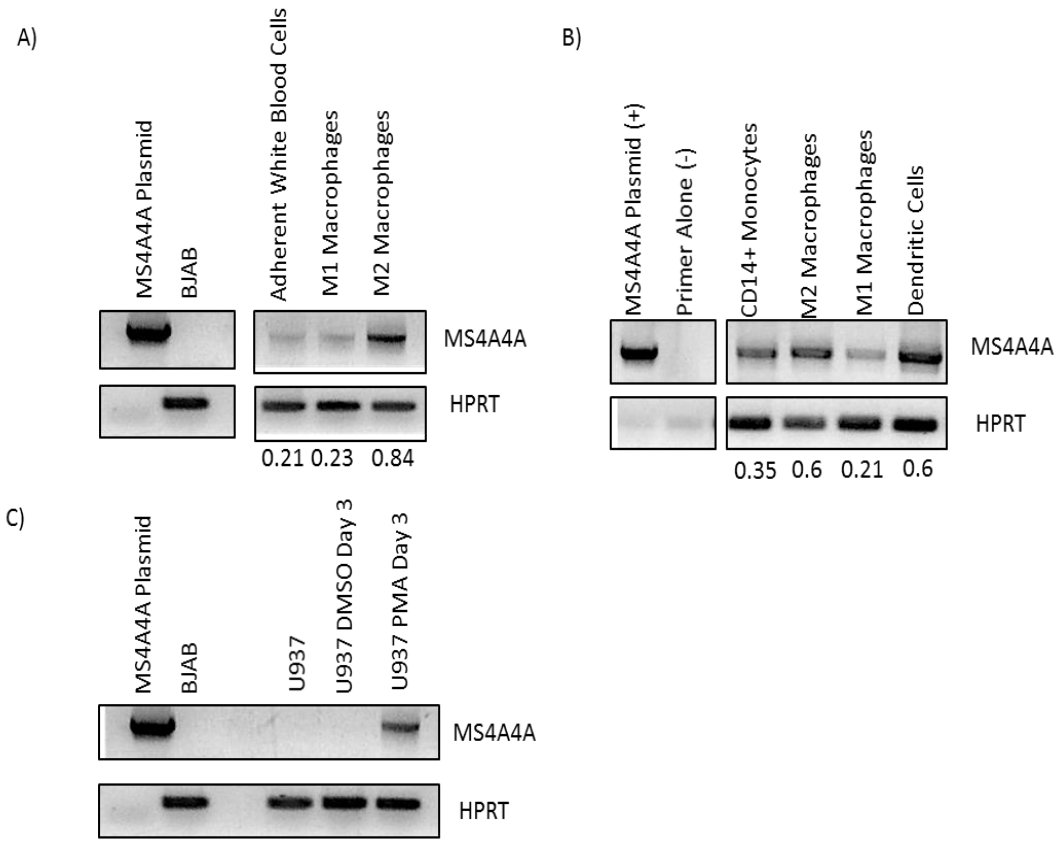

Figure 4.5: MS4A4A mRNA expression in primary monocytes, monocyte derived macrophages, and PMA Differentiated U937 cells. A) Primary adherent and monocyte derived M1 and M2 macrophages were analyzed by PCR for MS4A4A mRNA expression. B) MS4A4A mRNA expression was subsequently re-evaluated by qualitative PCR alongside pure CD14+ monocytes, DC cells and among C) DMSO and PMA treated U937 cells. Densitometry analysis was performed for select samples relative to the HPRT controls and is represented by numerical values.

Here, MS4A4A mRNA expression was evaluated in CD14+ monocytes, alongside monocyte derived macrophage subsets (M1 and M2) and dendritic cells. The dendritic cells were donated by the lab of Dr. Christopher Mody and were also derived from monocytes, by exposure to GM-CSF and IL-4 for 5 days, followed by incubation with TNF for an additional 2 days. RT-PCR analysis (Figure 4.5B) demonstrated that MS4A4A mRNA was expressed at elevated levels in monocytes, up-regulated by approximately 2-fold following differentiation into M2 macrophages and dendritic cells, and selectively down- regulated following differentiation into the M1 macrophage subset. Collectively, the MS4A4A mRNA expression data were in accordance with MS4A4A protein analysis in monocytes and macrophage subsets (Figure 4.2; Figure 4.3). To evaluate MS4A4A mRNA in parental, DMSO treated, and PMA differentiated U937 cells, total RNA was similarly extracted and amplified by RT-PCR. As shown in Figure 4.3C, MS4A4A mRNA was detected in PMA differentiated U937 cells but not parental or DMSO treated cells. These data were consistent with MS4A4A protein expression (Figure 4.4).

4.6 The Effect of Anti-MS4A4A on BJAB-MS4A4A-HA Cell Apoptosis

Anti-MS4A1 (Rituximab) is capable of inducing cellular apoptosis in B-lymphocytes (Cragg, 2005). Similarly, anti-MS4a4B is capable of inducing cellular apoptosis in T-lymphocytes (Yan et al., 2013). Since MS4A4A shares sequence and structural similarity with its mouse homolog, MS4a4B, as well as with human MS4A1 (CD20) (Liang & Tedder, 2001), and displays restricted patterns of protein expression, we investigated the ability of anti-MS4A4A to induce cellular apoptosis. Previously, we

generated 3 mouse monoclonal IgG1 antibodies (3F2, 4H2, and 5C12) directed against extracellular epitopes of MS4A4A. Cross-blocking experiments performed by previous members of our lab suggested that anti-MS4A4A 3F2 and 4H2 may bind the same cell surface epitopes whereas anti-MS4A4A 5C12 may bind a distinct epitope. As a result, we evaluated the ability of anti-MS4A4A 4H2 and 5C12 but not anti-MS4A4A 3F2, to induce cellular apoptosis. Here, BJAB cells which ectopically expressed MS4A4A-HA, were cultured in the presence of soluble or immobilized anti-MS4A4A or mouse IgG1 isotype control. Anti-MS4A4A and mouse IgG1 were diluted in PBS at three different concentrations (5ug, 10ug, or 20ug per ml) for the soluble condition while anti-MS4A4A was immobilized by covering the wells of polyethylene plates with anti-MS4A4A (20ug per ml) for 3 hours at 37°C. The ability of both soluble (limited-crosslinking) and immobilized anti-MS4A8B (high-crosslinking) to induce cellular apoptosis was evaluated because *in vivo,* antibody-Fc receptor binding may induce high levels of immunoglobulin crosslinking (Falk, 2007). As a positive control, cells were also incubated with soluble anti-IgM, which is known to induce cellular apoptosis in BJAB cells. Following a 08 or 16 hour incubation, BJAB-MS4A4A-HA cells were stained with Annexin-V-FITC and propidium iodide. Annexin V-FITC binds to phosphatidylserine, an integral membrane protein which is localized in the inner-leaflet of the plasma membrane. However, following apoptosis, membrane flipping and the loss of membrane symmetry induces the translocation of phosphatidylserine to the outer leaflet of the plasma membrane, allowing for Annexin-V-FITC binding (van Engeland, Nieland, Ramaekers, Schutte, &

Reutelingsperger, 1998). In contrast, propidium iodide is a DNA stain, which is capable of intercalating itself between nucleotides. Propidium iodide is used to identify cell viability since it is normally excluded from live and early apoptotic cells but is capable of binding to the DNA of necrotic cells and late stage apoptotic cells (Inoue, 2001). As shown in Figure 4.6A, flow cytometry analysis of Annexin-V-FITC and propidium iodide staining can be used to identify cells that are either: alive (PI and Annexin V-FITC negative), necrotic (PI and Annexin V-FITC positive), or apoptotic (PI negative and Annexin V-FITC positive). When we evaluated the ability of anti-MS4A4A 4H2 and 5C12 to induce cellular apoptosis in BJAB-MS4A4A-HA cells, the levels detected did not statistically differ with respect to the isotype control (Figure 4.6B). This was observed after both 8 and 16 hours of treatment for both soluble (Figure 4.6B (A)) and immobilized antibody conditions (Figure 4.6B (B)).

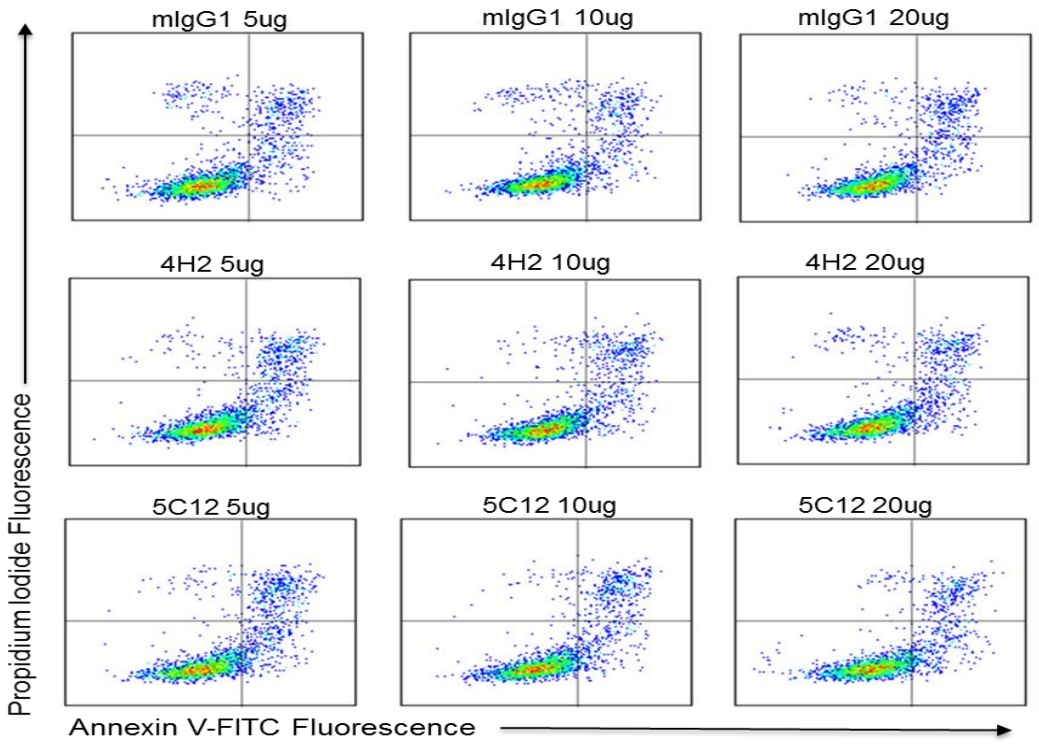

Figure 4.6a: The effect of soluble anti-MS4A4A (4H2 and 5C12) on BJAB-MS4A4A HA cell apoptosis. BJAB-MS4A4A HA cells were seeded at a density of $2.0x10^5$ and treated with either mIgG1, anti-MS4A4A 4H2 or anti-MS4A4A 5C12 antibodies. For each condition the cells were exposed to either 5, 10, or 20 micrograms per ml of media of the aforementioned antibody. After 16 hours the treated BJAB-MS4A4A HA cells were stained with Annexin V-FITC for 30 minutes and propidium iodide (PI) for 1 minute and subsequently evaluated using flow cytometry. Note, this figure represents the staining pattern for a single trial at 16 hours. The collective results from the N=4 experiments are displayed in Figure 4.6b, which shows that anti-MS4A4A 4H2 and 5C12 have no effect on cell apoptosis (N=4: four independent experiments, each performed with duplicate samples).

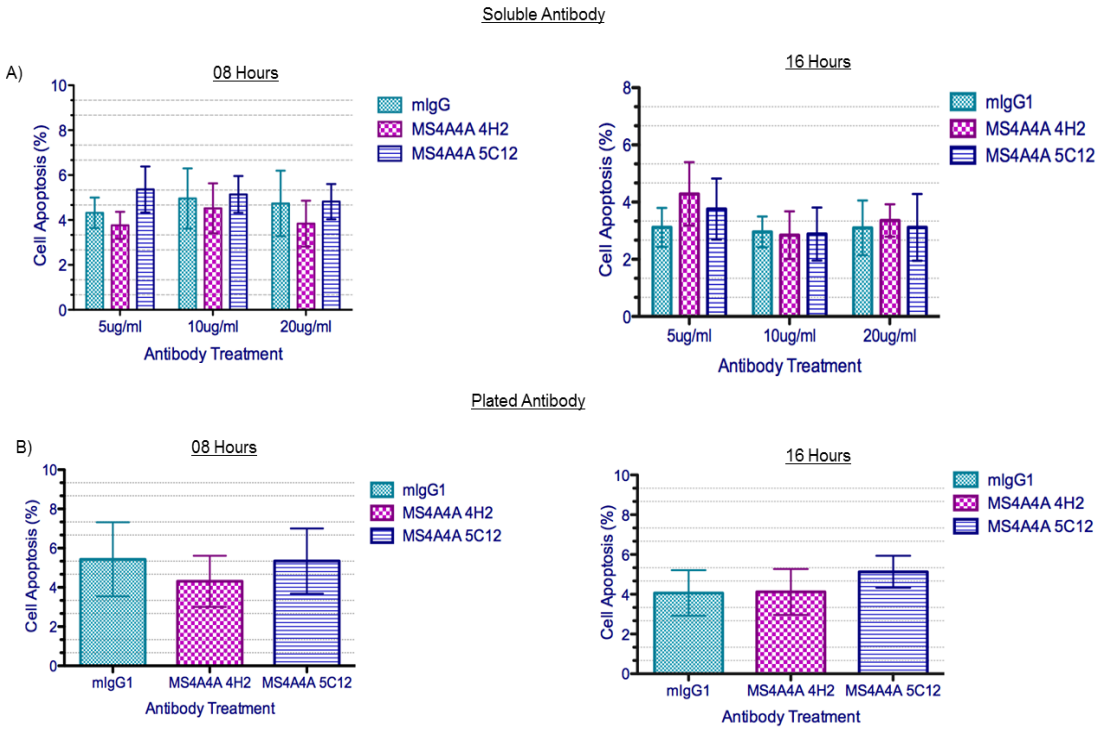

Figure 4.6b: The effect of anti-MS4A4A (4H2 and 5C12) on BJAB-MS4A4A HA cell apoptosis. BJAB-MS4A4A HA cells were seeded at a density of $2.0x10^5$ and treated with either soluble (A) or plated (B) mIgG1, anti-MS4A4A 4H2 or anti-MS4A4A 5C12 antibodies as indicated. For the soluble condition (A), cells were exposed to either 5, 10, or 20 micrograms per ml of media of the aforementioned antibodies. For the plated condition (B) cells were cultured in polyethylene plates coated with 20ug of antibody or mouse IgG1 (per ml of PBS). After 8 or 16 hours the treated BJAB-MS4A4A HA cells were stained with Annexin V-FITC for 30 minutes and propidium iodide for 1 minute and subsequently evaluated using flow cytometry. Note as a positive control cells were incubated with 25ug of anti-IgM per ml of media for 8 hours (10.8 % apoptosis) and 16 hours (11.6% apoptosis) (N=4: four independent experiments, each performed with duplicate samples).

4.7 The Effect of Anti-MS4A4A 4H2 and 5C12 on PMA Differentiated U937 Cell Apoptosis

We also evaluated the capability of anti-MS4A4A 4H2 and 5C12 to induce cellular apoptosis in PMA differentiated U937 cells. As previously shown (Figure 4.6B), anti-MS4A4A was not able to induce cellular apoptosis in BJAB-MS4A4A-HA cells. The BJAB-MS4A4A-HA cell line ectopically expressed MS4A4A. Consequently, we questioned whether anti-MS4A4A 4H2 and 5C12 may be able to induce cellular apoptosis in cells which natively express MS4A4A. PMA differentiated U937 cells express MS4A4A at elevated levels following 2 days of treatment. Here, PMA differentiated U937 cells were cultured in the presence of soluble (5ug, 10ug, or 20ug) or immobilized anti-MS4A4A or mouse IgG1 isotype control. Following a 08 hour incubation, PMA differentiated U937 cells were stained with Annexin-V-FITC and propidium iodide and analyzed by flow cytometry. The flow cytometric analysis of three independent experiments, each performed with duplicate samples, indicated that the levels of apoptosis were not influenced by soluble or immobilized anti-MS4A4A 4H2 or 5C12 (Figure 4.7). The data suggested that anti-MS4A4A 4H2 and 5C12 were not able to induce cellular apoptosis in PMA differentiated U937 cells.

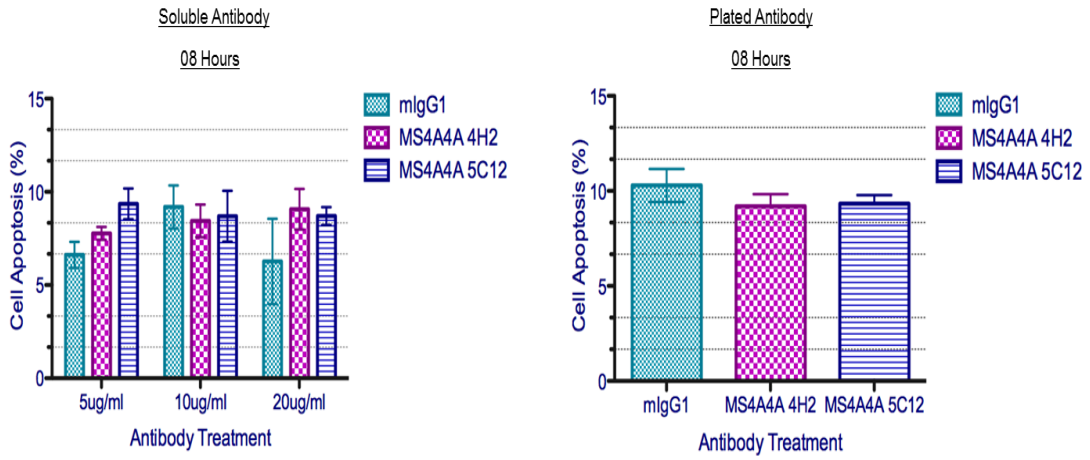

Figure 4.7: The effect of anti-MS4A4A (4H2 and 5C12) on PMA differentiated U937 cell apoptosis. U937 cells were seeded at a density of $5.0x10^5$ and differentiated with 20ng of PMA per ml of growth media for 48 hours. During the process, the cells were also treated with either soluble (left) or plated (right) mIgG1, anti-MS4A4A 4H2 or anti-MS4A4A 5C12 antibodies as indicated. **F**or the soluble condition (A), cells were exposed to either 5, 10, or 20 micrograms of the aforementioned antibody. For the plated condition (B) cells were cultured in polyethylene plates coated with 20ug of antibody or mouse IgG1 (per ml of PBS). After 16 hours, the treated PMA U937 cells were stained with Annexin V-FITC for 30 minutes and propidium iodide (PI) for 1 minute. PMA differentiated U937 cells were subsequently evaluated using flow cytometry (N=3: three independent replicates performed with doublet samples).

4.8 The Effect of Anti-MS4A4A 4H2 and 5C12 on BJAB-MS4A4A-HA Homotypic Adhesion

Certain anti-MS4A1 antibodies are capable of inducing homotypic adhesion of BJAB-MS4A1 cells. Homotypic adhesion is defined as the cellular adhesion of identical cells and is a property that is correlated with its therapeutic efficacy of specific anti-MS4A1 monoclonal antibodies (Cragg, 2005). In addition, BJAB cells are known to undergo homotypic adhesion. Since we previously transfected BJAB cells to ectopically express MS4A4A-HA, we questioned whether anti-MS4A4A 4H2 and 5C12 may influence homotypic adhesion in BJAB-MS4A4A-HA cells. Here, BJAB-MS4A4A-HA cells were cultured in the presence of soluble or immobilized mouse IgG1, anti-MS4A4A 4H2, or anti-MS4A4A 5C12. For the soluble condition, cells were exposed to either 5, 10, or 20 micrograms of antibody per ml of culture media. Following, 0, 4, 8, 16, and 24 hours of treatment the cells were evaluated for homotypic adhesion by light microscopy. Since BJAB cells intrinsically undergo homotypic adhesion, we looked for changes in the kinetics of homotypic adhesion. Analysis of four independent experiments, each with duplicate samples, indicated that BJAB-MS4A4A-HA homotypic adhesion was not influenced by either soluble (5ug, 10ug, and 20ug per ml) or immobilized anti-MS4A4A 4H2 or anti-MS4A4A 5C12 (Figure 4.8).

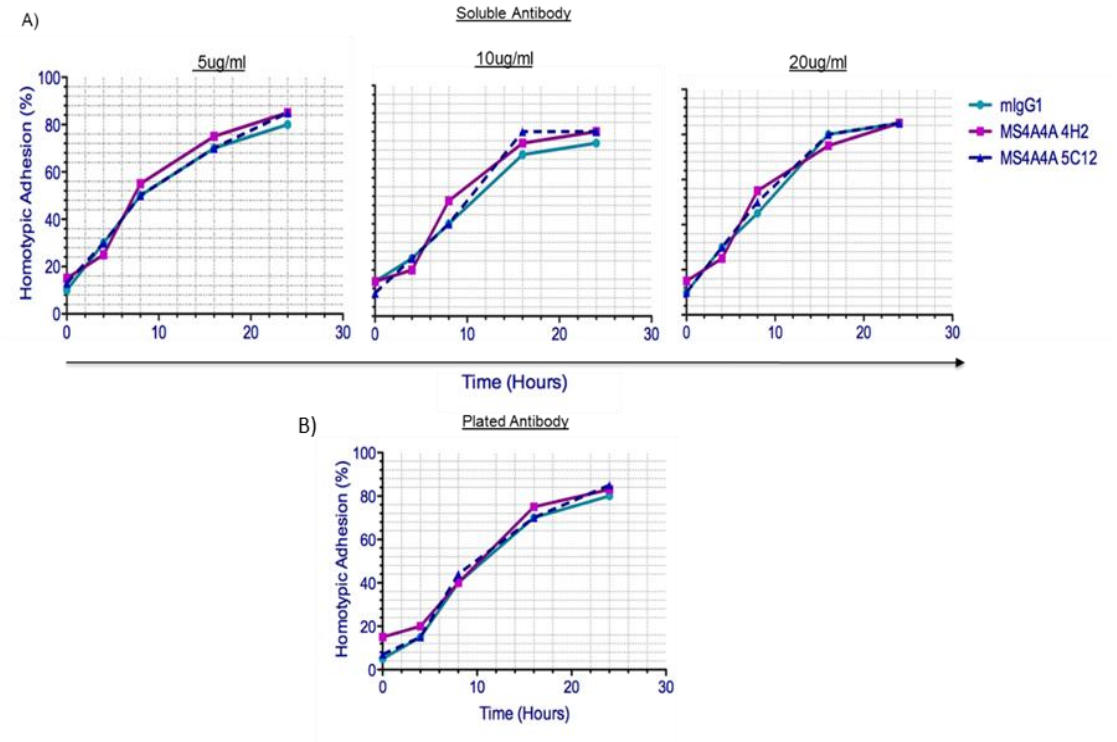

Figure 4.8: Effect of anti-MS4A4A (4H2 and 5C12) on BJAB-MS4A4A-HA homotypic adhesion. BJAB-MS4A4A HA cells were seeded at a density of $2.0x10^5$ and treated with either soluble (A) or plated (B) mIgG1, anti-MS4A4A (4H2 or 5C12) antibodies as indicated. For the soluble condition (A), cells were exposed to either 5, 10, or 20 micrograms per ml of culture media of the aforementioned anti-MS4A4A antibodies. For the plated condition (B) cells were cultured in polyethylene plates coated with 20ug of antibody or mouse IgG1 (per ml of PBS). Upon 0 and after 4, 8, 16 and 24 hours the cells were evaluated for homotypic adhesion by light microscopy. Homotypic adhesion was quantified by visually evaluating the number of clumps of homotypic adherent cells within a defined region and expressing it as a function of the total number of free cells and adherent clumps (N=4: four independent experiments with each performed with

4.9 The Effect of Anti-MS4A4A on PMA Induced U937 Differentiation

Many disorders are characterized by an abundance of macrophages and the ability to regulate their differentiation could be potentially useful (Wynn, Chawla, & Pollard, 2013). Multiple antibody based immunotherapeutics are capable of affecting the cellular differentiation processes (Sliwkowski & Mellman, 2013). Therefore our lab questioned whether anti-MS4A4A could affect the differentiation of MS4A4A expressing cells. In order to evaluate this, we used U937 cells and cultured them in the presence of PMA and either anti-MS4A4A or mouse IgG1 isotype control. The experiments were performed in the presence or absence of soluble antibody or immobilized anti-MS4A4A. If anti-MS4A4A affected cellular differentiation of PMA treated U937 cells, then indicators of PMA differentiation could be expected to differ between the isotype treated and anti-MS4A4A treated samples within the soluble or immobilized antibody conditions. For U937 cells, four indicators are commonly used to evaluate the PMA induced differentiation into macrophages: these include the expression of CD14, changes in granularity, size, and morphological features (Minafra et al., 2011). As shown in Figure 4.9A, CD14 expression was increased in PMA differentiated U937 cells but not in the DMSO treated control. When treated with anti-MS4A4A or the mouse IgG1 isotype control, CD14 expression did not differ under either soluble antibody or immobilized antibody conditions (Figure 4.9B). By using flow cytometry, the granularity and the size of PMA differentiated U937 cells can also be compared.

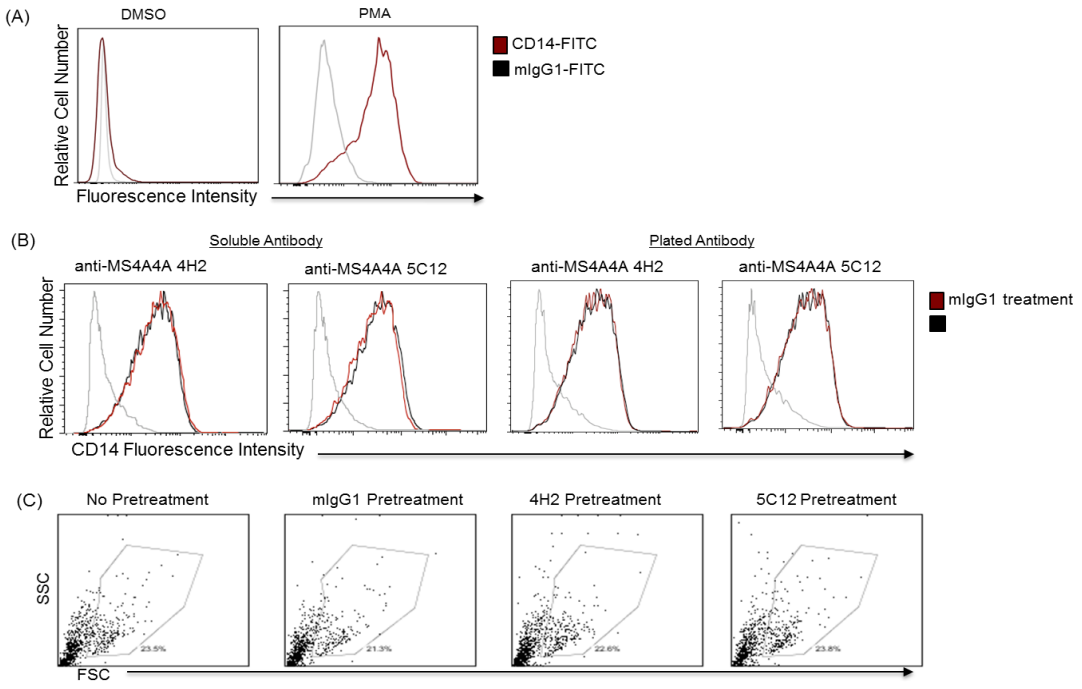

Figure 4.9: The effect of anti-MS4A4A (4H2 and 5C12) on PMA induced U937 differentiation. (A) DMSO treated and PMA U937 differentiated cells were stained for CD14-FITC and mIgG1-FITC to ensure that DMSO, the reagent in which PMA is dissolved, does not affect U937 differentiation. In (B) U937 cells were seeded at a density of $5.0x10^5$ cells per ml and differentiated with 20ng PMA per ml for 48 hours. During the process, the cells were treated with either (A) 20 ug of soluble mIgG1 (red) or anti-MS4A4A 4H2 (black) antibody per ml (left) or with plated anti-MS4A4A 4H2 and mIgG1 (right). In either case, PMA differentiated cells were subsequently evaluated by flow cytometry for changes in CD14 expression as well as FSC and SSC (C), both established markers for the identification for U937 differentiation into macrophages. Note, in all cases, anti-MS4A4A-4H2 and anti-MS4A4A 5C12 did not effect PMA induced CD14 expression or changes in FSC and SSC (N=2).

Specifically, as cells become more granular their side scatter increases and as they become larger in size their forward scatter increases. As shown in Figure 4.9C, no difference in forward or side scatter was observed when cells were cultured in the presence of, mouse IgG1, anti-MS4A4A 4H2, anti-MS4A4A 5C12, and no treatment. Collectively, the data suggested anti-MS4A4A does not affect the PMA induced differentiation of U937 cells.

C. Discussion

The results described herein support the restricted protein expression of MS4A4A in peripheral whole white blood cell gated monocytes (Figure 4.2) and monocyte derived M2 macrophages (Figure 4.3). They also support the absence of MS4A4A expression in monocyte derived M1 macrophages (Figure 4.3) as well as peripheral whole white blood cell gated resting lymphocytes and granulocytes (Figure 4.2). Given that MS4A4A shares substantial sequence and structural similarity with MS4A1 (Liang & Tedder, 2001) and displayed restricted protein expression, we also investigated its potential to induce cellular apoptosis and influence both cellular differentiation as well as homotypic adhesion. However, both soluble and immobilized anti-MS4A4A (4H2 and 5C12) did not: I) induce cellular apoptosis in PMA differentiated U937 (Figure 4.7) or BJAB-MS4A8B-HA cells (Figure 4.6), II) influence the homotypic adhesion of BJAB-MS4A4A-HA cells (Figure 4.8), or III) influence the PMA induced differentiation of U937 cells (Figure 4.9).

Among peripheral whole white blood cells, consistent MS4A4A mRNA and protein expression was identified in monocytes (Figure 4.2). The expression was in accordance with previous gene profiling reports from various database searches (Shin et al., 2011; Wu et al., 2009). Monocytes can be classified as classical, alternative, and intermediate populations based upon the expression of human CD14 and CD16 (Jaipersad et al., 2014; Tallone et al., 2011). Here, MS4A4A expression was observed in CD14- and CD14+ as well as CD16- and CD16+ monocytes (Figure 4.2). The data indicate that MS4A4A is expressed across the classical, alternative, and intermediate monocytic subsets. The expression of MS4A4A in all monocytes suggests a function that conserved within the classical, alternative, and intermediate monocytic populations. In contrast MS4A4A expression was not detected in resting peripheral blood granulocyte or lymphocyte subsets. These data are in concordance with the previous analysis of MS4A4A mRNA expression within select hematopoietic tissue, where our lab demonstrated that MS4A4A mRNA is not expressed in peripheral blood T- and B-lymphocytes. MS4A4A mRNA was also undetectable in the thymus, which is characterized by multiple T-cell subsets (Jonathan Zuccolo, 2010).

Here we also report the novel identification of MS4A4A protein and mRNA expression in M2 monocyte derived macrophages (Figure 4.3). Protein analysis indicates that MS4A4A is differentially expressed in the M2 macrophage subset at levels that are logarithmically higher than the isotype control, while expression is almost completely absent in M1 macrophages. In addition, the differential expression of MS4A4A in M2

macrophages was consistent among different blood donors and among all repetitions. Consequently, the consistently high differential expression of MS4A4A within M2 macrophages make it a suitable cell surface marker for monocyte derived M1 and M2 classification.

Despite the expression of MS4A4A in peripheral whole white blood cell gated monocytes, MS4A4A is not expressed in the U937 cell line (Figure 4.4). Though both cells are monocytic and human in origin, the U937 cell line differs from primary circulating monocytes in that it is a pro-monocytic cell line which lacks markers of mature circulating monocytes (CD14 and CD16); furthermore it is a cancer line (Minafra et al., 2011). The difference in expression suggests MS4A4A may not be expressed on the surface of immature monocytes. It could also suggest that MS4A4A protein expression may be down-regulated in monocytes that are cancerous. Indeed, this phenomenon is known to occur with respect to the cell surface expression of mouse MS4a4B. Specifically, Xu and colleagues (2006) demonstrated that MS4a4B expression is absent in a series of T-lymphocyte cell lines which are oncogenic (Xu et al., 2010). Nonetheless, the PMA induced differentiation of the U937 cell line resulted in both MS4A4A mRNA and MS4A4A protein expression (Figure 4.4). PMA is capable of inducing a series of functional and phenotypic changes in U937 cells that result in a macrophage like phenotype (Minafra et al., 2011). Complete differentiation of U937 cells typically occurs within 2 to 3 days of PMA treatment (Minafra et al., 2011). Here, MS4A4A expression was shown to rapidly increase during differentiation, with elevated

expression by 24 hours and maximum expression by 48 hours of PMA treatment (Figure 4.4). PMA differentiated U937 cells also express cell surface proteins such as CD86 (Hida et al., 2000) and CD206 (Minafra et al., 2011) and therefore phenotypically resemble both M1 and M2 macrophages. In that respect, it is interesting that MS4A4A expression not only occurs in primary monocyte derived M2 macrophages but also in PMA differentiated U937 cells which partially resemble the M2 subset.

Lung tissue is characterized by an abundance of alveolar macrophages. Here, the alveolar macrophages are exposed to a variety of airborne pathogens and particulate matter which they must clear (Murray & Wynn, 2011). The constant exposure to airborne pathogens suggests alveolar macrophages may adopt a phenotype resembling M1 macrophages. However, it has been reported that due to the constant tissue repair, approximately 50% of human alveolar macrophages actually express CD206 and resemble M2 macrophages (Pechkovsky et al., 2010). Previously, our lab evaluated the mRNA expression of MS4A4A among a panel of solid human tissues. Among the 18+ human tissues tested, mRNA expression of MS4A4A was detected only in the lung (J. Zuccolo et al., 2013). Given that lung tissue is characterized by an abundance of alveolar macrophages which are characterized by a M2 phenotype, it is conceivable that the previously identified restricted tissue MS4A4A mRNA expression reflects the presence of MS4A4A in M2 macrophages lining the lung tissue.

MS4A4A displays elevated and restricted protein expression in hematopoietic cells, shares substantial sequence and structural similarity with MS4A1 as well as

MS4a4B and contains two short extracellular loops (Liang & Tedder, 2001). Given these features, MS4A4A has the potential to function as an immunotherapeutic target. We evaluated the effects of anti-MS4A4A on three cellular functions in select MS4A4A expressing cells: I) cell apoptosis, II) cellular differentiation, and III) homotypic adhesion. In each case the cellular effects evaluated were limited to those which were not Fc receptor dependent. The limitations were necessary since all of our anti-MS4A4A monoclonal antibodies were repeatedly identified as of the mouse IgG1 isotype. Consequently it is not capable of mediating cellular effects that are dependent on Fc receptor-antibody crosslinking (Bruhns, 2012; Falk, 2007; Mancardi et al., 2013). Therefore, complement dependent killing, antibody-mediated cytotoxicity, and cellular phagocytosis could not be evaluated using human cells. Mouse IgG2a and IgG2b are the major mediators of complement activation. Therefore we could not evaluate complement dependent killing. Similarly, in the mouse system, mouse Ig2a and mouse IgG2b, but not mouse IgG1 are capable of mediating cellular effects dependent upon Fc receptor-antibody crosslinking (Falk, 2007). Therefore, since anti-MS4A4A is of the mouse IgG1 isotype we could also not evaluate the ability of anti-MS4A4A to induce the aforementioned antibody mediated functions in the mouse system.

BJAB-MS4A4A-HA cells were evaluated for cellular apoptosis following 8 and 16 hours of anti-MS4A4A treatment (Figure 4.6). Within this time frame, anti-MS4A1 antibodies have been shown to induce cellular apoptosis in MS4A1+ cells (Shan, Ledbetter, & Press, 1998). However, in PMA differentiated U937 cells apoptosis was

evaluated following 08 hours of antibody treatment. Here, apoptosis could not be evaluated for extended time periods due to several limitations. First, PMA treatment induces U937 cells to undergo several morphological and functional changes that are associated with their differentiation (Minafra et al., 2011). Among these are changes in the cellular adherence of PMA differentiated U937 cells with polyethylene plates. Following short periods of culture in PMA, we found that differentiated cells did not adhere tightly to polyethylene plates and can be gently removed without considerably affecting cellular vitality. However, when PMA differentiated U937 cells are cultured for extended periods of time they become tightly adherent and the conditions required for their removal induces extensive cell death which confounds the analysis of apoptosis.

Here we show that both soluble and immobilized anti-MS4A4A 4H2 and 5C12 antibodies did not induce cellular apoptosis (Figure 4.6; Figure 4.7) or influence homotypic adhesion (Figure 4.8) and the cellular differentiation (Figure 4.9) of MS4A4A expressing cells. Nevertheless, it is still conceivable that antibodies directed against the extracellular epitopes of MS4A4A may be capable of inducing the aforementioned effects. The concept is best illustrated by considering the effects of monoclonal antibodies directed against the extracellular epitopes of human CD20. Currently, there are several antibodies that are directed against distinct CD20 cell surface epitopes. Depending upon the epitope, targeted monoclonal anti-CD20 antibodies are capable of inducing differing cellular effects with varying effectiveness (Cragg, 2005; Deans et al., 2002). Consider for instance the anti-CD20 IF5 and anti-CD20 B1 monoclonal antibodies.

Both antibodies are of the IgG2a isotype and target a distinct CD20 cell surface epitope. Among these, only anti-CD20 B1 has the capability to induce homotypic adhesion and cellular apoptosis (Cragg, 2005; Deans et al., 2002). Consequently, it is possible that antibodies directed against MS4A4A cell surface epitopes distinct from those targeted by anti-MS4A4A 4H2 and 5C12, may be capable of inducing cellular apoptosis or influencing homotypic adhesion and cellular differentiation.

MS4a4B, a mouse homolog of MS4A4A, is known to regulate G1 to S phase cell cycle progression of T-lymphocytes (Xu et al., 2010). Several immunotherapeutic antibodies have been reported to modulate cell cycle progression (Cragg, 2005; Sliwkowski & Mellman, 2013). Therefore we questioned whether anti-MS4A4A 4H2 and 5C12 could modulate the cell cycle progression of MS4A4A expressing cells. Despite MS4A4A expression in peripheral blood monocytes (Figure 4.2), monocyte derived M1 and M2 macrophages (Figure 4.3), and PMA differentiated U937 cells (Figure 4.4), we restricted our analysis to the effects of anti-MS4A4A on BJAB-MS4A4A-HA cell cycle progression. The limitation was necessary since monocytes, their differentiated progeny, and PMA treated U937 cells have limited *in vitro* proliferation potential. Here, we incubated BJAB-MS4A4A-HA cells with soluble or immobilized anti-MS4A4A followed by staining with propidium iodide and flow cytometric analysis. Propidium iodide is a nuclear stain which is capable of differentiating between cells which are in the G1, S, and G2/M phase of the cell cycle (Inoue, 2001). BJAB-MS4A4A-HA cells intrinsically undergo homotypinc adhesion during cell culture. In preliminary experiments, we could not measure the

effects of anti-MS4A4A on BJAB-MS4A4A-HA cell cycle progression. Literature review and further analysis indicated that homotypic adhesion interferes with the ability of propidium iodide and other indicators to identify cell cycle phases (Inoue, 2001).

Chapter V
Summary and Future Directions

In this thesis I have described absence of MS4A8B protein expression in peripheral blood gated monocytes, resting granulocytes and lymphocytes as well as the absence of MS4A8B expression in monocyte derived M1 and M2 macrophages. Collectively, the data indicates that MS4A8B is not expressed in the hematopoietic cell populations that we evaluated. Therefore, the patterns of human MS4A8B expression differ with respect to its mouse homolog, MS4a8A, which is expressed in M2 macrophages (Schmieder et al., 2011). Here, we also confirm the expression of MS4A8B in the NCI-H69 cell line, but at levels that are logarithmically lower from those reported by Bangur and colleagues (Bangur et al., 2004).

Recently, two independent studies evaluated the expression of MS4A8B. The first identified MS4A8B expression in normal but not cancerous colonic epithelium (Michel et al., 2013) while a second study identified that MS4A8B is preferentially over-expressed in prostate cancer cells (Ye et al., 2014). Both cells types are of epithelial origin. Collectively, our data and the recent studies indicate that though MS4A8B is not expressed in the hematopoietic cell populations evaluated, it does display expression in select cells of epithelial origin. Consequently, additional studies could evaluate the expression of MS4A8B in normal and cancerous epithelial cells of tissue where MS4A8B mRNA was previously identified (J. Zuccolo et al., 2013). Evaluating MS4A8B expression

in both cancerous and healthy cells may be important since recent studies have shown that MS4A8B is differentially expressed between the two. If MS4A8B displays restricted protein expression, future studies could investigate whether antibodies directed against its extracellular epitopes are capable of inducing cellular apoptosis and additional effects in MS4A8B+ cells. Since MS4A8B was recently shown to regulate cell cycle progression in prostate cancer cells and the LNCaP prostate cancer cell line (Ye et al., 2014) it would be interesting to determine whether anti-MS4A8B is capable of influencing cell cycle progression.

In a preliminary investigation we confirmed that MS4A8B is expressed in the LNCaP cell line at levels that would allow for molecular biology and functional assays. With respect to functional assays, immunoprecipitation experiments of MS4A8B in the LNCaP cell line may help elucidate the proteins that MS4A8B associates with in order to regulate cell cycle progression. In addition, siRNA mediated down-regulation of MS4A8B and over-expression studies may also help determine whether MS4A8B is involved in the regulation of additional cellular roles, such as cellular differentiation, a function which has been reported for its mouse homolog, MS4a8A (Michel et al., 2013). In addition, multiple MS4A family members, such as MS4A1 and MS4A12, are known to regulate extracellular calcium conductance (Cragg, 2005; Koslowski et al., 2008). Since MS4A8B shares substantial sequence and structural similarity with both MS4A1 and MS4A12 it may also regulate calcium conductance (Liang & Tedder, 2001).

Using our monoclonal anti-MS4A4A antibodies we also evaluated the expression of MS4A4A within hematopoietic cell subsets. Herein, we report that MS4A4A is not expressed in resting lymphocytes or granulocytes. However, it is still possible that MS4A4A may be expressed in activated lymphocytes or granulocytes. Similarly, T-lymphocytes and B-lymphocytes can also be separated into multiple populations based upon various cell surface markers, their anatomical location and stage of development (Murphy K, 2008). Consequently, future studies could investigate whether MS4A4A is expressed in T- or B- lymphocyte sub-populations as well as activated peripheral blood T- or B-lymphocytes. In this thesis I report that MS4A4A is expressed in peripheral blood monocytes. Monocytes can be classified according to the expression of CD14 and CD16 as classical, intermediate, and alternative monocytes (Tallone et al., 2011). MS4A4A protein was found to be expressed in CD14- and CD14+ as well as CD16- and CD16+ monocytes, indicating that MS4A4A is expressed across monocytic subsets.

We also analyzed the expression of MS4A4A in peripheral blood monocyte derived M1 and M2 macrophages. Here, we report that MS4A4A is consistently expressed in M2 but not M1 macrophages. Its consistent, elevated, and restricted expression within the M2 but not M1 macrophage subset make it a suitable cell surface marker for their classification. However, M2 macrophages can also be sub-classified and differentiated to M2a, M2b, M2c, and tumor associated macrophages (Mantovani et al., 2004; Martinez & Gordon, 2014). Each subset is involved in the regulation of specific cellular functions and displays different cell surface markers (Mantovani et al., 2004).

Future investigations will evaluate the expression of MS4A4A within M2 macrophage subsets. If MS4A4A also displays differential expression within M2 macrophage subsets, it could potentially be used as a cell surface marker for their sub-classification.

With the identification of MS4A4A protein expression in monocytes and macrophages its functional role can now be elucidated. The mouse homolog of MS4A4A, MS4a4B, is known to regulate cell cycle progression and cellular apoptosis in T-lymphocytes (Xu et al., 2010; Yan et al., 2013). A similar function may be performed by MS4A4A in monocytes, PMA differentiated U937 cells, or monocyte derived M2 macrophages. To investigate whether MS4A4A is involved in the regulation of similar and/or additional functions, MS4A4A siRNA mediated down-regulation and ectopic expression studies can be performed, followed by analysis with a series of functional and molecular biology assays. Interestingly, in a preliminary experiment we identified that anti-MS4A4A is capable of co-immunoprecipitating a unique product in PMA differentiated U937 cells (MS4A4A+).

Here we also report that both soluble and immobilized anti-MS4A4A (4H2 and 5C12) did not induce cellular apoptosis in PMA differentiated U937 cells and BJAB-MS4A8B-HA cells, influence the homotypic adhesion of BJAB-MS4A4A-HA cells, or the PMA induced differentiation of U937 cells. Nonetheless, it is still possible that targeting MS4A4A via immunoglobulin molecules can influence the aforementioned functions. As previously discussed, the ability of an antibody to induce cellular apoptosis or influence cellular functions such as homotypic adhesion depends upon the epitope it targets

(Cragg, 2005). Consequently, as additional antibodies are developed against MS4A4A, future studies may re-evaluate their ability to induce cellular apoptosis and influence other cellular functions. In our experiments, we evaluated the ability of anti-MS4A4A to induce apoptosis and influence cellular functions that were not dependent on immunoglobulin-Fc receptor binding. As previously mentioned, the limitation was necessary since our monoclonal anti-MS4A4A antibodies were identified as of the mouse IgG1 isotype. Mouse IgG1 cannot bind to human Fc receptors (Mancardi et al., 2013) and therefore we could not evaluate the ability to anti-MS4A4A to induce antibody-dependent cytotoxicity. Since mouse IgG2a and mouse IgG2b but not mouse IgG1 are capable of activating complement we could not evaluate the ability to anti-MS4A4A to induce complement dependent killing. For Rituximab, antibody dependent cytotoxicity and complement dependent killing are believed to be among the most important effector mechanisms regulating its action (Cragg, 2005). Here, the short extracellular loop of MS4A1, against which Rituximab binds, is believed to allow the engagement of Rituximab near the plasma membrane and allow for the efficient activation of complement dependent killing and antibody mediated cytoxicity (Lim et al., 2010). Since MS4A4A also possess short extracellular loops (Cragg, 2005; Lim et al., 2010), it would be interesting to determine whether anti-MS4A4A can induce complement dependent killing and antibody mediated cytotoxicity. In order to evaluate this, the isotype of anti-MS4A4A would first need to be changed to one which is capable of binding human Fc receptors and activating complement, such as human IgG1. This

could be achieved by cloning the complementary regions of anti-MS4A4A within a vector containing the human IgG1 backbone (Sliwkowski and Mellman, 2013).

In conclusion, in this thesis I have demonstrated that MS4A4A but not MS4A8B is expressed in the hematopoietic cell populations evaluated. MS4A4A was expressed consistently in primary monocytes, PMA differentiated U937 cells and M2 macrophages while MS4A8B expression was confirmed in the NCI-H69 cell line. We also show that anti-MS4A4A is not capable of inducing cellular apoptosis or effecting select cellular functions in MS4A4+ cells.

References

Adra, C. N., Lelias, J. M., Kobayashi, H., Kaghad, M., Morrison, P., Rowley, J. D., & Lim, B. (1994). Cloning of the cDNA for a hematopoietic cell-specific protein related to CD20 and the beta subunit of the high-affinity IgE receptor: evidence for a family of proteins with four membrane-spanning regions. *Proc Natl Acad Sci U S A, 91*(21), 10178-10182.

Arista, S., Ferraro, D., Cascio, A., Vizzi, E., & di Stefano, R. (1995). Detection of IgM antibodies specific for measles virus by capture and indirect enzyme immunoassays. *Res Virol, 146*(3), 225-232.

Bangur, C. S., Johnson, J. C., Switzer, A., Wang, Y. H., Hill, B., Fanger, G. R., . . . Retter, M. W. (2004). Identification and characterization of L985P, a CD20 related family member over-expressed in small cell lung carcinoma. *Int J Oncol, 25*(6), 1583-1590.

Baselga, J., Cortes, J., Kim, S. B., Im, S. A., Hegg, R., Im, Y. H., . . . Group, C. S. (2012). Pertuzumab plus trastuzumab plus docetaxel for metastatic breast cancer. *N Engl J Med, 366*(2), 109-119. doi: 10.1056/NEJMoa1113216

Bruhns, P. (2012). Properties of mouse and human IgG receptors and their contribution to disease models. *Blood, 119*(24), 5640-5649. doi: 10.1182/blood-2012-01-380121

Carter, P. J. (2006). Potent antibody therapeutics by design. *Nat Rev Immunol, 6*(5), 343-357. doi: 10.1038/nri1837

Clark, E. A., & Shu, G. (1987). Activation of human B cell proliferation through surface Bp35 (CD20) polypeptides or immunoglobulin receptors. *J Immunol, 138*(3), 720-725.

Clynes, R. A., Towers, T. L., Presta, L. G., & Ravetch, J. V. (2000). Inhibitory Fc receptors modulate in vivo cytotoxicity against tumor targets. *Nat Med, 6*(4), 443-446. doi: 10.1038/74704

Coiffier, B., Lepretre, S., Pedersen, L. M., Gadeberg, O., Fredriksen, H., van Oers, M. H., . . . Robak, T. (2008). Safety and efficacy of ofatumumab, a fully human monoclonal anti-CD20 antibody, in patients with relapsed or refractory B-cell chronic lymphocytic leukemia: a phase 1-2 study. *Blood, 111*(3), 1094-1100. doi: 10.1182/blood-2007-09-111781

Correia, I. R. (2010). Stability of IgG isotypes in serum. *MAbs, 2*(3), 221-232.

Cragg, M., Walshe, CA., Ivanov, AO., and Glennie, MJ. . (2005). The biology of CD20 and its potential as a target for mAb therapy. *Current DIrections in Autoimmunity, 8*, 140-174.

Davis, W., Harrison, P. T., Hutchinson, M. J., & Allen, J. M. (1995). Two distinct regions of FC gamma RI initiate separate signalling pathways involved in endocytosis and phagocytosis. *EMBO J, 14*(3), 432-441.

Davoine, F., Lavigne, S., Chakir, J., Ferland, C., Boulay, M. E., & Laviolette, M. (2002). Expression of FcgammaRIII (CD16) on human peripheral blood eosinophils increases in allergic conditions. *J Allergy Clin Immunol, 109*(3), 463-469.

Deans, J. P., Li, H., & Polyak, M. J. (2002). CD20-mediated apoptosis: signalling through lipid rafts. *Immunology, 107*(2), 176-182.

Dinkel, H., Van Roey, K., Michael, S., Davey, N. E., Weatheritt, R. J., Born, D., . . . Gibson, T. J. (2014). The eukaryotic linear motif resource ELM: 10 years and counting. *Nucleic Acids Res, 42*(Database issue), D259-266. doi: 10.1093/nar/gkt1047

Donato, J. L., Ko, J., Kutok, J. L., Cheng, T., Shirakawa, T., Mao, X. Q., . . . Adra, C. N. (2002). Human HTm4 is a hematopoietic cell cycle regulator. *J Clin Invest, 109*(1), 51-58. doi: 10.1172/JCI14025

Falk, N., Jeffrey V. Ravtech.,. (2007). Fc-receptors as regulators of immunity. *Advances in Immunology, 96*, 179-204.

Gillis, C., Gouel-Cheron, A., Jonsson, F., & Bruhns, P. (2014). Contribution of Human FcgammaRs to Disease with Evidence from Human Polymorphisms and Transgenic Animal Studies. *Front Immunol, 5*, 254. doi: 10.3389/fimmu.2014.00254

Golay, J. T., Clark, E. A., & Beverley, P. C. (1985). The CD20 (Bp35) antigen is involved in activation of B cells from the G0 to the G1 phase of the cell cycle. *J Immunol, 135*(6), 3795-3801.

Grage-Griebenow, E., Flad, H. D., & Ernst, M. (2001). Heterogeneity of human peripheral blood monocyte subsets. *J Leukoc Biol, 69*(1), 11-20.

Hari, S. B., Lau, H., Razinkov, V. I., Chen, S., & Latypov, R. F. (2010). Acid-induced aggregation of human monoclonal IgG1 and IgG2: molecular mechanism and the effect of solution composition. *Biochemistry, 49*(43), 9328-9338. doi: 10.1021/bi100841u

Hida, A., Kawakami, A., Nakashima, T., Yamasaki, S., Sakai, H., Urayama, S., . . . Eguchi, K. (2000). Nuclear factor-kappaB and caspases co-operatively regulate the activation and apoptosis of human macrophages. *Immunology, 99*(4), 553-560.

Houser, B. (2012). Bio-Rad's Bio-Plex(R) suspension array system, xMAP technology overview. *Arch Physiol Biochem, 118*(4), 192-196. doi: 10.3109/13813455.2012.705301

Hupp, K., Siwarski, D., Mock, B. A., & Kinet, J. P. (1989). Gene mapping of the three subunits of the high affinity FcR for IgE to mouse chromosomes 1 and 19. *J Immunol, 143*(11), 3787-3791.

Inoue, S. (2001). [Analyses of cell cycle and DNA]. *Rinsho Byori, 49*(9), 835-841.

Ishibashi, K., Suzuki, M., Sasaki, S., & Imai, M. (2001). Identification of a new multigene four-transmembrane family (MS4A) related to CD20, HTm4 and beta subunit of the high-affinity IgE receptor. *Gene, 264*(1), 87-93.

Jaipersad, A. S., Lip, G. Y., Silverman, S., & Shantsila, E. (2014). The role of monocytes in angiogenesis and atherosclerosis. *J Am Coll Cardiol, 63*(1), 1-11. doi: 10.1016/j.jacc.2013.09.019

Jimenez, R., Salazar, G., Baldridge, K. K., & Romesberg, F. E. (2003). Flexibility and molecular recognition in the immune system. *Proc Natl Acad Sci U S A, 100*(1), 92-97. doi: 10.1073/pnas.262411399

Jin, H., Yang, R., Zheng, Z., Romero, M., Ross, J., Bou-Reslan, H., . . . Merchant, M. (2008). MetMAb, the one-armed 5D5 anti-c-Met antibody, inhibits orthotopic pancreatic tumor growth and improves survival. *Cancer Res, 68*(11), 4360-4368. doi: 10.1158/0008-5472.CAN-07-5960

Jones, D. H., Nusbacher, J., & Anderson, C. L. (1985). Fc receptor-mediated binding and endocytosis by human mononuclear phagocytes: monomeric IgG is not endocytosed by U937 cells and monocytes. *J Cell Biol, 100*(2), 558-564.

Jonsson, T., Arnason, J. A., & Valdimarsson, H. (1986). Enzyme-linked immunosorbent assay (ELISA) screening test for detection of rheumatoid factor. *Rheumatol Int, 6*(5), 199-204.

Kiesel, S., Haas, R., Moldenhauer, G., Kvalheim, G., Pezzutto, A., & Dorken, B. (1987). Removal of cells from a malignant B-cell line from bone marrow with immunomagnetic beads and with complement and immunoglobulin switch variant mediated cytolysis. *Leuk Res, 11*(12), 1119-1125.

Kohler, G., & Milstein, C. (1975). Continuous cultures of fused cells secreting antibody of predefined specificity. *Nature, 256*(5517), 495-497.

Koslowski, M., Sahin, U., Dhaene, K., Huber, C., & Tureci, O. (2008). MS4A12 is a colon-selective store-operated calcium channel promoting malignant cell processes. *Cancer Res, 68*(9), 3458-3466. doi: 10.1158/0008-5472.CAN-07-5768

Krausgruber, T., Blazek, K., Smallie, T., Alzabin, S., Lockstone, H., Sahgal, N., . . . Udalova, I. A. (2011). IRF5 promotes inflammatory macrophage polarization and TH1-TH17 responses. *Nat Immunol, 12*(3), 231-238. doi: 10.1038/ni.1990

Kuijpers, T. W., Bende, R. J., Baars, P. A., Grummels, A., Derks, I. A., Dolman, K. M., . . . van Lier, R. A. (2010). CD20 deficiency in humans results in impaired T cell-independent antibody responses. *J Clin Invest, 120*(1), 214-222. doi: 10.1172/JCI40231

Kuster, H., Zhang, L., Brini, A. T., MacGlashan, D. W., & Kinet, J. P. (1992). The gene and cDNA for the human high affinity immunoglobulin E receptor beta chain and expression of the complete human receptor. *J Biol Chem, 267*(18), 12782-12787.

Kutok, J. L., Yang, X., Folkerth, R., & Adra, C. N. (2011). Characterization of the expression of HTm4 (MS4A3), a cell cycle regulator, in human peripheral blood cells and normal and malignant tissues. *J Cell Mol Med, 15*(1), 86-93. doi: 10.1111/j.1582-4934.2009.00925.x

Lefebvre, M. L., Krause, S. W., Salcedo, M., & Nardin, A. (2006). Ex vivo-activated human macrophages kill chronic lymphocytic leukemia cells in the presence of rituximab: mechanism of antibody-dependent cellular cytotoxicity and impact of human serum. *J Immunother, 29*(4), 388-397. doi: 10.1097/01.cji.0000203081.43235.d7

Lewis, G. D., Figari, I., Fendly, B., Wong, W. L., Carter, P., Gorman, C., & Shepard, H. M. (1993). Differential responses of human tumor cell lines to anti-p185HER2 monoclonal antibodies. *Cancer Immunol Immunother, 37*(4), 255-263.

Lewis Phillips, G. D., Li, G., Dugger, D. L., Crocker, L. M., Parsons, K. L., Mai, E., . . . Sliwkowski, M. X. (2008). Targeting HER2-positive breast cancer with trastuzumab-DM1, an antibody-cytotoxic drug conjugate. *Cancer Res, 68*(22), 9280-9290. doi: 10.1158/0008-5472.CAN-08-1776

Li, H., Ayer, L. M., Polyak, M. J., Mutch, C. M., Petrie, R. J., Gauthier, L., . . . Deans, J. P. (2004). The CD20 calcium channel is localized to microvilli and constitutively associated with membrane rafts: antibody binding increases the affinity of the association through an epitope-dependent cross-linking-independent mechanism. *J Biol Chem, 279*(19), 19893-19901. doi: 10.1074/jbc.M400525200

Liang, Y., Buckley, T. R., Tu, L., Langdon, S. D., & Tedder, T. F. (2001). Structural organization of the human MS4A gene cluster on Chromosome 11q12. *Immunogenetics, 53*(5), 357-368.

Liang, Y., & Tedder, T. F. (2001). Identification of a CD20-, FcepsilonRIbeta-, and HTm4-related gene family: sixteen new MS4A family members expressed in human and mouse. *Genomics, 72*(2), 119-127. doi: 10.1006/geno.2000.6472

Lim, S. H., Beers, S. A., French, R. R., Johnson, P. W., Glennie, M. J., & Cragg, M. S. (2010). Anti-CD20 monoclonal antibodies: historical and future perspectives. *Haematologica, 95*(1), 135-143. doi: 10.3324/haematol.2008.001628

Liu, Y. C., Zou, X. B., Chai, Y. F., & Yao, Y. M. (2014). Macrophage Polarization in Inflammatory Diseases. *Int J Biol Sci, 10*(5), 520-529. doi: 10.7150/ijbs.8879

Lu, J., Ellsworth, J. L., Hamacher, N., Oak, S. W., & Sun, P. D. (2011). Crystal structure of Fcgamma receptor I and its implication in high affinity gamma-immunoglobulin binding. *J Biol Chem, 286*(47), 40608-40613. doi: 10.1074/jbc.M111.257550

Maloney, D. G., Grillo-Lopez, A. J., White, C. A., Bodkin, D., Schilder, R. J., Neidhart, J. A., . . . Levy, R. (1997). IDEC-C2B8 (Rituximab) anti-CD20 monoclonal antibody therapy in patients with relapsed low-grade non-Hodgkin's lymphoma. *Blood, 90*(6), 2188-2195.

Mancardi, D. A., Albanesi, M., Jonsson, F., Iannascoli, B., Van Rooijen, N., Kang, X., . . . Bruhns, P. (2013). The high-affinity human IgG receptor FcgammaRI (CD64) promotes IgG-mediated inflammation, anaphylaxis, and antitumor immunotherapy. *Blood, 121*(9), 1563-1573. doi: 10.1182/blood-2012-07-442541

Mantovani, A., Sica, A., Sozzani, S., Allavena, P., Vecchi, A., & Locati, M. (2004). The chemokine system in diverse forms of macrophage activation and polarization. *Trends Immunol, 25*(12), 677-686. doi: 10.1016/j.it.2004.09.015

Martinez, F. O., & Gordon, S. (2014). The M1 and M2 paradigm of macrophage activation: time for reassessment. *F1000Prime Rep, 6*, 13. doi: 10.12703/P6-13

Martinez, F. O., Gordon, S., Locati, M., & Mantovani, A. (2006). Transcriptional profiling of the human monocyte-to-macrophage differentiation and polarization: new molecules and patterns of gene expression. *J Immunol, 177*(10), 7303-7311.

Matsuda, A., Okayama, Y., Ebihara, N., Yokoi, N., Gao, P., Hamuro, J., . . . Kinoshita, S. (2008). High-affinity IgE receptor-beta chain expression in human mast cells. *J Immunol Methods, 336*(2), 229-234. doi: 10.1016/j.jim.2008.05.006

Michel, J., Schonhaar, K., Schledzewski, K., Gkaniatsou, C., Sticht, C., Kellert, B., . . . Schmieder, A. (2013). Identification of the novel differentiation marker MS4A8B and its murine homolog MS4A8A in colonic epithelial cells lost during neoplastic transformation in human colon. *Cell Death Dis, 4*, e469. doi: 10.1038/cddis.2012.215

Minafra, L., Di Cara, G., Albanese, N. N., & Cancemi, P. (2011). Proteomic differentiation pattern in the U937 cell line. *Leuk Res, 35*(2), 226-236. doi: 10.1016/j.leukres.2010.07.040

Morsy, D. E., Sanyal, R., Zaiss, A. K., Deo, R., Muruve, D. A., & Deans, J. P. (2013). Reduced T-dependent humoral immunity in CD20-deficient mice. *J Immunol, 191*(6), 3112-3118. doi: 10.4049/jimmunol.1202098

Murphy K, T. P., Walport M. (2008). *Janeways Immunobiology*. Newyork: Garland Science.

Murphy K., T. P., and Walport M. . (2008). *Janeway's Immunobiology 7th Edition* (7 ed.). Newyork: Graland Science.

Murray, P. J., & Wynn, T. A. (2011). Protective and pathogenic functions of macrophage subsets. *Nat Rev Immunol, 11*(11), 723-737. doi: 10.1038/nri3073

Nimmerjahn, F., & Ravetch, J. V. (2008). Fcgamma receptors as regulators of immune responses. *Nat Rev Immunol, 8*(1), 34-47. doi: 10.1038/nri2206

Nissim, A., & Chernajovsky, Y. (2008). Historical development of monoclonal antibody therapeutics. *Handb Exp Pharmacol*(181), 3-18. doi: 10.1007/978-3-540-73259-4_1

Okeley, N. M., Miyamoto, J. B., Zhang, X., Sanderson, R. J., Benjamin, D. R., Sievers, E. L., . . . Alley, S. C. (2010). Intracellular activation of SGN-35, a potent anti-CD30 antibody-drug conjugate. *Clin Cancer Res, 16*(3), 888-897. doi: 10.1158/1078-0432.CCR-09-2069

Olafsen, T. (2012). Fc engineering: serum half-life modulation through FcRn binding. *Methods Mol Biol, 907*, 537-556. doi: 10.1007/978-1-61779-974-7_31

Pechkovsky, D. V., Prasse, A., Kollert, F., Engel, K. M., Dentler, J., Luttmann, W., . . . Zissel, G. (2010). Alternatively activated alveolar macrophages in pulmonary fibrosis-mediator production and intracellular signal transduction. *Clin Immunol, 137*(1), 89-101. doi: 10.1016/j.clim.2010.06.017

Polyak, M. J., Li, H., Shariat, N., & Deans, J. P. (2008). CD20 homo-oligomers physically associate with the B cell antigen receptor. Dissociation upon receptor engagement and recruitment of phosphoproteins and calmodulin-binding proteins. *J Biol Chem, 283*(27), 18545-18552. doi: 10.1074/jbc.M800784200

Polyak, M. J., Tailor, S. H., & Deans, J. P. (1998). Identification of a cytoplasmic region of CD20 required for its redistribution to a detergent-insoluble membrane compartment. *J Immunol, 161*(7), 3242-3248.

Press, O. W., Appelbaum, F., Ledbetter, J. A., Martin, P. J., Zarling, J., Kidd, P., & Thomas, E. D. (1987). Monoclonal antibody 1F5 (anti-CD20) serotherapy of human B cell lymphomas. *Blood, 69*(2), 584-591.

Radbruch, A., Bruggemann, M., Liesegang, B., & Rajewsky, K. (1982). Isolation of immunoglobulin class-switch and variable-region variants from mouse myeloma and hybridoma cell lines. *Adv Exp Med Biol, 158*, 93-105.

Radbruch, A., Liesegang, B., & Rajewsky, K. (1980). Isolation of variants of mouse myeloma X63 that express changed immunoglobulin class. *Proc Natl Acad Sci U S A, 77*(5), 2909-2913.

Reff, M. E., Carner, K., Chambers, K. S., Chinn, P. C., Leonard, J. E., Raab, R., . . . Anderson, D. R. (1994). Depletion of B cells in vivo by a chimeric mouse human monoclonal antibody to CD20. *Blood, 83*(2), 435-445.

Rey-Giraud, F., Hafner, M., & Ries, C. H. (2012). In vitro generation of monocyte-derived macrophages under serum-free conditions improves their tumor promoting functions. *PLoS One, 7*(8), e42656. doi: 10.1371/journal.pone.0042656

Robak, T., & Robak, E. (2011). New anti-CD20 monoclonal antibodies for the treatment of B-cell lymphoid malignancies. *BioDrugs, 25*(1), 13-25. doi: 10.2165/11539590-000000000-00000

Roopenian, D. C., & Akilesh, S. (2007). FcRn: the neonatal Fc receptor comes of age. *Nat Rev Immunol, 7*(9), 715-725. doi: 10.1038/nri2155

San Jose, E., Sahuquillo, A. G., Bragado, R., & Alarcon, B. (1998). Assembly of the TCR/CD3 complex: CD3 epsilon/delta and CD3 epsilon/gamma dimers associate indistinctly with both TCR alpha and TCR beta chains. Evidence for a double TCR heterodimer model. *Eur J Immunol, 28*(1), 12-21.

Schmieder, A., Schledzewski, K., Michel, J., Schonhaar, K., Morias, Y., Bosschaerts, T., . . . Goerdt, S. (2012). The CD20 homolog Ms4a8a integrates pro- and anti-inflammatory signals in novel M2-like macrophages and is expressed in parasite infection. *Eur J Immunol, 42*(11), 2971-2982. doi: 10.1002/eji.201142331

Schmieder, A., Schledzewski, K., Michel, J., Tuckermann, J. P., Tome, L., Sticht, C., . . . Goerdt, S. (2011). Synergistic activation by p38MAPK and glucocorticoid signaling mediates induction of M2-like tumor-associated macrophages expressing the novel CD20 homolog MS4A8A. *Int J Cancer, 129*(1), 122-132. doi: 10.1002/ijc.25657

Schroeder, H. W., Jr., & Cavacini, L. (2010). Structure and function of immunoglobulins. *J Allergy Clin Immunol, 125*(2 Suppl 2), S41-52. doi: 10.1016/j.jaci.2009.09.046

Shan, D., Ledbetter, J. A., & Press, O. W. (1998). Apoptosis of malignant human B cells by ligation of CD20 with monoclonal antibodies. *Blood, 91*(5), 1644-1652.

Shi, C., & Pamer, E. G. (2011). Monocyte recruitment during infection and inflammation. *Nat Rev Immunol, 11*(11), 762-774. doi: 10.1038/nri3070

Shin, G., Kang, T. W., Yang, S., Baek, S. J., Jeong, Y. S., & Kim, S. Y. (2011). GENT: gene expression database of normal and tumor tissues. *Cancer Inform, 10*, 149-157. doi: 10.4137/CIN.S7226

Sliwkowski, M. X., & Mellman, I. (2013). Antibody therapeutics in cancer. *Science, 341*(6151), 1192-1198. doi: 10.1126/science.1241145

Takahashi, K., Takata, M., Suwaki, T., Kawata, N., Tanimoto, Y., Soda, R., & Kimura, I. (1993). New flow cytometric method for surface phenotyping basophils from peripheral blood. *J Immunol Methods, 162*(1), 17-21.

Tallone, T., Turconi, G., Soldati, G., Pedrazzini, G., Moccetti, T., & Vassalli, G. (2011). Heterogeneity of human monocytes: an optimized four-color flow cytometry protocol for analysis of monocyte subsets. *J Cardiovasc Transl Res, 4*(2), 211-219. doi: 10.1007/s12265-011-9256-4

Taylor, R. P., & Lindorfer, M. A. (2008). Immunotherapeutic mechanisms of anti-CD20 monoclonal antibodies. *Curr Opin Immunol, 20*(4), 444-449. doi: 10.1016/j.coi.2008.05.011

Teeling, J. L., French, R. R., Cragg, M. S., van den Brakel, J., Pluyter, M., Huang, H., . . . Glennie, M. J. (2004). Characterization of new human CD20 monoclonal antibodies with potent cytolytic activity against non-Hodgkin lymphomas. *Blood, 104*(6), 1793-1800. doi: 10.1182/blood-2004-01-0039

Teeling, J. L., Mackus, W. J., Wiegman, L. J., van den Brakel, J. H., Beers, S. A., French, R. R., . . . van de Winkel, J. G. (2006). The biological activity of human CD20 monoclonal antibodies is linked to unique epitopes on CD20. *J Immunol, 177*(1), 362-371.

Teicher, B. A. (2009). Antibody-drug conjugate targets. *Curr Cancer Drug Targets, 9*(8), 982-1004.

van der Poel, C. E., Spaapen, R. M., van de Winkel, J. G., & Leusen, J. H. (2011). Functional characteristics of the high affinity IgG receptor, FcgammaRI. *J Immunol, 186*(5), 2699-2704. doi: 10.4049/jimmunol.1003526

van Engeland, M., Nieland, L. J., Ramaekers, F. C., Schutte, B., & Reutelingsperger, C. P. (1998). Annexin V-affinity assay: a review on an apoptosis detection system based on phosphatidylserine exposure. *Cytometry, 31*(1), 1-9.

van Vugt, M. J., Heijnen, A. F., Capel, P. J., Park, S. Y., Ra, C., Saito, T., . . . van de Winkel, J. G. (1996). FcR gamma-chain is essential for both surface expression and function of human Fc gamma RI (CD64) in vivo. *Blood, 87*(9), 3593-3599.

Venkataraman, C., Schaefer, G., & Schindler, U. (2000). Cutting edge: Chandra, a novel four-transmembrane domain protein differentially expressed in helper type 1 lymphocytes. *J Immunol, 165*(2), 632-636.

Verreck, F. A., de Boer, T., Langenberg, D. M., van der Zanden, L., & Ottenhoff, T. H. (2006). Phenotypic and functional profiling of human proinflammatory type-1 and anti-inflammatory type-2 macrophages in response to microbial antigens and IFN-gamma- and CD40L-mediated costimulation. *J Leukoc Biol, 79*(2), 285-293. doi: 10.1189/jlb.0105015

Weiner, L. M., Surana, R., & Wang, S. (2010). Monoclonal antibodies: versatile platforms for cancer immunotherapy. *Nat Rev Immunol, 10*(5), 317-327. doi: 10.1038/nri2744

Wild, D. (2013). *The Immunoassay Handbook - Theory and Application of Ligand Binding, ELISA, and Related Techniques*. Oxford, United Kingdoms: Elsevier Science.

Woof, J. M., & Burton, D. R. (2004). Human antibody-Fc receptor interactions illuminated by crystal structures. *Nat Rev Immunol, 4*(2), 89-99. doi: 10.1038/nri1266

Wu, C., Orozco, C., Boyer, J., Leglise, M., Goodale, J., Batalov, S., . . . Su, A. I. (2009). BioGPS: an extensible and customizable portal for querying and organizing gene annotation resources. *Genome Biol, 10*(11), R130. doi: 10.1186/gb-2009-10-11-r130

Wynn, T. A., Chawla, A., & Pollard, J. W. (2013). Macrophage biology in development, homeostasis and disease. *Nature, 496*(7446), 445-455. doi: 10.1038/nature12034

Xu, H., Williams, M. S., & Spain, L. M. (2006). Patterns of expression, membrane localization, and effects of ectopic expression suggest a function for MS4a4B, a CD20 homolog in Th1 T cells. *Blood, 107*(6), 2400-2408. doi: 10.1182/blood-2005-08-3340

Xu, H., Yan, Y., Williams, M. S., Carey, G. B., Yang, J., Li, H., . . . Rostami, A. (2010). MS4a4B, a CD20 homologue in T cells, inhibits T cell propagation by modulation of cell cycle. *PLoS One, 5*(11), e13780. doi: 10.1371/journal.pone.0013780

Yan, Y., Li, Z., Zhang, G. X., Williams, M. S., Carey, G. B., Zhang, J., . . . Xu, H. (2013). Anti-MS4a4B treatment abrogates MS4a4B-mediated protection in T cells and ameliorates experimental autoimmune encephalomyelitis. *Apoptosis, 18*(9), 1106-1119. doi: 10.1007/s10495-013-0870-2

Yang, H. J., Zheng, L., Zhang, X. F., Yang, M., & Huang, X. (2014). Association of the MS4A2 gene promoter C-109T or the 7th exon E237G polymorphisms with asthma risk: a meta-analysis. *Clin Biochem, 47*(7-8), 605-611. doi: 10.1016/j.clinbiochem.2014.01.022

Ye, L., Yao, X. D., Wan, F. N., Qu, Y. Y., Liu, Z. Y., Shen, X. X., . . . Ye, D. W. (2014). MS4A8B promotes cell proliferation in prostate cancer. *Prostate, 74*(9), 911-922. doi: 10.1002/pros.22802

Zhang, H., Cui, W., & Gross, M. L. (2014). Mass spectrometry for the biophysical characterization of therapeutic monoclonal antibodies. *FEBS Lett, 588*(2), 308-317. doi: 10.1016/j.febslet.2013.11.027

Zheng, K., Bantog, C., & Bayer, R. (2011). The impact of glycosylation on monoclonal antibody conformation and stability. *MAbs, 3*(6), 568-576. doi: 10.4161/mabs.3.6.17922

Zuccolo, J. (2010). *Analysis of MS4A Genes.* (Masters of Science), University of Calgary, Calgary.

Zuccolo, J., Bau, J., Childs, S. J., Goss, G. G., Sensen, C. W., & Deans, J. P. (2010). Phylogenetic analysis of the MS4A and TMEM176 gene families. *PLoS One, 5*(2), e9369. doi: 10.1371/journal.pone.0009369

Zuccolo, J., Deng, L., Unruh, T. L., Sanyal, R., Bau, J. A., Storek, J., . . . Deans, J. P. (2013). Expression of MS4A and TMEM176 Genes in Human B Lymphocytes. *Front Immunol, 4*, 195. doi: 10.3389/fimmu.2013.00195